Thermogravimetric Analysis Coupled with Mass Spectrometry and Inductively Coupled Plasma-Optical Emission Spectroscopy for Sediment Fingerprinting: Tracing the Sources of Sediment to the Coral Reefs of Montserrat

Anna Isobel Hook

“This thesis is submitted for the degree of Masters by Research in Environmental Science”

Lancaster University

Lancaster Environment Centre

Submitted September 2024

Abstract

Coral reef survival is threatened by sediment deposition, particularly those surrounding volcanic islands, where sudden and larger sediment loads enhance threats. Tracing the sources of this sediment is vital for erosion mitigation, land-use and conservation, and is achieved through sediment fingerprinting, a technique with little application to coral reefs. In this study, the novel application of TGA-MS to identify potential tracers was used, alongside ICP-OES, on ghaut and reef samples from the volcanic island of Montserrat in the Caribbean, where knowledge of soil compositions and the effect of recent eruptions is severely understudied. Sediment from within 40 ghauts (steep-sided ephemeral watercourses) in the north-west and 7 coral reefs on the western coast of Montserrat were sampled. For TGA-MS, a heating rate of 10°C/min from ~30°C to 1000°C was used, identifying OM, clay and calcite weight loss percentages, and exsolved H_2O and CO_2. ICP-OES analysed 11 elemental concentrations: Al, Ca, Cu, Fe, Mg, Mn, Ni, P, Pb, Si and Zn. The three-step method for tracer selection was used, producing a final tracer suit of clay, Fe, Mn and Si, with 100% reclassification accuracy. A MixSIAR unmixing model was applied to 5 marine samples, determining ghauts further south, in close proximity to the Belham River and Soufrière Hills Volcano, were the largest contributors to sediment deposition (>67%). Laboratory analysis and field observations implied the sediment was volcanically derived and particle size analysis indicated the predominant grain size on the reefs were fine sediment <0.5mm in diameter. The inclusion of clay identified that volcanic deposits were transported via terrestrial landscapes prior to deposition. The wider significance of the study is highlighted in terms of land-use planning, erosion mitigation and coral reef conservation, with a particular emphasis on the importance of considering varying processes on catchments experiencing unique processes, such as those of volcanism.

Contents

List of Figures

List of Tables

Glossary and Abbreviations

Table 1: A list of commonly used abbreviations for this study and their meanings.

Abbreviation	***Meaning***
ANOVA	Analysis of Variance
DSC	Differential Scanning Calorimetry
DTG	Derivative Thermogravimetry
ICP-OES	Inductively Coupled Plasma-Optical Emission Spectroscopy
LDA	Linear Discriminant Analysis
MS	Mass Spectrometry
OM	Organic Matter
PSA	Particle Size Analysis
TGA	Thermogravimetric Analysis
TGA-MS	Thermogravimetric Analysis Coupled with Mass Spectrometry

Table 2: A list of commonly used terms for this study and their definitions.

Term	***Definition***
Conservative	Applying to a tracer. In which chemical and mineralogical properties of the sediment remain unchanged during transportation.
DTG	The rate of change of the weight of a sample in relation to changing temperature or time.
Ghauts	Steep-sided ephemeral watercourses, incised during periods of heavy rain and flooding.
ICP-OES	A laboratory technique used to identify the concentrations of elements in liquid or gas samples.
Source Site	In sediment fingerprinting, the sites which sediment are believed to have potentially derived from.
Target Site	In sediment fingerprinting, the sites which receive sedimentation, the sediment of which is being traced to their original sources.
Tracer	In sediment fingerprinting, a variable or component of sediment used to identify the source of sediment.
TGA	A laboratory method used to analyse the change of weight of a sample as it is incrementally heated.
TGA-MS	A laboratory method combining TGA with mass spectrometry, during which the exsolved gases from TGA are measured in real time.

Acknowledgements

In the completion of this work, I would firstly like to thank Lancaster University and Lancaster Environment Centre for the opportunity, funding and resources offered in order to complete this project. Personally, I would like to express my deepest thanks to Dr Hugh Tuffen and Professor John Quinton for their continued and innumerable guidance, support and assistance. The time and patience they have dedicated to myself, and this project is truly appreciated along with the skills and knowledge I have gained from having the pleasure to work with them. I would also like to thank Professor Carly Stevens and Professor Phil Haygarth for their involvement in the planning and completion of the field sampling, along with the guides and locals in Montserrat. Furthermore, I would like to express great appreciation to Dr Pedro Batista for his time and willing involvement of the project, offering invaluable expertise and assistance on the completion of the sediment fingerprinting procedure. Further acknowledgments go to Dr Vassil Karloukovski, Dr Catherine Wearing and Dr Clare Benskin for all their extensive help and assistance with laboratory analysis. My sincerest appreciation is also extended to Dr Mengyi Gong and Dr Natalia Lipiejko for their time and help with statistical analysis.

I am also grateful to the entire LEC Soils Research Group and my office colleagues for their continued support and advice throughout my time spent on this project, it was a pleasure to work alongside each of them. Finally, the completion of this project could not have been done without the personal support of all my family and friends. Their faith in me when confidence was lacking motivated me to achieve my goals and ambitions, offering support and encouragement through every step of the journey and for that I am forever grateful.

Chapter 1: Introduction

1.1 Introduction

Coral reefs are important ecosystems covering <0.1% of the world's oceans (Jones *et al*., 2022) in tropical/subtropical marine environments, yet are one of the most vulnerable. They are important regions as they sustain the largest diversity of unique marine organisms on Earth (Jones *et al*., 2022) along with providing ecosystem services such as fishing and tourism. Coral reefs across the globe are under threat, including those surrounding Montserrat. Eutrophication, acidification, increased sea surface temperatures and more frequent/violent storms (Lesser, 2021; Negri *et al.,* 2011; Scoffin, 1993) are just some of the processes threatening coral reefs. Some have been exacerbated via climate change and global warming but there are also direct and indirect anthropogenic causes. The exponential rise in human population has resulted in increasing tourism, agriculture and land development. These have caused physical damage/breakages to corals from boats, anchors and people, along with increased inputs of nutrients, waste and sediment to coral reefs (Zainal Abidin and Mohamed, 2014). The inputs of these substances are threatening coral reefs through physical disturbances and changes in water quality which must remain in an optimum state for coral reefs to thrive.

The deposition of sediment (sedimentation) onto coral reefs is a significant threat requiring further investigation, experiencing little quantification in modern or ancient times (Lokier, 2021). This threat to coral reef ecosystems relates to the amount and type of sediment that is deposited and so varies across environments. Therefore, when studying sedimentation of coral reefs, each target and source should be investigated independently to account for differing sediment types deposited. In this way, knowledge of the sources of sediment deposited is crucial. Sediment can enter a coral reef through a number of various transfer routes as described in Figure 1. These include terrestrial runoff, aeolian deposits, anthropogenic activity and, in the case of Montserrat, through volcanic deposits (Lokier, 2021). When considering sediment in marine environments, acknowledging the various routes in which sediment may travel from terrestrial/source to marine environments is essential (DelValls *et al*., 1998). Determining sediment sources is not only imperative when investigating the potential impacts their deposition may have on various ecosystems, but also in terms of identifying areas experiencing soil erosion. Heightened soil erosion impacts soil stability and structure, as well as nutrient cycling (Quinton *et al.,* 2010), making areas experiencing high rates of erosion especially vulnerable during periods of heavy rainfalls and storm events. Identifying these areas is important for land use planning, land

management practices, agriculture and pollution mapping, particularly in regard to the development of mitigation measures. For a small island limited in land-use capacity and who are yet to receive significant modern research in sedimentation, Montserrat is an example of somewhere in desperate need of research in this area of study.

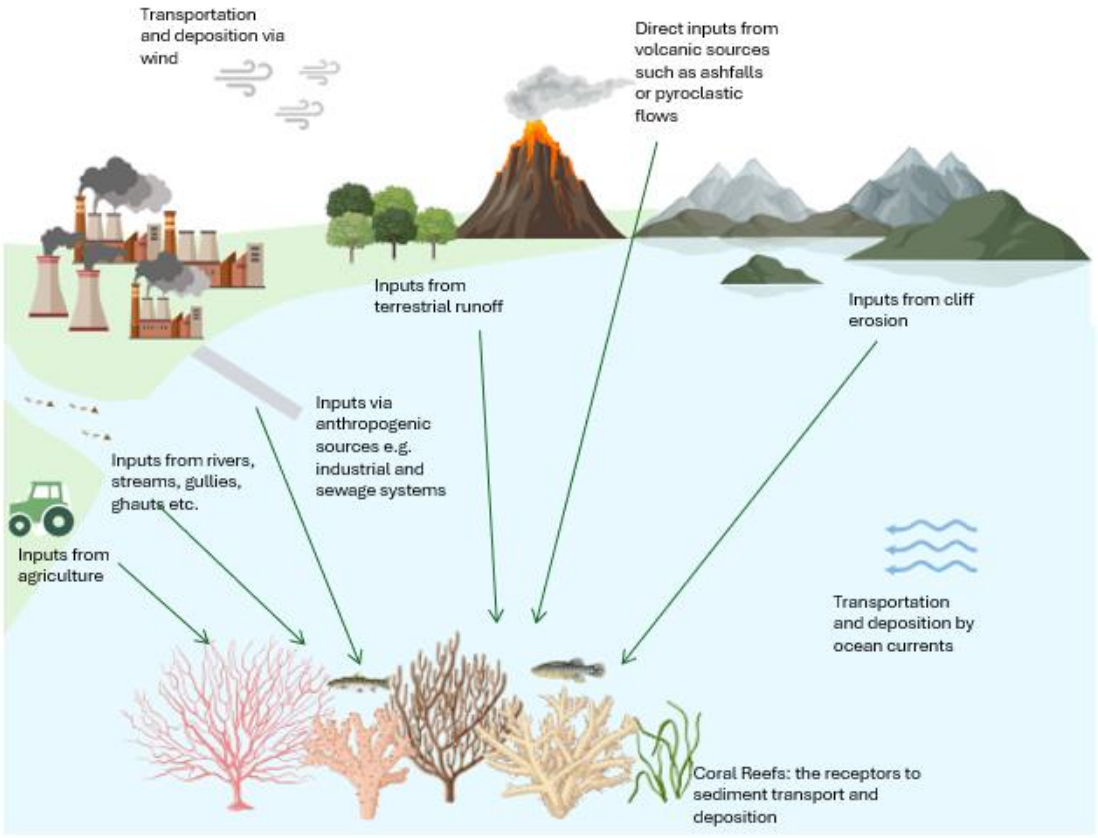

Figure 1: A conceptual diagram demonstrating a variety of sources of sediment to coral reef ecosystems. Created with BioRender.com

Montserrat is a Caribbean Island located in the Lesser Antilles with a total land area of 102 km^2 (Flower *et al*., 2020), with extensive terrestrial and marine ecosystems provided by Montserrat's unique topography. This has been influenced by a three-million-year history of volcanic activity from multiple volcanic centres: Silver Hills, Centre Hills and (South) Soufrière Hills (Figure 2). Since the onset of recent volcanic activity in 1995, the island has been divided into an Exclusion Zone in the southern two-thirds and a safe zone in the northern third of the island. Each volcanic centre (Figure 2) features steeply eroded valleys heading towards the coast (Barclay *et al*., 2006). One key topographical feature of interest are these ghauts; steep-sided ephemeral

watercourses, incised during periods of heavy rain and flooding (Hemmings *et al*., 2015). Montserrat is a tropical island lying in the north of the Intertropical Convergence Zone (ITCZ), where the rainfall season runs from April to November with peaks in September and May and an average rainfall of approximately 890mm yr^{-1} (Barclay *et al*., 2006). However, this rainfall varies across Montserrat depending on the topography. As Montserrat has a steep topography, air cools adiabatically, leading to large amounts of rain concentrated on mountain tops with much less in coastal regions (Barclay *et al*., 2006). The coastline (49km in total (Flower *et al*., 2020)) is key to Montserrat as it contains coral reefs along the eastern and north-eastern shelves of the island, averaging around 10% in coral cover (Flower *et al*., 2020), attracting tourists and assisting the local economy.

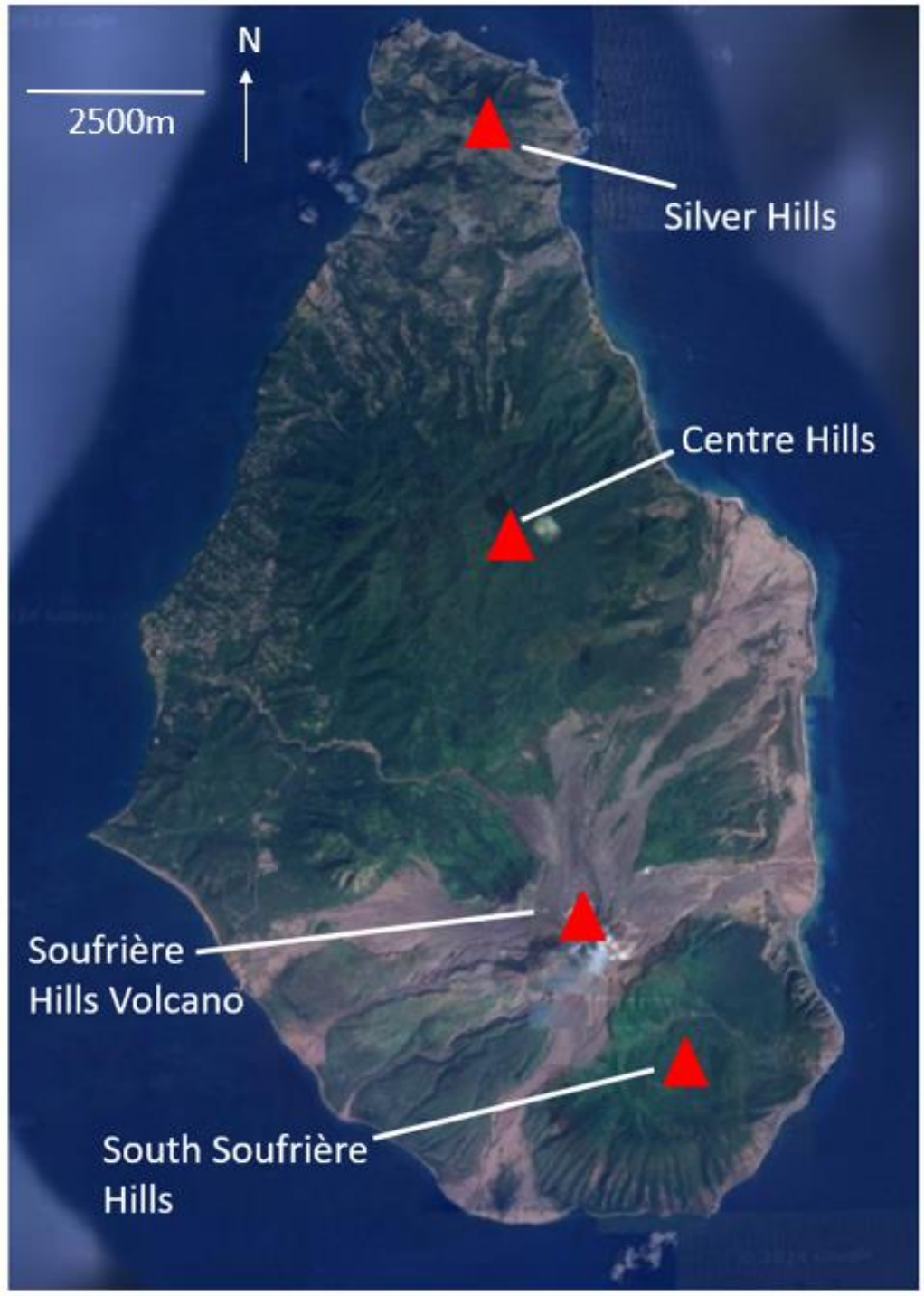

Figure 2: The locations of 4 main volcanic centres on Montserrat: Silver Hills, Centre Hills, Soufrière Hills Volcano and South Soufrière Hills. Base map from Google Earth.

In Montserrat, sediment deposition onto the coral reefs may be a significant issue due to the recent volcanic activity (Barclay *et al.,* 2007; Lokier 2021). The distribution of volcanic deposits, as well as potentially heightened soil erosion associated with volcanic activity, may increase the movement of sediment across terrestrial environments leading into the marine. As a result,

discovering where the sediment on coral reefs is sourced is imperative in mitigating soil movement and erosion.

One way of determining the sources of sediment is through a technique called sediment fingerprinting. Sediment fingerprinting is a source apportionment method where sediment properties from various potential sources are compared, and the unique properties (tracers) are used to determine the origin of material delivered elsewhere (Smith and Blake, 2014). There are a number of different properties which can be used as fingerprint tracers. Batista *et al*. (2022) describe potential fingerprints which include: fallout radionuclides, geochemistry, colour and magnetic properties. Koiter *et al*. (2013) demonstrate the wide range of uses of sediment fingerprinting at vast spatial and temporal scales, as well as identifying sources of sediment as small as <10µm. Sediment fingerprinting is used for a variety of purposes including land use management, waterway management, agriculture, identifying pathways of pollutants and developing strategies to reduce erosion as well as providing information for wider areas of research such as sediment budgets/dynamics and fluvial processes (Walling, 2013). Despite the beneficial applications of sediment fingerprinting, it does face challenges in reliability. During sediment transport there are a number of natural processes that may influence the chemical, biological and physical composition of sediment (Koiter *et al*., 2013). This brings uncertainty when comparing sediment properties to sources as it requires differentiating between those properties directly connected to the source and those which have arisen through additional environmental factors. Despite this, sediment fingerprinting has the potential to offer extremely powerful insight in the determination of sediment source contributions to coral reefs, however, it requires important consideration into the choice of tracers selected to perform at its full capacity.

1.2 Aims and Objectives

The first aim of this project is to assess which ghauts the sediment found on the coral reefs surrounding Montserrat was derived from. The second aim is to apply and test the application of thermogravimetric analysis coupled with mass spectrometry (TGA-MS) to sediment fingerprinting, assessing the suitability of this method. Inductively coupled plasma-optical emission spectroscopy (ICP-OES) data will be used alongside this. This will minimise some of the current gaps in research surrounding soil erosion and sediment pollution on Montserrat and will provide the first use of TGA-MS in its application to sediment fingerprinting.

To achieve the aims of this study, several objectives were set. The main objectives are:

1. To use both thermogravimetric analysis and ICP-OES to characterise key chemical components of the sediment collected from both reefs and ghauts on Montserrat.
2. To use thermogravimetric analyses coupled with mass spectrometry to aid the identification of chemical/mineralogical components of ghaut and reef sediment samples from Montserrat through the use of CO_2 and H_2O exsolved gas analysis.
3. Through the use of statistical testing, determine whether there are significant differences within and between ghaut and reef sediment samples from Montserrat in terms of their chemical/mineralogical compositions.
4. To implement sediment fingerprinting methods to evaluate which ghauts on Montserrat transport and deposit sediment onto the coral reefs surrounding the island.

1.3 Thesis Outline

This thesis is presented as a selection of chapters. As such, many chapters have their own aims and objectives outlined which work towards fulfilling the main aim of the project as previously stated. The chapters are as follows:

Chapter 1: Introduction – The purpose of this chapter is to introduce the key topics of the entire project and to highlight the issues the project aims to address. The overall aims and objectives are also outlined.

Chapter 2: Literature Review – This chapter navigates the current literature surrounding the topics of interest in the project. Broad concepts and ideas are summarised, emphasising the current research gaps and further highlighting the need for this study.

Chapter 3: Field Sampling – The purpose of this short chapter is to explain the field sites and samples collected for use in the rest of the project. Explanations on the way samples were collected and details on the sampling sites are outlined.

Chapter 4: Development of TGA Methodology – Chapter 4 discusses the preliminary TGA testing conducted on samples from Chapter 3. The aim is to outline the way in which the TGA methodology used for suitable data attainment was developed. The chapter includes a methodology for the preliminary testing, the results of these tests and a discussion on their implications, concluding on the final TGA methodology used for Chapters 5 and 6.

Chapter 5: Identification of TGA Signals – The inclusion of Chapter 5 offers an in-depth explanation on the way in which the identity of the mineralogical components in the tested samples were discovered through the procurement of DTG signals. An in-depth literature review, along with laboratory and statistical testing acts to justify the conclusions drawn.

Chapter 6: Sediment Fingerprinting - The most substantial chapter in the thesis and that which addresses the main aim of the project: successfully completing sediment fingerprinting to discover which ghauts on Montserrat transport and deposit sediment onto the coral reefs. This chapter outlines the parameters used as tracers, the sediment fingerprinting method and results, as well as including particle size analysis data, resulting in a discussion and explanation of the observations.

Chapter 7: Overall Discussion and Conclusion – The final chapter of the thesis acts as a broad discussion of the findings of the study and the implications for other areas of science. Limitations and recommendations for future studies are also included, ending with a broad conclusion of the thesis as a whole.

Chapter 2: Literature Review

2.1 Anthropogenic Impacts on Coral Reefs

Many people depend on coral reefs for their livelihoods. Tens of millions of people benefit from coral reef fisheries across tropical and subtropical regions (McManus *et al*., 2000). Around 20% of the global population lives within 100km of the shoreline at high densities (Duprey *et al*., 2016), with tourism providing employment and revenue for over 100 countries and territories (Spalding *et al*., 2017), including Montserrat. However, these benefits are also putting increased pressure on coral reef ecosystems, along with damages to corals through tourism. Overfishing is threatening the extinction of coral reef fish due to exploitation from an increased demand for food for the rising population. Sherman *et al*. (2023) state that 59% of shark/ray species related to coral reefs are at risk of extinction, with overfishing being the main cause.

Indirectly, anthropogenically enhanced global warming and climate change are large factors controlling the current distribution of coral reefs. Coral reefs are located where the conditions are optimal for survival. These include minimum sea temperatures of around 18°C, with optimal ranges commonly around 24 to 27°C (Johansen *et al*., 2013), low nutrient levels, salinity within 25000-45000mg/L (Manzello and Lirman, 2003), shallow depths and clear waters (Kleypas *et al*., 1999). Climate change is having broad implications for coral reefs, with damage resulting from changes in sea temperatures, salinity and frequency and magnitude of storms. Global warming is increasing ocean temperatures at an average rate of almost 0.3°C per decade (Garcia-Soto *et al*., 2021). This has accelerated drastically from the rate of 0.06°C per decade seen during the 20th and early 21st century (Garcia-Soto *et al*., 2021). Johansen *et al*. (2013) demonstrate the effect of increasing temperatures on common coral fish. They found that at temperatures only a few degrees above the normal range (30°C and 33°C) swimming speeds dropped sharply and fish spent longer resting motionless on the bottom of the reef. The mobility of reef organisms is a factor in predator-prey interactions, energy intake and fitness of fish (Johansen *et al*., 2013), therefore influencing mortality rates of the fish themselves and other reef organisms, resulting in a destabilisation of the ecosystem community as a whole. Anthropogenic disturbances to nutrient and salinity levels are also of major concern in regard to water quality.

2.2 Impact of Water Quality on Coral Reefs

Extensive research has been undertaken on the impacts of water quality on coral reefs (Bell, 1992; De'ath and Fabricius, 2010; Duprey *et al*., 2016; Rogers, 1990). One main factor influencing water quality is the abundance of nutrients. Coral reefs thrive in conditions where nutrient levels are low, so excessive inputs have the ability to impact all levels of an ecosystem through creating a nutrient surplus. Eutrophication and the addition of excess nutrients, minerals and heavy metals to water bodies has the potential to debilitate entire ecosystems. The formation of algal blooms reduces light attenuation and disrupts the water quality, leading to various physiological challenges. Nutrient enhancement has been found to increase coral diseases and bleaching (Vega Thurber *et al*., 2013), leading to mass mortality, but also reducing skeletogenesis (Marubini and Davies, 1996). Marubini and Davies (1996) offer useful insight into the way in which coral may respond to added nutrients from eutrophication or the deposition of nutrient-high or contaminated sediment through the completion of a controlled experiment, whereby nitrate was added to coral species and the physiological effects were observed. The results showed that around 50% of coral experienced a reduction in skeletogenesis. Using models, they theorised this was due to the observed increase in zooxanthellae which preferentially used the limited CO_2 supply, reducing that which could be used for coral calcification.

Alongside the enhanced supply of nutrients, heavy metals should also be considered. Heavy metal pollution in water bodies will have a number of consequences for corals due to binding of the molecules to proteins in corals. These consequences include reproductive stress (Reichelt-Brushett and Harrison, 2005), disruption to cellular functions (Kuzminov *et al.,* 2013), changes in rates of photosynthesis, physiological stress (Baumann *et al.,* 2009) and mass mortality. Not only this, but the threat from metal pollution is enhanced by the longevity that heavy metals remain in the environment, influencing water quality many years after deposition (Guzmán and Jiménez, 1992).

Salinity is another main concern when studying the water quality of reefs. Salinity levels outside the optimum range can also lead to mass mortality, a significant modern threat as some suggest increases of up to 8% salinity due to enhanced global warming (Du *et al.,* 2019). The effects of salinity on marine organisms are vast with changes occurring to nerves, enzymes, metabolism and cellular electrochemical processes (Vernberg and Vernberg, 2012). For corals specifically, exposure to elevated salinity has shown reductions in photosynthesis, respiration and survival (Manzello and Lirman, 2003; Porter *et al*., 1999). The variations of photosynthesis and respiration on Porites Furcata, an abundant coral species in near-shore environments, were reported by Manzello and Lirman (2003). They discovered reductions in photosynthesis rates and observed

the retraction of polyps alongside excessive mucus production when exposed to salinity levels outside the normal. However, they also report insignificant variations in respiration rates and no sign of tissue mortality after 2, 4, 6 and 24 hours of exposure. However, the results of this study counteract those observed in other literature such as Porter *et al*. (1999) who describe the opposite after up to 36 hours of exposure. This suggests exposure time also is likely a key factor in the effects of salinity on coral species. Although these studies did not consider sediment, they are a good representation of the various ways in which coral reefs respond to the addition of different stressors to their environment, whilst also highlighting the need to consider how coral reefs respond to these changes over time. This is especially important in sediment studies as sediment can remain in the water column for extensive periods of time.

2.3 Impact of Sediment on Coral Reefs

Another major pressure to coral reef ecosystems is the addition of sediment. Terrestrial runoff has the ability to alter water quality of the surrounding reefs through the addition of inorganic nutrients, particulate organic matter and sediment deposition (Storlazzi *et al*., 2015). The deposition of terrestrial sediment onto coral reefs has widespread issues for the ecosystem. When sediment enters the water column, fine grained sediment may remain in suspension and cause reduced light attenuation through increased turbidity. Riegl and Branch (1995) demonstrated that there is an up to 75% decline in light availability from just 100mg of sediment per cm^2, reaching 97% when levels reach 400mg per cm^2. This reduction in light attenuation has adverse effects on corals including stunted growth and eventual bleaching.

Aside from light attenuation, sedimentation impacts coral reefs by smothering corals when settling on their surfaces. This may block polyps and inhibit feeding mechanisms as well as using up energy to remove it (Duckworth *et al*., 2017, Fourney and Figueiredo, 2017). This was found in terms of fine sediment on sponges by Bannister *et al*. (2012) where the inhalant canals and filtering mechanisms were blocked. Additionally, the mucus film the sponges produce to counteract the negative effects of sedimentation uses their energy reserves, reducing the energy they can use for feeding, reproduction and growth (Bannister *et al*., 2012). Although this study provides insight into the physiological impact on coral reef ecosystems and also considers grain size, it neglects to consider the chemical composition of the sediment itself, an important factor in how it will behave once in the water column. Similar issues arise in other literature concerning sediment and marine environments. Wenger *et al*. (2013) looked at the effects of sediment on coral reef fish. They described the challenges of increased turbidity reducing visibility and ability

to obtain food, therefore impacting growth, reproduction and potentially mortality. Wenger *et al*. (2013) also found that the development of fish was influenced by the presence of terrestrial sediments. For fish exposed to various levels of sediment, the pelagic larval development (PLD) was significantly longer than those receiving no extra sediment, disturbing the population demographics. Comparatively to the study by Bannister *et al*. (2012), they also fail to take into account the chemical composition of the terrestrial sediment, but also that of the grain size.

Sediment has a range of magnitudes and types of impacts on reefs. One factor to consider is sediment grain size. It is generally agreed that fine sediment will have a harsher impact on coral reef ecosystems through the increase in turbidity due to the ability for fine-grained sediment to stay in suspension for longer periods of time, having a prolonged impact. Kookana *et al*. (1998) also attribute worse responses to fine-grained sediments to the reduced gas exchange, increasing the ability to bind nutrients and biocides. These effects were demonstrated by Fourney and Figueiredo (2017) who compared the impacts of both fine (terrestrial) sediment and coarse (natural) sediment on corals. They found that exposure to coarse sediment reflected that of an undisturbed ecosystem and attributed this to the way coarse sediment settled relatively quickly allowing the lower turbidity to be retained. Their results concerning finer grained sediment reflected that of previous studies by Storlazzi *et al*. (2015) in which finer grained sediment reduced the photosynthetically active radiation (PAR) more so than coarser sediments, and Tebbett *et al*. (2017) who demonstrated that finer-grained sediment is more readily ingested by coral reef fish, negatively impacting their health (and the productivity of the fishing industry). Whilst these studies are useful in describing the mechanisms behind coral interactions with various grain sizes, chemical composition linked to grain sizes in samples is an important component that has not been studied.

In 2005, Harrington *et al*. incorporated both the grain size and mineralogy of sediment in a study on their influence on crustose coralline algae (CCA). In agreement with the later studies of Fourney and Figueiredo (2017) and Storlazzi *et al*. (2015), they also found harsher effects on the CCA when exposed to finer-grained sediment. In terms of sediment composition, they also demonstrated how sensitivity increases for silts in comparison to nutrient-poor calcareous sediment. The strengths of this study lie in its ability to integrate both sediment grain size and mineralogy into a concise evaluation of the consequential deposition of sediment in coral reefs, however, was limited in the chemical compositions of sediment considered.

2.4 Impact of Volcanic Deposits on Coral Reefs

When discussing the influence of sediment on coral reefs surrounding volcanic islands it is important to also consider that of volcanic deposits. Volcanic deposits may enter the water column through numerous pathways such as pyroclastic density currents, lahars or direct ashfalls (Alexander *et al.,* 2010; Barclay *et al.,* 2007; Lokier, 2021). These volcanic deposits may settle on and compact coral reefs, whilst also influencing corals and water quality in similar ways to terrestrial sediment and nutrients. Fine-grained volcanic ash can affect light attenuation and may alter water quality through variations in alkalinity and the concentration of various ions (Reuter and Piller, 2011) indirectly effecting coral reefs. Sediment may also contain heavy metals and/or be high in nutrients which would then enter the water column upon deposition.

In terms of the composition of sediment, many studies (Reuter and Piller, 2011; Vroom and Zgliczynski, 2011) acknowledge the struggle imposed on coral reef flora and fauna when volcanic deposits enter the water column, with Vroom and Zgliczynski (2011) finding that many fish species became non-existent when subjected to volcanic ash deposits. Along with the reduction in light attenuation by fine-grained volcanic ash, Reuter and Piller (2011) discuss how tissue necrosis and other physiological stresses are amongst the range of consequences to corals when they are even only partially covered by volcaniclastics. These studies contribute to the literature by providing insight into the specific threats facing coral reefs surrounding volcanic islands through the sediment they study, whilst other literature discussed is more general in terms of the coral reef locations. Evidence from the geological record (Lokier, 2021) also indicate many cases of coral reef mortality following inundation by volcanic sediments. However, quantifying the impact of volcanic deposits on coral reefs specific to Montserrat remains challenging due to a lack of research, data and surveying prior to volcanic events.

2.5 Sediment on Montserrat

The last in-depth, comprehensive soil analysis done on Montserrat was a land-use survey completed by Lang in 1967, following previous soil mapping by Hardy and Rodrigues in 1949. Lang (1967) classifies soils into four main groups: protosols, young soils, latosolics and smectoid clays. These were further subdivided based on location, weathering and slope. Hardy and Rodrigues split Montserrat into 7 general soil types: lithosols, alluvial-colluvial soils, brown earth soil, rendzina soil, yellow earth soil, terras soil and shoal soil. Since these, there have been fewer comprehensive studies considering the soils of Montserrat. One study is that concerning the weathering on Montserrat by Jones *et al*. (2010) who state that Andisols are the predominant

soil type in Montserrat, similar to other islands in the Lesser Antilles. They describe the soil as coarse with soil aquifers in the island's centre due to the high infiltration rates. Despite the lack of extensive soil mapping in recent years, other literature (Feller *et al*., 2006; Ranatunga *et al*., 2009) agree andisols are the dominant soil type of Montserrat due to the andesitic composition of Soufrière Hills volcano.

The presence of andisols implies volcanic deposits are a large contributing source of sediment in many areas of Montserrat. Jones *et al*. (2010) discuss how, from the onset of the eruption of Soufrière Hills volcano in 1995 up to 2010, the amount of volcanic material erupted from the volcano was equal to approximately 1km^3. Other literature discuss the presence of sediment derived from volcanic deposits also. For example, Edmonds *et al*. (2006) describe how the volcanic activity in 2003 caused the deposition of various tephra deposits, stating that approximately 90% of the island was covered. These deposits can be evidenced on Montserrat in the exclusion zone, where there are deposits of ash seen atop buildings and other structures (Figure 3). Figure 3 represents the layers of deposits built up and compressed over time from numerous volcanic eruptions.

Figure 3: A photograph showing layers of sediment and ash deposited on top of a building's roof in Montserrat. Photography credited to Professor John Quinton.

Another source of sediment within and downstream of ghauts may be the ghauts themselves (Figure 1). When completing the soil mapping in 1949, Hardy and Rodrigues acknowledged that it was likely that “deepening, widening and backward cutting” of the ghauts was occurring, with evidence of wall collapse in newer ghauts at the time. Hautmann *et al*. (2013) used Bouguer gravity data to investigate the structures of Montserrat and theorised that some of the larger ghauts may have been formed due to the structural discontinuity between high-density andesitic lava and flank deposits (of lower density). This would have caused increased erosion, carving out the ghauts and potentially continuing today during flood events (Alexander *et al.,* 2010; Barclay *et al.,* 2007) due to structural instability.

2.6 Transfer Routes: Terrestrial to Marine Environments

The input of sediment and volcanic deposits to marine environments has potentially devastating consequences for coral reef populations. Therefore, it is important to know where this sediment is coming from and how it is transported to these environments. This presents a challenge as there are multiple pathways through which sediment can be transported before it is deposited (Figure 1). On volcanic islands experiencing ongoing eruptions, the sediment load to marine environments may be vast. For example, Jones *et al*. (2010) predict that approximately 75-90% of volcanic material erupted from Soufrière Hills Volcano between 1995 and 2010 was deposited in the oceans after moving across the terrestrial environment. Similar results have been seen across the islands of the Lesser Antilles as Cassidy *et al*. (2014) stated that around 84% of volcanic material erupted from the islands in the last 100ka has been transferred to marine basins.

The identification of transfer routes is becoming increasingly important due to heightened soil erosion brought about by a more intense hydrological cycle and evidence that increased precipitation encourages soil erosion at faster rates (García-Ruiz *et al.,* 2015; Nearing *et al*., 2004). Sediment can be transferred between environments in a number of ways, including by wind, water and anthropogenic activity. For example, land management practices can displace soil, encouraging erosion and the ease of movement across landscapes. Movement of sediment has been heightened due to both land-use changes and the increased frequency and ferocity of storms via global warming, presenting a large threat to islands of the Lesser Antilles specifically during the wet season of July-November (Biguenet *et al*., 2021; Chalaux-Clergue *et al*., 2024). Identifying sources of erosion and their transfer routes is essential due to its linkages to pollutant transfer, sediment build up in water columns, degradation of soil health and stability and negative impacts on water ecosystems (Chalaux-Clergue *et al*., 2024). Not only this but Walling

(2013) state that fine sediment is a key vector in particle transfers from terrestrial to marine environments. This includes heavy metal pollutants as the sediment acts as a substrate to which they can adsorb. It is worth noting that in many studies involving sediment transfer, an integrated approach is not often taken. Álvarez-Romero *et al*. (2011) discuss how, especially in the conservation of marine protected areas, terrestrial and marine environments are often considered separately as opposed to broadly connected ecosystems with linkages impacting the functioning of both.

The topography of the island of Montserrat aids the ease of transfer due to the presence of ghauts. These ephemeral waterways transport sediment from the ghauts and deposit it at sea. Therefore, the transfer of sediment from terrestrial to marine environments is dependent on the drainage and transport loads of waterways, influenced by rainfall. Reid and Laronne (1995) investigated the differences in sediment transport across ephemeral, seasonal and perennial streams. It was found that the ephemeral stream had a significantly greater bed load transport efficiency than all other seasonal and perennial streams included in the study. Reid and Laronne (1995) concluded that this was because the ephemeral beds were not armoured, so transport of sediment is higher and more reflective of flow rates. The ghauts in Montserrat that this study surrounds are also ephemeral valleys and therefore there is potential for large amounts of sediment transfer to the sea via ghauts (Alexander *et al.,* 2010).

2.7 Sediment Fingerprinting

As previously discussed, sediment fingerprinting is a source apportionment method used to identify the potential sources of material, their relative contributions and potential transfer routes to secondary locations by the use of tracers. In order to do this, the relevant tracer type of choice is measured through field or laboratory experiments and the data is compiled and undergoes a series of statistical tests. It is generally agreed in modern research that the selection of fingerprints is a multistep process (Mukundan *et al*., 2010). The first step in sediment fingerprinting involves a series of statistical tests on the individual tracers. The non-conservative tracers can also be removed from further testing. Discriminant analyses are used to identify each tracer's ability to individually identify sources (Mukundan *et al*., 2010). Often studies then decide whether tracers are redundant and choose to keep only those tracers in which the majority of variation within the dataset can be explained. This is referred to as multiple discriminant function analysis (DFA). Principal component analysis and cluster analyses may also be used as a visual means of confirming clear discrimination is achieved (Walling, 2013). Studies choosing to also

investigate each sources relative contributions to the secondary location may then use mixing models to achieve this.

Sediment fingerprinting studies are wide and diverse. One example of sediment fingerprinting in fluvial applications is that of García-Comendador *et al*. (2017) who applied sediment fingerprinting to layers of accumulated sediment after wildfire events. They used sediment fingerprinting to discuss how sediment, ash and other particles introduced to a landscape after a wildfire can be transported across the landscape via streams during a storm event.

Many sediment fingerprinting studies have taken place on agricultural land. For example, Lamba *et al.,* (2015) used sediment fingerprinting for source apportionment in the USA and found that 45-97% of suspended sediment in the watershed was from agricultural sources. A similar study by Stewart *et al.* (2014) saw similar trends with agricultural sources of sediment being the dominant contributor at 53%. Both studies used geochemical elements as their sediment tracers. Soil erosion is a large concern for agricultural land, but sediment fingerprinting has also been suggested as a potential management tool. The degradation of crop-bearing soil health, reduced soil stability and loss of essential nutrients threatens the agriculture industry as well as runoff from fertilisers causing widespread aquatic issues in terms of eutrophication and pollution. As a result, sediment fingerprinting has been applied as a management tool to regulate sediment budgets and daily loads (Mukundan *et al.*, 2012).

As indicated, sediment fingerprinting is a developed tool with successful applications in a number of areas. Therefore, it has the potential to act as a powerful tool in understanding the sources of sediment on Montserrat and how those might impact the coral reefs surrounding the island. The tracers used for this would be the imperative part of the procedure, to maximise the possibility of sediment fingerprinting being effective. The ways in which tracers and differences between sources and target locations are uncovered differ in each sediment fingerprinting application. One novel way to potentially fulfil this is through the use of thermogravimetric analyses coupled with mass spectrometry, a method yet to be applied to sediment fingerprinting.

2.8 Thermogravimetric Analyses

Thermogravimetric analyses (TGA) is a technique used to quantify the weight loss of samples that is associated with thermal decomposition when subjected to heating in a controlled environment (Saadatkhah *et al*., 2019; Xu *et al.,* 2005). During thermogravimetric analyses, a small sample is placed in a crucible on a balance. The weight of the sample is then recorded over

time in comparison to a reference crucible. These crucibles remain inside a furnace where the temperature is raised incrementally according to the temperature regime chosen. The temperature is recorded alongside the weight using a thermocouple. From this, accurate weight, time, temperature and heat flow data are recorded. Finding the derivative weight (DTG) allows the identification of the rate of mass loss, to identify how much mass is lost at different temperature peaks (Martí-Rosselló *et al.,* 2018). Mass will decrease as decomposition and evaporation occurs, allowing the interpretation of chemical properties of the sample (Bish and Duffy, 1990; Földvári, 2011). Coupling TGA with mass spectrometry (TGA-MS) is an advanced technique giving the ability to identify the gases released over time as mass decreases and temperature increases (David *et al.,* 2018). As a result, complex analysis of samples can be achieved. When connected to a mass spectrometer, capillary tubes are connected so the gases released during the experiment are transported to a mass spectrometer where the gases are identified in real time. As a result, the components of the sample being heated at various temperature peaks can be identified through peaks in mass spectrometer readings (Applegarth *et al.,* 2013). An example thermogram is shown in Figure 4.

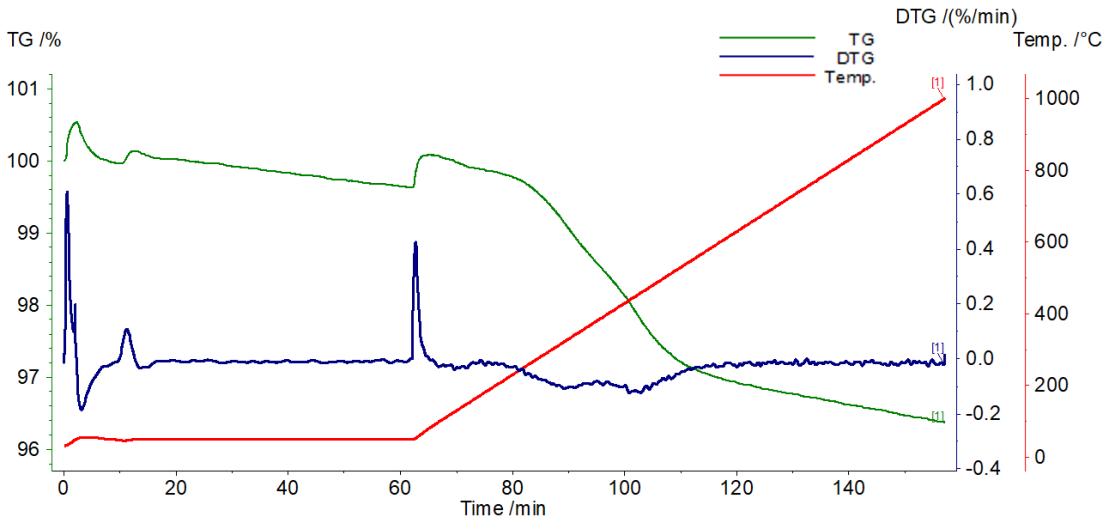

Figure 4: An example thermogram of the LB1 sample (Chapter 3). Curves representing the TG (%), DTG (%/min) and temperature (°C) are shown with the time (minutes) of the test on the x-axis. The procedure followed that described in Section 4.4.4.

Chauhan *et al.* (2020) describes the benefits of using TGA for soil samples, namely the detailed analysis of both organic and inorganic fractions of soil and their respective reaction mechanisms whilst being accurate and repeatable. Components of soil that can be identified using TGA include organic carbon, inorganic carbon and mineralogical fractions such as various clays. For example, Lebron *et al.* (2023) investigated the effectiveness of using TGA to differentiate the

various pools of organic carbon, finding it a suitable method for monitoring soil carbon long-term. TGA has also been applied to soil samples to identify carbon stocks in terms of cycling (Yanardağ *et al.,* 2014). Whilst the applications of TGA (and specifically TGA-MS) on soil chemistry have been less extensive than other more common practices, there have been various studies on the use of TGA for soil microplastics analysis. Dümichen *et al*. (2017) used TGA coupled with GC-MS (gas chromatography mass spectrometry) to measure masses of polypropylene and polyethylene released during decomposition with positive results. In 2018, a similar study was conducted by David *et al*. whereby TGA-MS was used for microplastic detection and demonstrated very low limits of detection and quantification, suggesting it is a suitable method to use alongside existing methods for soil analysis.

Zethof *et al.* (2019) attempted to use TGA to differentiate graphite in soil from other carbon sources. However, in this study, overlapping mass losses meant identification using this technique alone was challenging, thus suggesting the need for coupling with additional techniques such as mass spectrometry. Although not applied for sediment fingerprinting, a similar idea was used in terms of using TGA to differentiate sources, as is done in sediment fingerprinting.

To date, TGA-MS has not been used as a sediment fingerprinting tool. Standalone, TGA has been used in some source apportionment studies (Chauhan *et al.,* 2020; Jaramillo *et al.,* 2022). For example, Chauhan *et al.* (2020) used TGA in combination with chemometric methods in a linear discrimination function model to assign unknown soil samples into groups based on locations. Additionally, Jaramillo *et al.* (2022) used TGA as a way of distinguishing the sources of respirable coal mine dust. This is a significant hazard in terms of both health and explosivity of mines. They used TGA for source apportionment on dust samples by determining the levels of the three main components: coal, carbonates and non-carbonates, each of which show different TGA curves. Jaramillo *et al.* (2022) were able to use this information to successfully determine the sources of the dust samples, demonstrating the successful application of TGA to source apportionment studies.

When investigating sediments using TGA, few studies have highlighted the importance of considering the preparation and grain sizes of the samples tested. A recent study by Zentar *et al.* (2023) investigated the influence of various drying methods on test results, including TGA, of marine sediments. They found percentage mass loss varied for marine sediment based on air, oven and freeze-drying, highlighting the need for consistent preparation across samples prior to TGA analyses. The grain size has been shown to impact oxidation rates, combustion rates and

percentage mass loss. For example, Kaplin and Brochu (2014) investigated the variation in TGA results between conventional and cryomilled samples of NiCoCrAlY. They found that oxidation rates were lower for cryomilled samples but the difference between them is less significant at higher temperatures. Farivar *et al.* (2021) also studied the significance of grain size on TGA and Derivative Thermogravimetry (DTG) results. The influence of grain size on DTG was more pronounced in this study. They found that peaks of water and oxygen loss did not vary significantly with size, however combustion of carbon did (Farivar *et al.*, 2021). It was shown that the temperature peak for carbon combustion increased as particle size increased, and this occurred for all material types tested due to the higher surface area of smaller particles, increasing their reactivity. Therefore, slower combustion kinetics in larger grains are responsible for the higher peak temperatures of carbon combustion (Farivar *et al.*, 2021). These studies demonstrate how grain size can have various influences on TGA and DTG results depending on the reaction processes focused on. Therefore, it is important when conducting thermogravimetric analyses to consider sample grain size so as to not misinterpret results.

2.9 ICP-OES

Inductively coupled plasma-optical emission spectroscopy (ICP-OES) is an analytical technique used to discover the presence and abundance of up to 70 elements in a sample (Khan *et al*., 2021). Hou *et al*. (2006) describe how in this technique, liquid or gas samples can be used directly, where the sample is injected into the ICP-OES radiofrequency-induced argon plasma and converted to an aerosol, where it is vaporized by the 10000K temperature sustained. Solid materials (such as sediment) may also be used but must undergo acid digestion in order to form a solution which can be injected. The radiofrequency discharge causes the excitation of atoms/ions and results in the spontaneous emission of photons (Khan *et al*., 2021). Different wavelengths of emission correspond to different elements and thus the abundance of elements can be determined.

ICP-OES has had successful applications into a variety of industries and branches of research. Some of these include pharmaceuticals (Pinheiro *et al.,* 2021), forensics, textiles (Rezić and Steffan, 2007), agriculture, food analysis, geological and environmental studies. For example, in 2007, Rezić and Steffan conducted a study using ICP-OES for textiles. They used ICP-OES to determine the metal content of textiles such as polyester, wool and cotton as metals can pose consumer health hazards and issues with production. Using ICP-OES they were able to successfully determine whether materials were following industry standards.

Recently ICP-OES has been the focus of a study by Sim *et al*. (2024) for agricultural and geographical tracing purposes. In the food and agriculture industries, quality control is essential, just as it is in pharmaceuticals. An element of this involves tracing the geographical origin of produce. Sim *et al.* (2024) conducted a study showing how ICP-OES could be used to do this with onions from China and Korea. The ICP-OES results of 60 elements meant that the determination of the country of origin was accurate 100% of the time (study sample size of 52).

Soil/sediment is one material which has been studied using ICP-OES extensively. Table 3 shows a selection of studies conducted within the past two decades surrounding the use of ICP-OES on soil and sediment samples. For example, Shaheen *et al.* (2022) conducted a study on agricultural soils in Egypt, applying the ICP-OES technique in order to quantify the presence of heavy metals in the soil and assess whether toxic levels had accumulated. They were also able to use this to successfully identify different sources of pollution using cluster analysis. Similarly, Ling *et al.* (2023) used ICP-OES as a way to quantify the presence of heavy metals in coastal sediments in Malaysia. Whilst heavy metals are indicators of pollution, as presented by Shaheen *et al.* (2022), they are also indicators of mineralogy. Ling *et al*. (2023) were able to show how different minerals have varying adsorption properties which in turn influences the concentrations of heavy metals found in the sediment through ICP-OES. Many other sediment-focused studies use ICP-OES in similar ways with promising results (Habineza *et al*., 2023; Olutona, 2023). It has proven popular in soil and sediment studies due to its high accuracy and sensitivity, fast operating time and multiple-element analysis capability.

Furthermore, ICP-OES has also been applied to coral reef studies. For example, Cantarero *et al.* (2016) used ICP-OES to simultaneously investigate the ratios of Sr, Ca and Ba in Scleractinian corals and demonstrated a comparable accuracy and precision to the pre-established ICP-MS technique commonly used.

Table 3: Studies surrounding the use of ICP-OES for various applications in soil/sediment studies. The table includes the broad application area and a list of some of the elements which were analysed using ICP-OES. Those listed with a ** are studies where ICP-OES has been used for sediment fingerprinting purposes.

Author(s)	Date	Application Area	Elements Studied
Giancoli Barreto *et al*.	2004	Identifying potentially available metals in lake sediment.	Included Mg, Al, Cr, Mn, Fe, Co, Ni, Cu, Zn, Cd and Pb.
Lunderberg *et al.*	2008	Trace metal analysis of freshwater lake sediment in Michigan, US.	Included Al, Cd, Co, Cr, Cu, Fe, Mn, Ni, Pb, V and Zn.
Silva *et al.*	2011	Assessing major and trace elements in sediment from the Itupararanga reservoir.	Included Cd, Cr, Cu, Pb and Ni.
** Blake *et al.*	2012	Tracing sediment sources in agricultural catchments in comparison to geochemical fingerprinting.	Al, As, Ba, Ca, Cr, Cu, Fe, K, La, Mg, Mn, Ni, Pb, Sr, Ti, V, Y and Zn.
** Ajaj *et al.*	2018	Sediment Fingerprinting on soils across the United Arab Emirates.	22 elements including Al, Ca, Cd, Cu, Fe, Na, P and Zn.
** Habibi *et al.*	2019	Sediment Fingerprinting reservoir sediments.	53 elements – 4 were used as tracers (Cr, Th, Bi, Pr).
Shaheen *et al.*	2022	Quantifying heavy metal concentrations in agricultural soils in Egypt.	12 including Mg, Cr, Mn, Fe, Co, Ni, Zr and Pb.
** Fatahi *et al.*	2022	Sediment Fingerprinting fine-grained river sediment in Iran.	43 elements including Al, Cu, Cr, Cs, Mg, Mn, Na, Ni, Zn, Pb and Ca.
** Cabral Nascimneto *et al.*	2022	Sediment Fingerprinting ephemeral streams in a Brazilian river basin.	22 elements including Al, Co, Cr, Fe, Mn, Ni, Pb, Sc, Th, V and Zr.
Ling *et al.*	2023	Quantifying the presence of heavy metals in coastal sediment in Malaysia.	Major and heavy metal elements including Ca, Fe, Mg, Ni, Cr, Zn, Pb and Co.

The application of ICP-OES for sediment fingerprinting purposes has been successful in previous studies, as demonstrated by the indicated studies in Table 3. For example, Habibi *et al*. (2019) used ICP-OES to analyse 53 elements in reservoir sediments and identify four (Cr, Th, Bi and Pr) as geochemical tracers which explained 96% of the variations between study sites and sources. Ajaj *et al*. (2018) also used ICP-OES in sediment fingerprinting in soils across the United Arab Emirates. They studied 22 elements, building fingerprints for each, aiding the determination of whether these metals were found in soils at permissible levels in various regions. Finally, more recently, Fatahi *et al*. (2022) used ICP-OES for sediment fingerprinting, identifying 33 conservative and 11 non-conservative tracers. For the purpose of their study on fine-grained river sediment in Iran, under different statistical tests, at least 12 of these tracers identified using ICP-OES came back as significant when used for sediment fingerprinting.

Despite the wide array of ICP-OES applications, it has not appeared to have been used extensively on Montserrat. Zellmer *et al*. (2003) investigated the geochemistry of the island, with similar techniques of using ICP-MS and trace elements. This proved helpful in inferring the petrological processes of Montserrat. However, this study focussed on volcanic deposits and processes rather than sediment and its transfer across the island into marine environments.

2.10 Conclusions

After reviewing the current literature, it is clear there is a large gap in research focusing on Montserratian soils within the last half century. There is a serious lack in knowledge of sediment sources to the coral reefs surrounding the islands, along with the ways in which it is being transferred across environments, with a substantial research gap of the application of sediment fingerprinting, not only on Montserrat, but in the wider Lesser Antilles Arc. Additionally, the type and composition of soil on Montserrat has not been studied in recent times, with the extent to which the ongoing Soufrière Hills eruption has impacted the composition unknown. ICP-OES is yet to be applied to sediment from this region to better understand sediment chemistry – another research area lacking focus.

Furthermore, this study will be the first to apply thermogravimetric analysis coupled with mass spectrometry to sediment fingerprinting. More generally, this study contributes to our knowledge to pollution mapping, threats to coral reefs on the island of Montserrat, which are relevant to both land management and agriculture.

Chapter 3: Field Sampling

The samples used in this study were collected as part of a previous project (Stevens *et al.,* 2023) concerning the mapping of Montserratian soils. Field sampling was undertaken by scientists from Lancaster University. The aim of this chapter is to give a brief overview of the fieldwork undertaken by these scientists to acknowledge how and where the samples used in this study were collected, relevant especially for Chapter 6 where the locations of the samples were used in the interpretations of the sediment fingerprinting results.

Two types of samples were collected and used for this project: sediment samples from ghauts and coral reefs. The following sections describe the sampling methods and locations.

3.1 Ghauts

A total of 200 sediment samples were collected from 40 ghauts in the north-west region of Montserrat (Figures 5 & 6) from the 29th of January to the 3rd of February 2023. The ghauts sampled are grouped into four regions: Little Bay and Carrs Bay (LB) (Figure 6a), Cudjoehead, Olveston and Woodlands (COW) (Figure 6b), sites in and around the Belham River (BP) (Figure 6c) and Plymouth (EX) (Figure 6d). Nine LB ghauts were sampled, 17 COW, 13 BP and one EX.

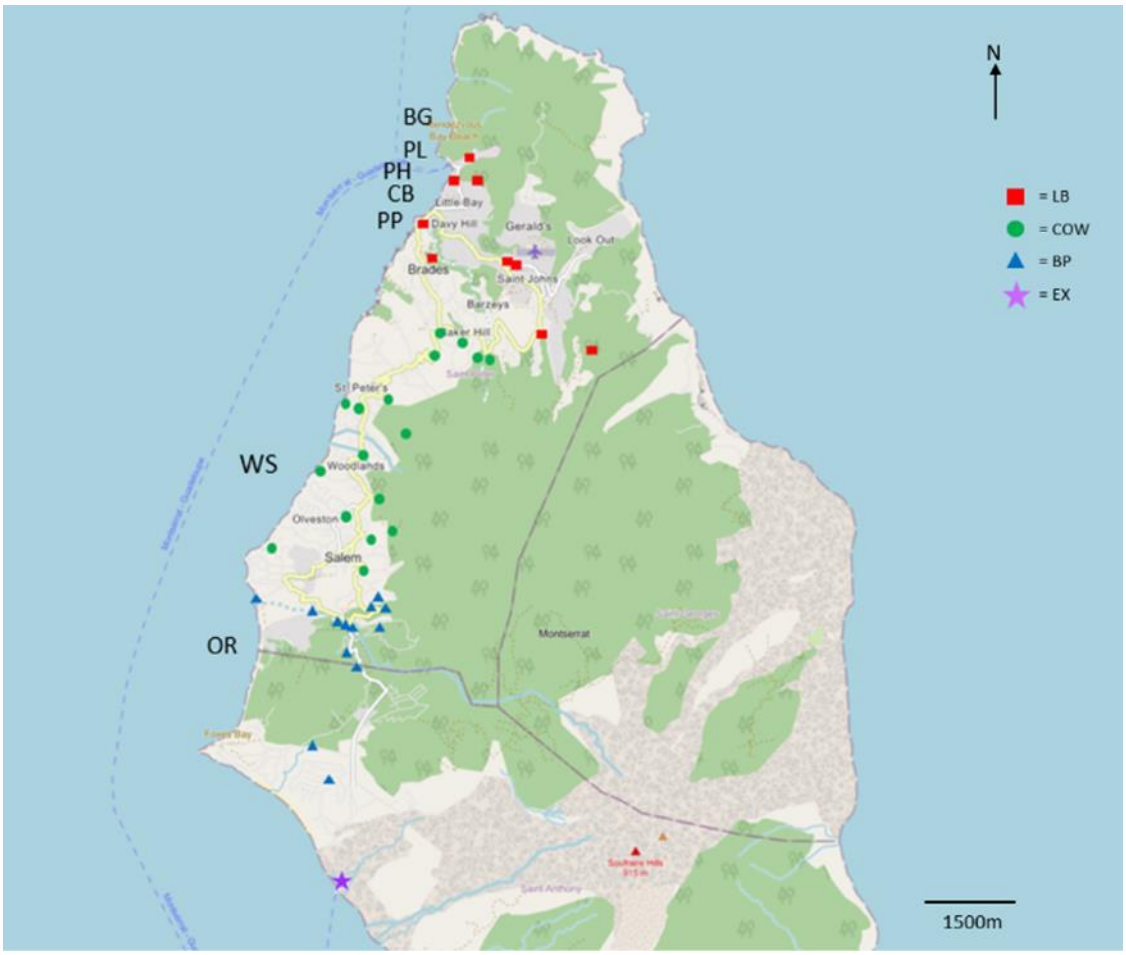

Figure 5: A map of Montserrat showing both ghaut and reef sample sites. The ghauts are represented by square, circle, triangle and star symbols based on the sample name and location. The reef samples are indicated by their respective initials (BG = Bantin Ghaut, PL = Port Little Bay, PH = Potato Hill, CB = Carr's Bay, PP = Piper's Pond, WS = Woodlands South, OR = Old Road Bay). Base map from ArcGIs Pro.

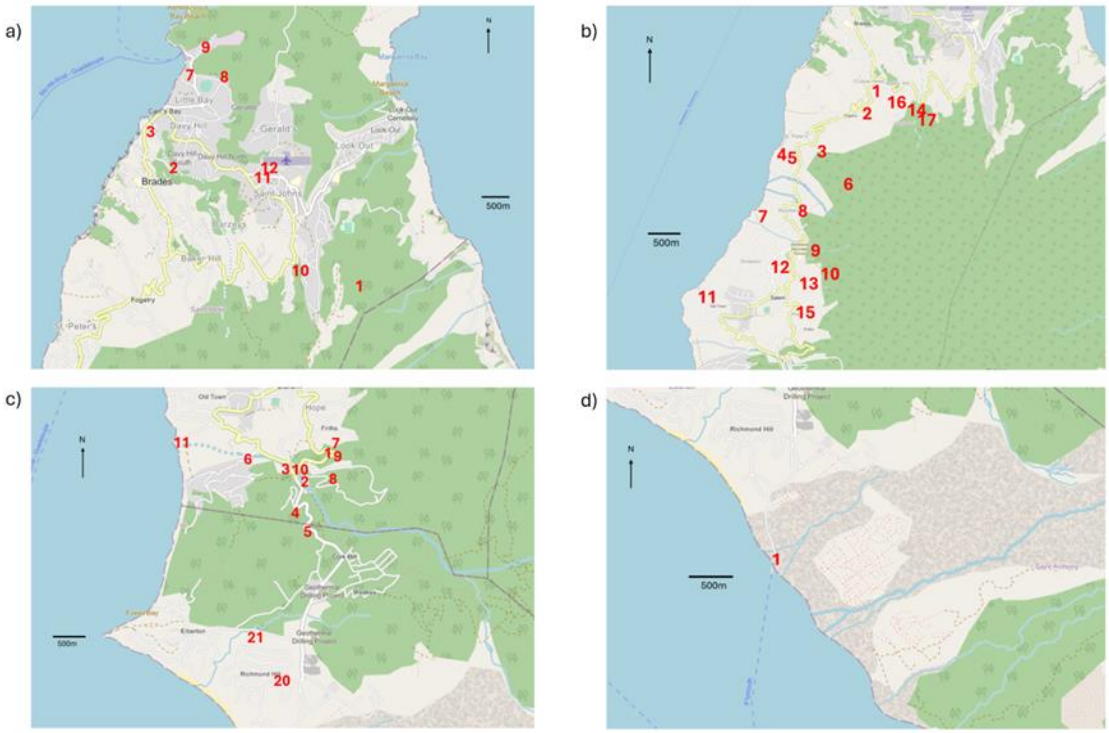

Figure 6: Maps of the ghaut sample locations from each of the 4 groupings: a) = LB locations, b) = COW locations, c) = BP locations and d) = EX location. Base maps from ArcGIs Pro.

Within each ghaut, five replicate samples were collected along a 20m transect starting from the midpoint of the ghaut and collected every 5m. Each of the five replicate samples was composed of four samples in an 'X' shape within 1m^2 of the sampling point and bulked. Each of the 200 samples consisted of approximately 150g of material with diameters <1cm. The texture of the material varied across ghauts, displaying sand, silt, gravel and mud-like textures. Some samples also showed signs of biological material (humus), whilst many marine samples also clearly contained shell and coral fragments.

3.2 Marine

Seven sediment samples were also collected by divers in early February 2023 from the coral reefs along the north-west coast of Montserrat (Figure 5). These sampling sites will henceforth be referred to as Old Road Bay (OR), Potato Hill (PH), Bantin Ghaut (BG), Woodlands South (WS), Piper's Pond (PP), Port Little Bay (PL) and Carr's Bay (CB). These samples were also bagged, labelled and brought back to Lancaster University for laboratory analysis.

Chapter 4: Development of the TGA Methodology

4.1 Introduction

One of the main aims and objectives of the project was to apply the use of TGA-MS to sediment fingerprinting. The development of the methodology was key, with preliminary testing undertaken to achieve a concise, uniform method. The focus on this methodology was essential as TGA has not been applied to sediment fingerprinting previously. This chapter outlines that preliminary testing, with descriptions of the results and implications drawn from them and a justification of the final methodology used and applied in further chapters.

4.2 Methods

On arrival at Lancaster University, the samples were oven dried at 105°C overnight and weighed prior to any laboratory experiments taking place.

4.2.1 TGA

For TGA analysis, tests were conducted on a TA SDT Q600 instrument (Figure 7), calibrated routinely through use of known samples to ensure accuracy was maintained. Around 40-75mg of each sample were used in alumina (Al_2O_3) crucibles (Figure 8) to identify mass loss up to 1000°C. All TGA tests experienced heating from room temperature to 1000°C at 10°C per minute in an oxidising atmosphere with air flow rate of 50mL/min.

Initially, pilot TGA testing was completed using the bulk dried sample. However, due to the variety of sizes of grains and the narrow diameter of the crucibles (6mm; Figure 8), representativeness was questioned with bias towards particles of smaller grain sizes. To combat this, grain size experimentation was conducted using the WS marine sample (Figure 5) to explore the potential variation in TGA and/or DTG results with grain size. The WS sample was sieved and split into 4 different grain size fractions: <125µm, 125-250µm, 250-500µm and 500-1000µm. TGA analysis was conducted on these using the same procedure described above. Data were processed and analysed on TA Universal Analysis 2000 software. The TGA and DTG results are shown in Figure 10 and 11 respectively.

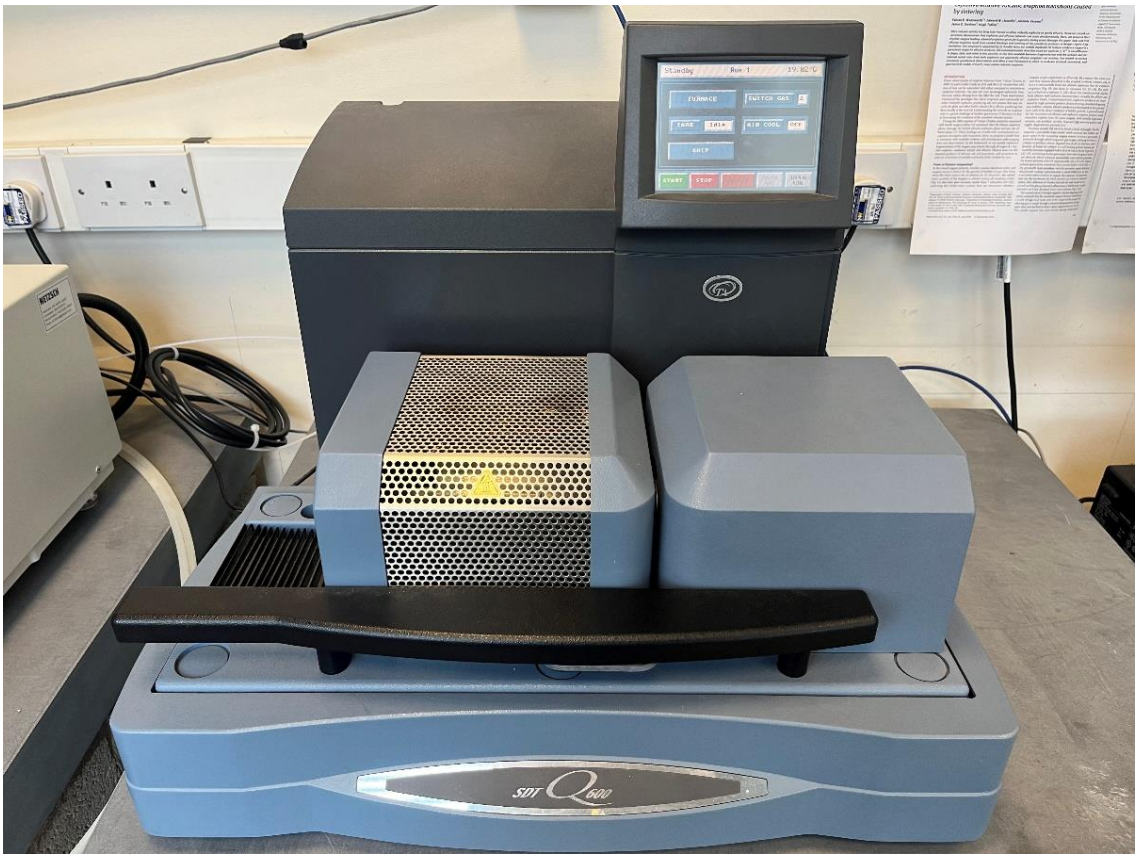

Figure 7: The SDT Q600 TGA used for thermogravimetric analysis.

Figure 8: An alumina crucible containing a small amount of the BP3 ghaut sample (Figure 6c).

After testing on grain sizes, pre-treatment on ghaut samples was undertaken. The five replicate samples of each ghaut were bulked together to obtain one sample per ghaut due to time and cost considerations. This involved weighing 3±0.1g of each replicate sample and bulking, sieving through 2mm and shaking for 1 hour at 200rpm on a KS 501 digital orbital shaker to ensure samples were well mixed. All ghaut and coral reef samples were then ball milled at 30Hz for one minute on a Retsch MM 400 ball mill to homogenise the samples (grain sizes <250µm), reduce variability between samples and accommodate the small masses required for analysis.

4.2.2 TGA-MS

To complete TGA-MS analysis of H_2O and CO_2, a Netzsch STA449C Jupiter TGA with a Hiden HPR20 mass spectrometer attached were used (Figure 9), calibrated routinely to maintain accuracy. Mass spectrometry data was collected for H_2O and CO_2 exsolved gases due to their recurrent nature as the main products when completing thermal degradation experiments on soils in oxidising atmospheres (Fernández *et al.,* 2012; Plante *et al.,* 2009).

In the TGA-MS experiments the heating rate mirrored that of TGA tests at 10°C per minute to 1000°C in an oxidising atmosphere (air flow rate of 50mL/min), however, equilibration at 30°C was added before heating took place rather than starting from room temperature.

Figure 9: Images of the Netzsch STA449C Jupiter TGA (left) and the Hiden HPR20 mass spectrometer (right) used for TGA-MS analysis.

Initial pilot testing was conducted with calcium oxalate (Figure 14) to ensure the instruments were calibrated accurately, followed by the Woodlands South ball milled sample. During this test an isothermal stage was added at 50°C for one hour to achieve stable mass spectrometer readings. Following this, the Bantin Ghaut (BG) ball milled reef sediment sample was tested with the one-hour isothermal at 50°C but also included an initial evacuation and refill. Evacuating and refilling the vacuum with O_2-free N_2 reduced blanks of CO_2 and H_2O that derived from air, and these were further decreased by addition of a 60-minute isothermal at 50°C (Figure 15). The tests were conducted in an oxidising atmosphere (air) with a flow rate of 50mL/min. A protective N_2 purge gas was used to protect the balance assembly, with a flow rate of 20mL/min.

Testing was conducted for all 40 ghaut samples and 7 marine samples on both the TA SDT Q600 and the Netzsch STA449C Jupiter TGA with a Hiden HPR20 mass spectrometer. A number of samples were tested multiple times on both instruments also to ensure repeatability and accuracy of the instruments and methods, with peak positions and mass losses highly repeatable.

4.2.3 Data Processing

Data was processed and analysed using Microsoft Excel, Netzsch Proteus Thermal Analysis software version 8.0.1, Hiden Analytical Version 5 and MATLAB R2020a. Calculations of percentage weight loss in varying temperature ranges (Chapter 5) were made in the Proteus software, along with the areas under the peaks to obtain values for the percentage weight loss within those peak temperatures. TGA and mass spectrometry data were combined and time corrections made where appropriate.

4.3 Results

4.3.1 TGA

The results of the grain size experiments are described in Figure 10 and 11. The TGA data demonstrates the weight loss as temperatures increased, whilst DTG describes the rate of weight loss as temperatures increase. The area under the DTG peaks represents the percentage of weight loss in that temperature range. This was calculated for all grain sizes for the temperature ranges 590-800°C and 800-1000°C, where peaks were present. This is described in Figure 12.

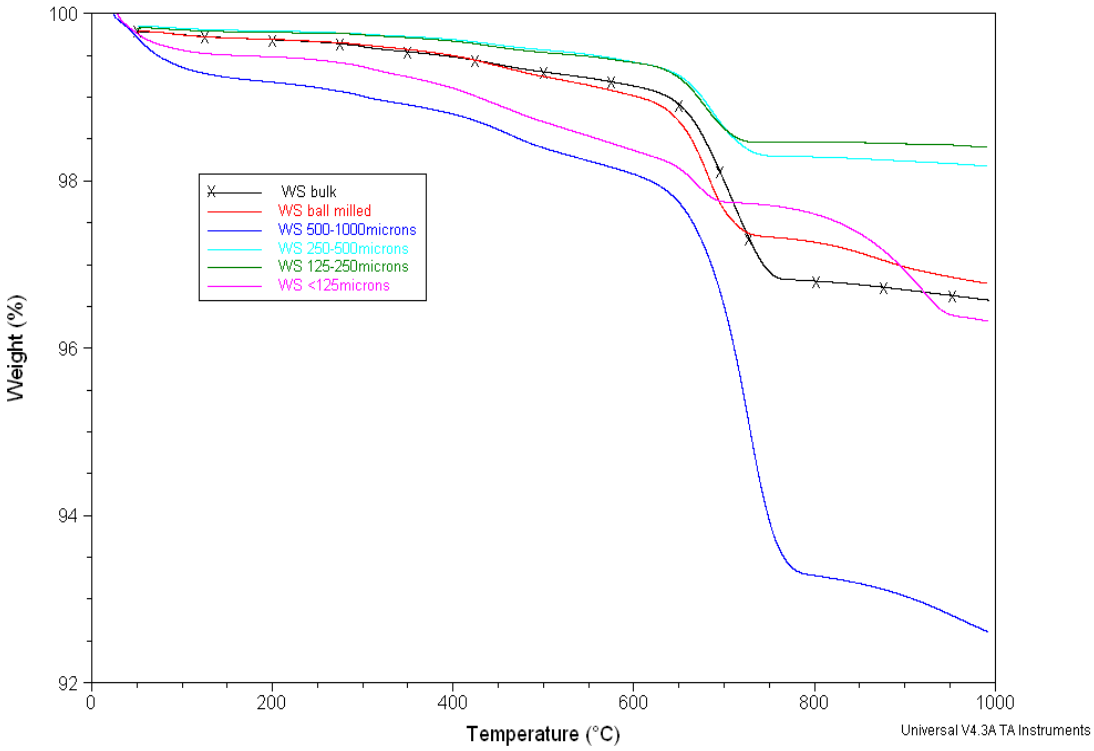

Figure 10: An overlay of the thermogravimetric data (TGA) for different grain sizes of the Woodlands South reef sediment sample, demonstrating the mass loss over the course of the experiment. Fractions include: 500-1000µm, 250-500µm, 125-250µm, <125µm. The overlay also includes the results for the bulk WS sample and a ball milled WS sample. All tests followed the same temperature regime of 10°C increases per minute to 1000°C. The higher mass loss on the 500-1000µm curve is noted due to the distinct composition of coarser-grained carbonate clasts.

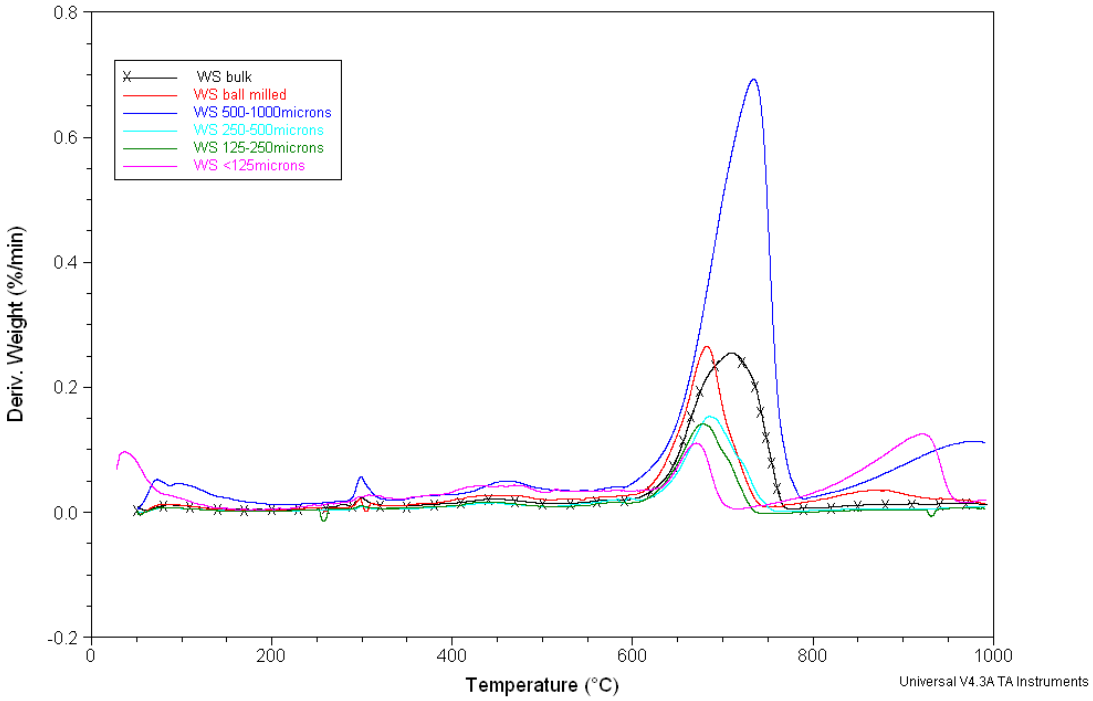

Figure 11: Derivative weight signals (DTG) for different grain fractions of the Woodlands South reef sediment sample. Fractions include: 500-1000µm, 250-500µm, 125-250µm, <125µm. The overlay also includes the results for the bulk WS sample and a ball milled WS sample. All tests followed the same temperature regime of 10°C increases per minute to 1000°C.

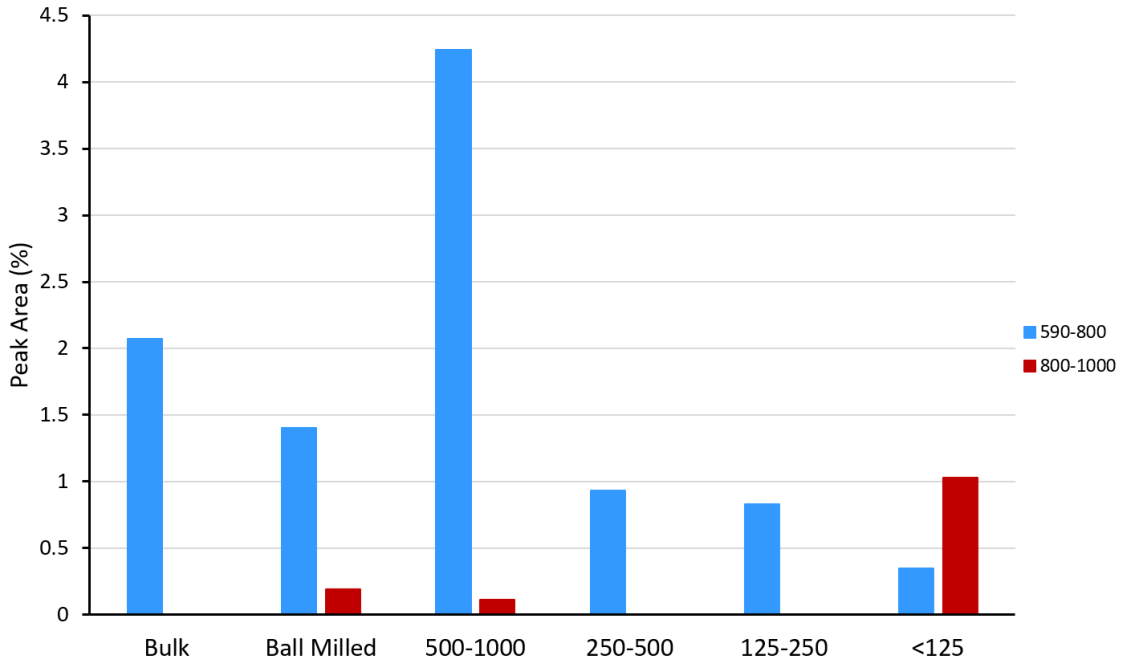

Figure 12: The area under the DTG peaks (Figure 11) of the different grain fractions of the Woodlands South reef sediment sample. Fractions include: 500-1000µm, 250-500µm, 125-250µm, <125µm. The overlay also includes the results for the bulk WS sample and a ball milled WS sample. All tests followed the same temperature regime of 10°C increases per minute to 1000°C. Values are given for peaks within the 590-800°C temperature range and the 800-1000°C temperature range (where peaks were present). Higher weight loss for the 500-1000µm is evident due to the abundance of carbonates in this range, reflecting that of Figure 10.

Differential Scanning Calorimetry data (DSC) is also collected during TGA experiments. This represents the heat flow over time and gives evidence of exothermic and endothermic reactions occurring during the analysis. These reactions may be in association with thermal breakdowns of the soil components such as the release of soil organic matter or clay minerals. DSC example results for the BG marine sample are presented in Figure 13.

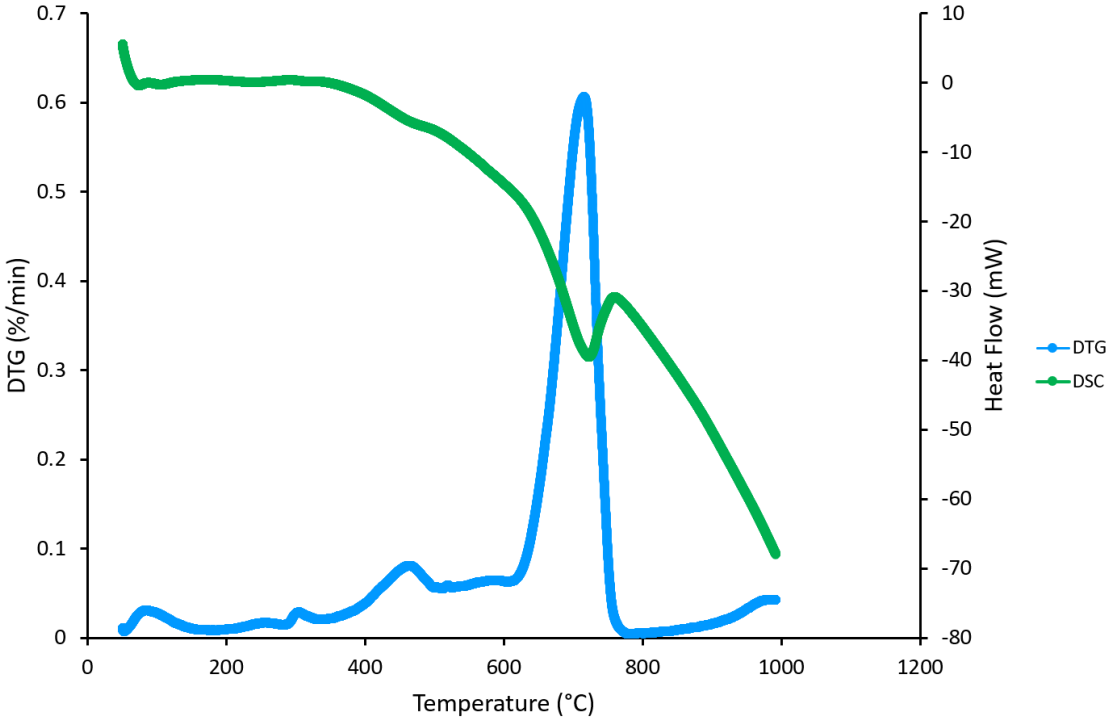

Figure 13: The derivative thermogravimetry (DTG) and heat flow (DSC) data for the Bantin Ghaut marine sample. The sample was ball milled prior to analysis. The heat flow represents the exothermic and endothermic reactions, with exothermic up. The prominent endothermic peak at ~730°C corresponds with the maximum rate of mass loss in a thermal decomposition reaction.

4.3.2 TGA-MS

The DTG, H_2O and CO_2 results of the initial pilot testing with calcium oxalate are demonstrated in Figure 14. CaOx gives three distinct peaks (East *et al.,* 2010), labelled A, B and C in Figure 14, so was used as a standard in TGA-MS testing. Peak A corresponds to the release of H_2O, whilst peaks B and C correspond to the release of CO_2. The positions of all DTG peaks align with the expected positions of the MS signals.

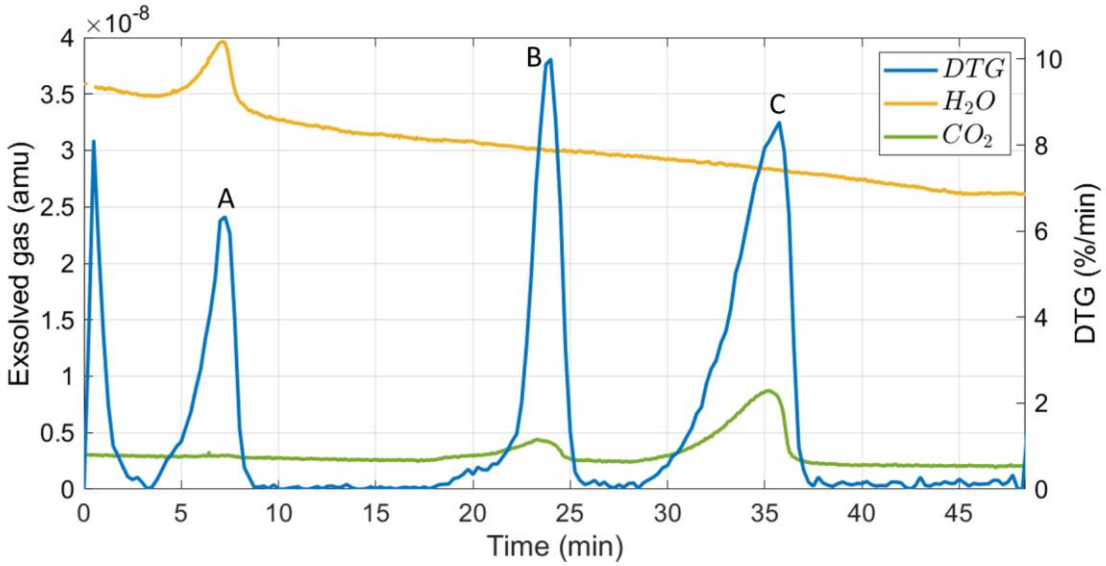

Figure 14: A plot demonstrating the DTG, H_2O and CO_2 curves of a calcium oxalate sample. The MS data (H_2O and CO_2) are displayed on the primary y-axis in amu, whilst the DTG data is displayed on the secondary y-axis in percentage/minute. The time the experiment was conducted over is on the x-axis in minutes. The three distinct DTG peaks are labelled A, B and C.

The results of the TGA-MS testing for all ghaut and marine samples can be found in Appendix B. However, the mass spectrometry readings of the BP1 ghaut sample are demonstrated in Figure 15, along with the DTG and MS signals of the EX1 and COW17 ghaut samples (Figures 16 and 17 respectively) as a way of demonstrating the impact of the buoyancy effect on the resultant signals (see section 4.4.3).

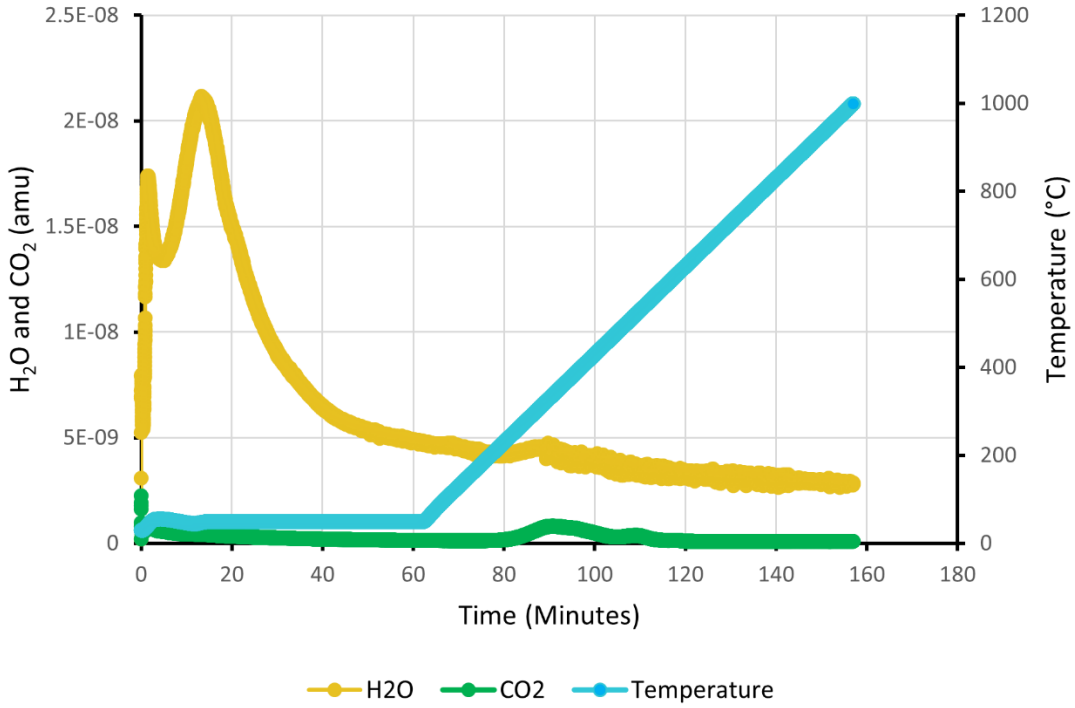

Figure 15: Graph showing the MS signals (H_2O and CO_2) in amu and temperature in °C against time in minutes for the BP1 ghaut sample (Figure 6c). The time of the experiment includes the initial two-minute heating from 30°C to 50°C, followed by the one-hour isothermal at 50°C, followed by the heating to 1000°C. Heating rate was 10°C/minute.

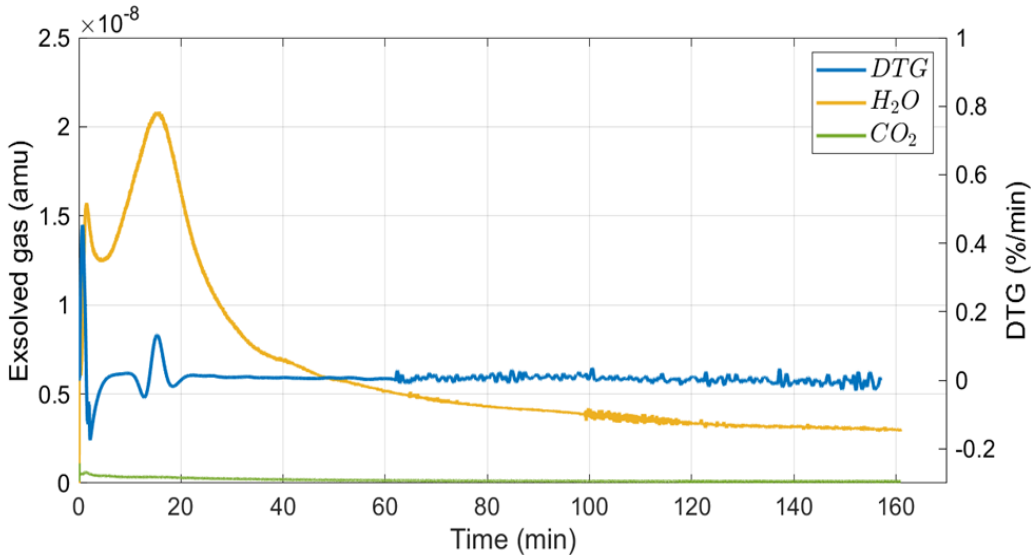

Figure 16: A plot demonstrating the DTG, H_2O and CO_2 curves of the EX1 sample. The MS data (H_2O and CO_2) are displayed on the primary y-axis in amu, whilst the DTG data is displayed on the secondary y-axis in percentage/minute. The time the experiment was conducted over is on the x-axis in minutes. The data contains that from the initial heat to 50°C, the isothermal at 50°C for one-hour and the subsequent heat to 1000°C at 10°C/min. Negligible DTG signals are displayed, demonstrating little mass loss and mostly displays background noise.

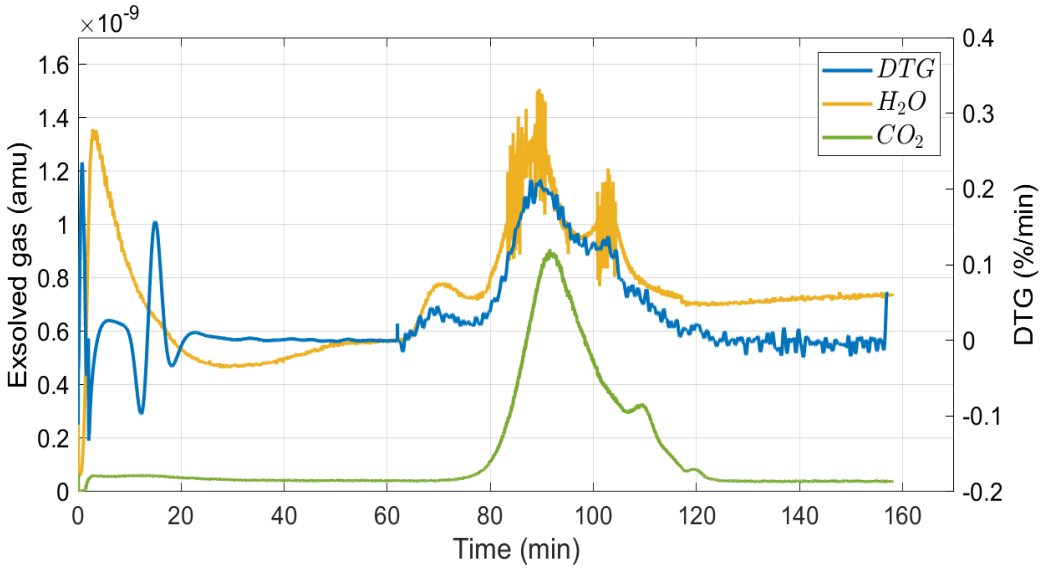

Figure 17: The MS (H_2O and CO_2, on the primary y-axis) and DTG (secondary y-axis) data for the COW17 ball milled sample (Figure 6b) against the time the experiment was conducted over. The graph includes data from the initial two-minute heat to 50°C, the isothermal at 50°C for one-hour and the subsequent heat to 1000°C. Heating rate 10°C/min.

4.4 Discussion

4.4.1 Grain Size Experiments

Figure 11 demonstrates how DTG is affected by the sample grain size. The curves are similar, showing a signature peak within the temperature range of 590-800°C, determined to be representing calcite (Chapter 5). Additional minor peaks of low magnitude are present, which have likely derived from individual grain differences between the samples. The peaks within the calcite range have variable magnitudes (Figure 10) and temperature for the different grain sizes, as the proportion of calcite will differ at different grain sizes. As a result, the 500-1000µm sample will contain more calcite than the finer sub-samples, explaining the general trend observed that smaller grain sizes have lower DTG magnitudes (Figure 10). These coarser clasts of calcium carbonate can be seen in the raw marine samples, displayed in Figure 18. The DTG magnitudes gradually increase as grain size increases whilst the peaks also experience a shift to the right. The shift in peak position relates to the kinetic control of temperature over grain size, with a slower diffuse breakdown of larger clasts, hence the peaks occur at higher temperatures. The shift towards higher peak position at increasing grain size reflects the greater surface area/volume ratio of smaller particles, which are therefore more reactive (Farivar *et al.,* 2012), requiring less

thermal energy for thermal degradation. The different peak positions reflect the influence of grain size on kinetics (Figure 11), whereas the differences in area reflect varying proportions of the material breaking down (Figures 11 and 12).

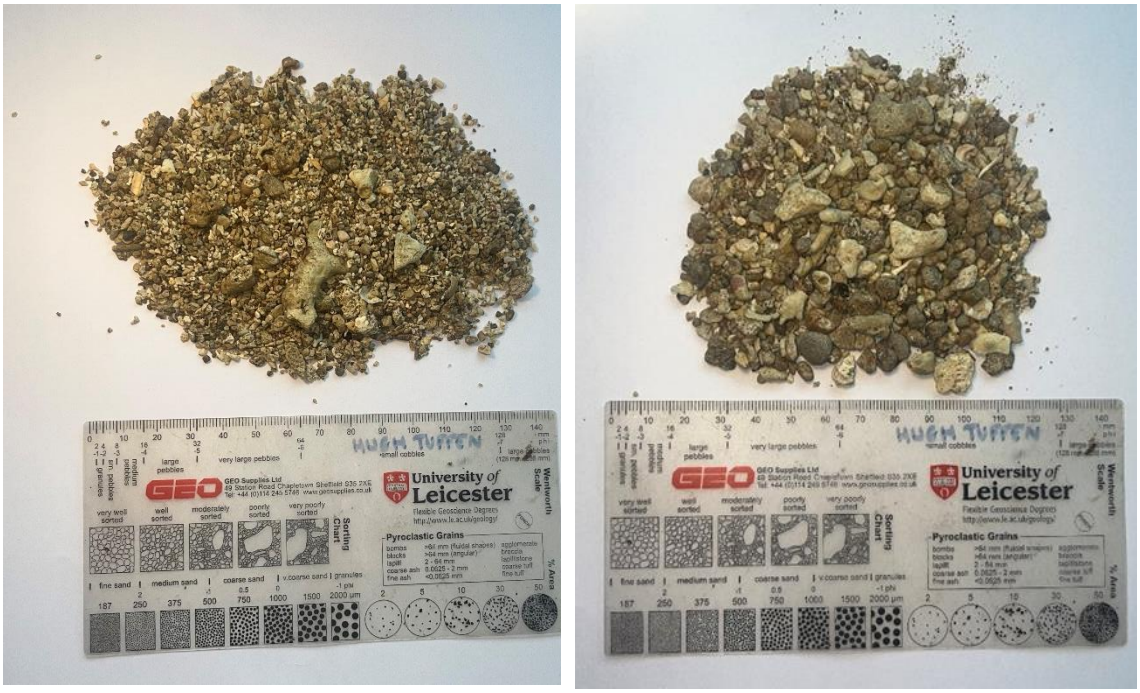

Figure 18: The bulk CB (left) and PP (right) marine samples.

It is noted that a stronger DTG peak was observed at around 900°C for the <125µm sample (Figures 11 and 12). This is interpreted as representing minerals derived from volcanic sources as these are typical temperature ranges for the breakdown of hydrous magmatic minerals such as amphibole or biotite (Földvári, 2011). These results suggest that the finer grained sand and silt samples may be volcanically derived, whereas the coarser materials are likely to be dominated by carbonates.

The ball milled WS sample demonstrates a DTG curve most resembling that of the 125-250µm curve (Figure 11). This was as expected as the grain size of the ball milled samples were <250µm, so the kinetic control would be similar. However, the area of the peak is greater than that of the 125-250µm curve. This indicates the ball milled sample contained more carbonate-rich material, which derived from coarser carbonate clasts.

The endothermic peak between 700-800°C in Figure 13 coincided with the mass loss associated with the thermal decomposition of calcite (Chapter 5). Such a relation is well documented in previous studies (Karunadasa *et al.,* 2019; Li *et al.,* 2017; Li *et al.,* 2020), mirrored by Karunadasa

et al. (2019) who found identical TGA-DSC calcium carbonate peaks, and although not used further here, DSC has potential to further characterise the decomposition reactions occurring in such soil/sediment samples.

4.4.2 Exsolved Gas Analysis

CO_2 and H_2O, amongst few others such as CO, have been reported multiple times as the main gases exsolved when conducting thermal analyses on soil, soil organic matter (SOM) and other humic substances, e.g. Lopez-Capel *et al.,* (2008) investigating thermal analyses on SOM in grasses, and Pitkanen *et al.,* (1999) when studying fuels. The use of exsolved gas analysis alongside TGA/DTG methods aids the identification of various exothermic and endothermic reactions with the use of DSC data (Figure 13) as well as differentiating overlapping thermal peaks. This is important for soil samples which may contain both SOM and minerals such as kaolinite and smectite clay minerals as the standard range for their combustion is similar, making it difficult to distinguish between them with TGA/DTG data alone (Lopez-Capel *et al.,* 2008).

In this study, MS peaks were mostly either absent or aligned with those of the TGA signals (Figs. 16 and 17), and assist identification of the DTG peaks (see Chapter 5). For example, CO_2 is released when SOM and carbonates are broken down (Idris *et al.,* 2010), whereas water adsorbed to clay minerals, specifically smectite, is released during their heating and degradation (Fernández *et al.,* 2012; Vidal and Dubacq, 2009). The lack of both DTG and MS peaks for the EX1 sample is notable. The TGA and DTG results; with negligible total weight loss, its location from amongst young pyroclastic deposits in Plymouth (Figure 6d), and appearance under the microscope, all indicate that EX1 is almost entirely composed of fresh volatile-poor volcanic ash deposited from the 1995-2010 eruption of Soufrière Hills volcano (Figure 16).

4.4.3 The Buoyancy Effect

TGA signals occurring at less than 200°C were ignored, due to the strong impact of the buoyancy effect from the isothermal stage of the analyses. The buoyancy effect is caused by the air in the furnace experiencing a decrease in density as temperatures are raised (Saadatkhah *et al.,* 2019). The buoyancy effect is seen on the DTG-MS curves during the initial heat and onset of the isothermal, demonstrated in Figures 16 and 17 between 0-20 minutes. When the buoyancy effect is present, the DTG signals are disturbed and clear peaks caused by the sample cannot be obtained. To combat this, any peaks witnessed within this temperature range of the samples were removed from further analysis.

4.4.4 Final Methodology

After the completion of various preliminary testing described, the methodology conducted on all 40 ghaut samples and 7 marine samples was as follows:

TGA: The ghaut samples used were those that were bulked and ball milled, the marine samples also ball milled. Tests were undertaken at a heating rate of 10°C/min from room temperature to 1000°C in an oxidising environment with an air flow rate of 50mL/min.

TGA-MS: The ghaut samples used were those that were bulked and ball milled, the marine samples also ball milled. The procedure included an initial evacuation and refill of the vacuum with O_2-free N_2 prior to heating from 30°C to 50°C at 10°C/min where a one-hour isothermal was held at 50°C. Heating from 50°C to 1000°C at 10°C/min then took place. All tests were conducted in an oxidising atmosphere with an air flow rate of 50mL/min and protective purge N_2 gas flow rate of 20mL/min.

Identical pre-treatment to samples were used across all final TGA methods for consistency. The use of ball milled samples meant grains of different sizes in the bulk sample could be used as to eliminate the bias against grains of larger sizes, but also removed the issue of having grain size affecting the results as seen in Figure 11. It was decided that ball milling the bulk samples prior to analyses was the preferred method, favoured over the use of solely the fine-grained fraction as in many sediment fingerprinting and wider catchment studies, due to the context of the study. Uniquely, Montserrat is an island where sediment has been observed to display little sorting across the catchments, with large clasts found spread across the landscape. This is explained through its volcanic history, where pyroclastic deposits are widespread and ashfalls have the ability to deposit larger clasts further across the region. For volcanic islands it is therefore sensible to overlook the fine-grained focus of many similar studies, instead favouring the bulk sample which is more representative of the catchment area. To incorporate these grain sizes in TGA experiments, it was therefore necessary to ball mill samples.

4.5 Conclusion

Preliminary TGA(-MS) testing was conducted with the aim of establishing a concise and representative method from which meaningful results could be drawn. The repeatability of the method was ensured through repeated testing of the same samples which demonstrated highly repeatable peak positions and mass loss percentages. Sources of error were minimised through routine calibrations of instruments and ensuring correct laboratory procedure was conducted. Grain size testing revealed shifts in peaks and their areas, drawing attention to the need to

homogenise grain sizes, achieved through ball milling. Alterations of the TGA-MS method also revealed a need to establish an accurate baseline for MS signals, achieved through the inclusion of evacuations, refills and an isothermal. In the completion of this pilot testing, the objectives set in this chapter were met, with the production of a robust method to be used in further chapters achieved.

Chapter 5: Identification of TGA Signals

5.1 Introduction

After completing preliminary TGA-MS analyses (Chapter 4), the signals obtained through completion of testing following the procedure outlined in section 4.4.4 were analysed and data extracted from DTG peaks. The presence of three main peaks were identified within temperature ranges: 200-430°C, 430-590°C and 590-800°C, similar to other studies using TGA for soil analysis (Table 4). We assumed them to represent organic matter (OM), clay and calcite respectively. Although other minerals create DTG peaks in these temperature ranges, OM, clay and calcite were assumed due to knowledge of the sample locations and likely mineral compositions indicated by pre-existing literature (Table 4). This chapter aims at justifying the assumptions made.

5.2 Methods

To assign identities to the three temperature ranges in which peaks were routinely present, an extensive literature review was undertaken. Studies surrounding soil and sediment using TGA were compared in terms of heating rates, atmospheres used and flow rates to establish similar methodologies and identify overlapping results.

To represent calcium carbonate peaks, coral and shell fragments were tested on the SDT Q600 TA (Figure 7). These fragments were hand-picked from the Piper's Pond (PP) marine sample (Figure 18). The same TGA procedure was used but the pre-treatment involved crushing the fragments using a pestle and mortar to grain sizes <250µm.

5.3 Results

The results of the literature review are demonstrated in Table 4, where the temperature range assigned to OM, clay and calcite in a number of studies are displayed, along with flow rates, temperature regimes and the presence of any exsolved gas analysis.

Table 4: A selection of TGA-based studies with the temperature (T) ranges identified and/or used for OM, clay and calcite. Also highlighted are the flow rates, temperature regimes and whether any exsolved gas analyses were included in the studies.

Author(s) and Date	**OM T range identified**	**Clay T ranges identified**	**Calcite T range identified**	**Flow Rate**	**Temperature Regime**	**Exsolved gas/DSC analysis (Yes/No)**
Miyazawa *et al*., 2000	200-280°C	N/A	N/A	Air and N_2 atmospheres	25 to 600°C at 15°C/min	No
Siewert, 2004	200-450°C	500-550°C	> 550°C	Air flow of 200mL/min	25°C to 950°C at 5°C/min	No
Critter and Airoldi, 2006	Around 300°C	200-580°C	N/A	N/A – was conducted in synthetic air or argon atmospheres	10°C/min to 1100°C	Yes
Pallasser *et al.,* 2013	200-430°C	430-590°C	> 600°C	60 ml/min O_2 and 40 ml/min N_2	10°C/min to 700°C, with 10-minute isothermals at 200°C and 700°C	Yes
Edmondson *et al.,* 2015	200-470°C	N/A	620-800°C	Air flow of 30mL/min	30°C/min from 20 to 1000°C	Yes
Kristl *et al.,* 2015	200-550°C	Around 350°C	>600°C	Air flow at 100mL/min	30 to 800°C at 10°C/min	No
Zethof *et al.,* 2019	Oxidation by 500°C	N/A	750-850°C	250mL/min O_2 and N_2	20°C/min to 1100°C	Yes
Chauhan *et al.,* 2020	200-280°C	430-600°C	> 600°C	100mL N_2	10°C/min to 645°C	No

Lebron *et al.,* 2023	By 375°C	375-650°C (noted this may also be due to charcoal particles)	650-1000°C	Air with 21% oxygen composition	6°C/min from 0-1000°C – also used 2°C/min and 10°C/min	Yes

The DTG signals from shell and coral samples are presented in Figures 19 and 20, alongside those of the 7 marine samples. Assuming these were pure samples and contained 100% calcite, the peak areas within the assumed calcite range (590-800°C) were used to estimate the relative percentage of calcite in each marine sample. The results are displayed in Table 5.

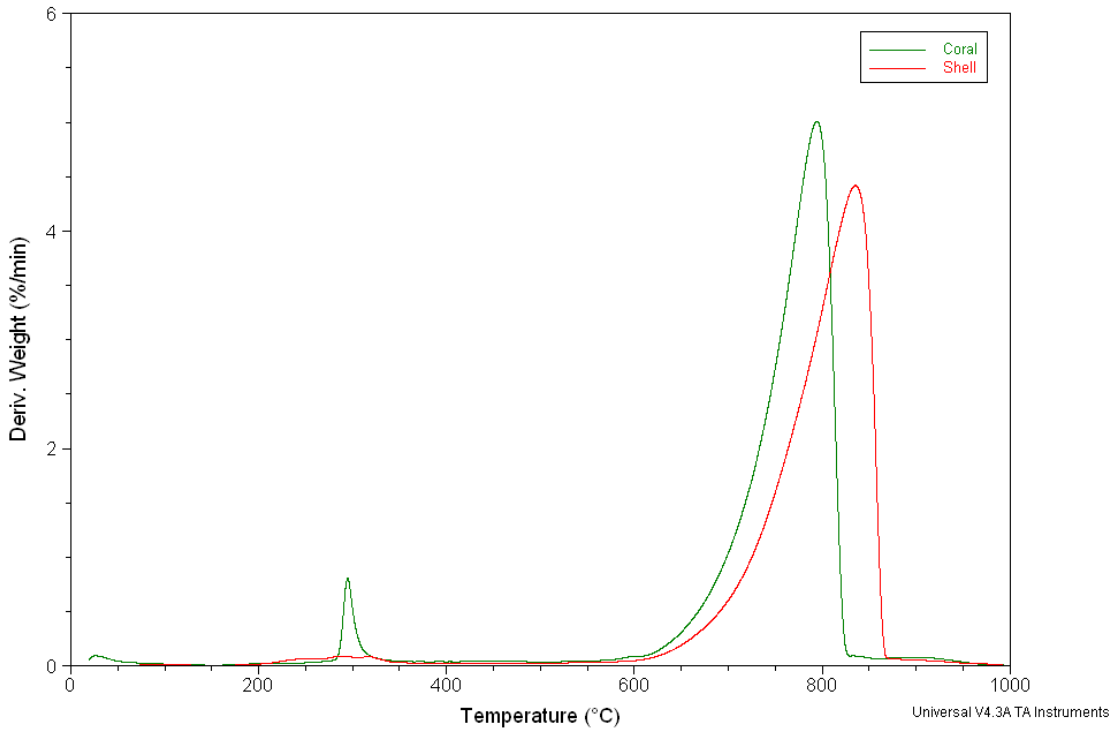

Figure 19: DTG peaks for ground shell fragments and ground coral fragments taken from the PP marine bulk sample.

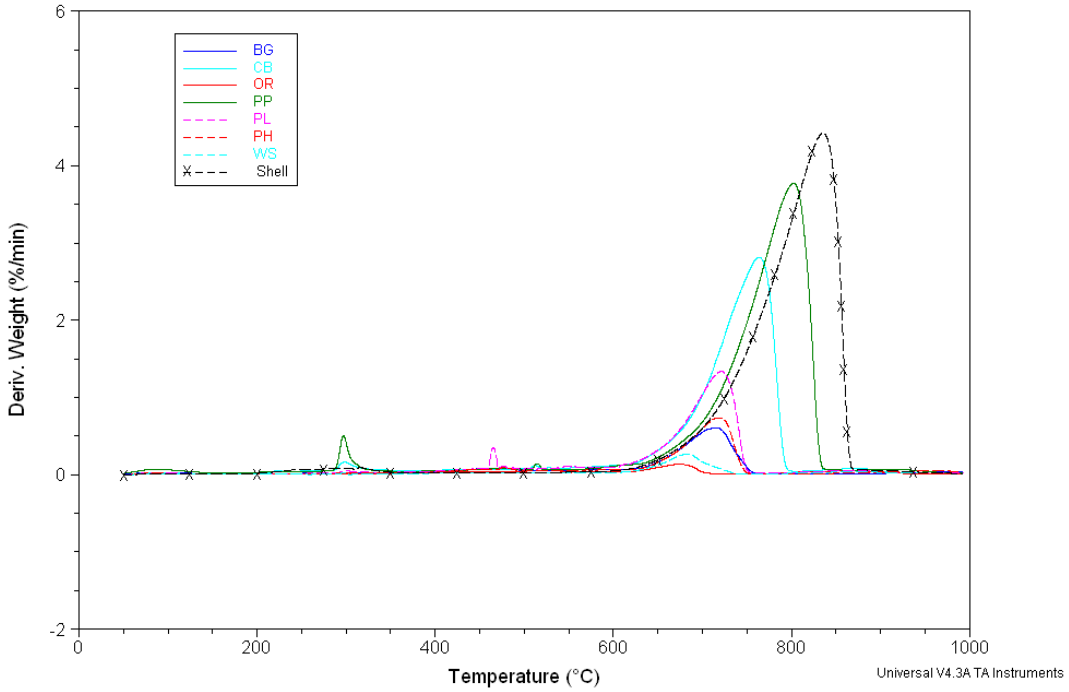

Figure 20: Overlay of all marine sample DTG signals as well as a pure shell sample from 0 to 1000°C at 10°C/min.

Table 5: The integrated area under the 590-800°C peak present in the DTG curves of the 7 marine samples and the shell sample. Under the assumption that the shell sample was composed of 100% calcium carbonate ($CaCO_3$), the proportions of the marine samples composed of calcium carbonate were estimated to two decimal places.

Sample	Peak Area	% $CaCO_3$
Shell	38.81	100.00
BG	3.67	9.47
CB	19.7	50.83
OR	0.57	1.47
PP	28.43	73.35
PL	7.87	20.30
PH	4.09	10.55
WS	1.39	3.59

5.4 Discussion

5.4.1 Organic Matter

Due to the importance of SOM for an abundance of ecosystem services, there has been much focus on calculating the presence in soils. A well-established thermal method for quantifying SOM is loss-on-ignition (LOI) experiments (Roper *et al.*, 2019). LOI experiments heat samples up to 500°C, ensuring complete removal of the SOM fraction (Jensen *et al.,* 2018). Other thermogravimetric experiments indicate OM burns off below 500°C (Critter and Airoldi, 2006; DeLapp and LeBoeuf, 2004), with temperature ranges often stated between 200-400°C (Chauhan *et al.,* 2020; Földvári, 2011; Pallasser *et al.,* 2013).

5.4.2 Clay

The most recent soil map of Montserrat (Lang, 1967) gives insight into the composition of soils that could be expected on the island. The presence of clay minerals across the island is explained, with clay fractions containing smectoid, kandoid and allophanoid minerals (Lang, 1967). The presence of smectites across other Lesser Antilles islands has also been documented, e.g., Parra *et al.* (1986) describe smectites and kaolinites dominating volcanic rocks originating from Martinique, found within the Venezuelan Basin. Gandais (1987) also found smectites and kaolinites when exploring the sources of clay minerals in the Grenada Basin, the only clay minerals provided by sediment from the Lesser Antilles Arc.

The handbook of minerals by Földvári (2011) list the temperature ranges for both kaolinite and smectite minerals, with many falling into the 430-590°C temperature range. For example, kaolinite has a thermogravimetric temperature range of 530-590°C, whilst certain smectite minerals, such as volkonskoite and nontronite, have ranges surrounding 400°C (Földvári, 2011). When using an identical heating rate to this study (10°C/min), clay minerals are known to express peaks from 430°C to around 600°C (Chauhan *et al.*, 2020; Pallasser *et al.*, 2013).

5.4.3 Calcite

Calcite (calcium carbonate) was the third component identified using the DTG peaks. Across the coral reef samples there were consistent peaks in the higher temperature ranges (Figure 20). Larger areas can be seen when the temperature peak is higher. This can be associated with the kinetic effect of larger particles such as calcium carbonate (Figure 18), which slows the

degradation, shifting the peak to the right. These peaks also appeared smaller in some of the ghaut samples. The positions of the DTG peaks reflect the compositions of the marine samples whereby the largest areas and peaks lying furthest to the right align with those which contain the highest percentages of estimated $CaCO_3$, those of the PP, CB and PL marine samples (Figure 20 and Table 5).

The results of the coral and shell tests were also used to justify the identification of calcite as peaks in this temperature range. Figures 19 and 20 demonstrate that $CaCO_3$ in these experiments is represented by DTG curves which experience significant increases after 600°C, with peaks around 800°C. It should be noted that in Figure 19 an additional peak was seen around 300°C for the coral sample. This was attributed to an impurity in the sample used originating from the bulk PP marine sample the coral was extracted from, seen also in Figure 20, and is likely that of organic matter so can be ignored when considering calcite peaks. Similar TGA and DTG curves were demonstrated by Li *et al.* (2017) when samples were tested containing both calcium carbonate and organic acids, with the temperature ranges identified mirroring that of this study.

Given the results of the coral and shell analyses and the knowledge that these fragments accounted for a large proportion of the coral reef samples, it was deduced that the peak in the high temperature ranges (590-800°C) would be attributed to calcium carbonate, in agreement with other thermogravimetric literature (Table 4). It is known that $CaCO_3$ begins to degrade in air above 600°C (Chauhan *et al.,* 2020; Galan *et al.,* 2012; Pallasser *et al.,* 2013), in different atmospheres.

The estimated percentage compositions of calcite (Table 5), demonstrate the PP and CB sediment samples contain a majority calcite, indicative of less terrestrially-derived sediment deposition occurring on these sites. However, very low percentage compositions seen in the OR and WS samples (Table 5) reflect their locations further south (Figure 5) than the other marine samples, where they are found on the coast, immediately adjacent to ash deposits from the 1995-2010 eruptions. The lack of other peaks within the 0-1000°C range tested implies the remainder of these samples may be composed of volcanically derived material, the breakdown of which would occur at higher temperatures, as stated in the handbook of minerals and seen in existing literature (Denton *et al.,* 2012; Földvári, 2011), potentially reflecting the deposition of materials from the ash fields.

Chapter 6: Sediment Fingerprinting

6.1 Introduction

The application of sediment fingerprinting allows the identification of sources of sediment to target samples, offering relative contributions of various sources. The aim in this study was to understand, using statistical evidence, which ghauts on Montserrat are supplying the majority of sediment to the coral reefs on the western coast of the island. The key objectives of this chapter were to:

1. Use a series of statistical tests to formulate an optimal tracer suite with a high reclassification rate.
2. Implement the selected tracer suite in a MixSIAR unmixing model to determine the relative contributions of ghauts to each coral reef.
3. Discuss the use of particle size analysis in offering explanations for the observed results.

6.2 TGA-MS and ICP-OES Methods

6.2.1 TGA

The TGA data used for sediment fingerprinting is described in chapters 4 and 5. However, calcite was rejected as a potential tracer for sediment fingerprinting (see Section 6.7.3) leaving just OM and clay (Table 6).

6.2.2 ICP-OES

In preparation for ICP-OES analysis, all 7 marine samples and 200 ghaut samples were ball milled at 30Hz for 1 minute on a Retsch MM 400 ball mill. The samples then underwent microwave digestion, where 5mL of nitric acid was added to 0.25±0.01g of each sample in a Teflon tube and left for 15-20mins before being secured with a bung. These were microwaved (1600W, 200°C) for around 30 minutes and left to cool for >one hour. The digested samples were then diluted to 20% and subsequently 2% nitric acid using deionised water. To accommodate both time and resource limitations, the 2% dilutions of the five replicate samples from each ghaut were bulked into one sample. This involved taking 2ml from each of the five samples and combining into one 10ml sample. These 40 ghaut samples and 7 marine samples were analysed using a Thermo ICAP duo ICP 6300. Blanks, standards and calibration standards were analysed to ensure accurate calibrations and readings.

For ICP-OES analysis, 11 elements were chosen to be analysed: Al, Ca, Cu, Fe, Mg, Mn, Ni, P, Pb, Si and Zn. The concentrations of these elements were calculated, and data was analysed using Microsoft Excel and R Studio Version 4.3.1. Both the concentrations for Ni and Pb in all the samples were below the instruments detection limit so were too low to be included accurately in the study. Ni and Pb were therefore removed from further analysis, along with Ca (Section 6.7.3).

6.2.3 Input Data

After preliminary data analysis and the subsequent rejection of certain variables, the final selection of variables used as potential tracers were implemented in the sediment fingerprinting procedure. Table 6 presents the variables used.

Table 6: The parameters obtained from TGA-MS and ICP-OES which were retained for use in the sediment fingerprinting procedure (Section 6.3) and those which were rejected as deemed unsuitable.

Method	**Parameters used as potential tracers**	**Parameters NOT used**
TGA-MS	OM and clay	Calcite, H_2O and CO_2
ICP-OES	Al, Cu, Fe, Mg, Mn, P, Si and Zn	Pb, Ni and Ca

6.3 Sediment Fingerprinting Method

Sediment fingerprinting studies begin with a three-step method (TSM) for selecting suitable tracers (Chalaux-Clergue *et al.,* 2024; Collins *et al.,* 2010; Sherriff *et al*., 2015). This includes:

1. An assessment of the conservative behaviour of each potential tracer
2. Analyses on the ability of each potential tracer to discriminate between sources
3. The construction of an optimal tracer suite demonstrating a high capacity to reclassify sources using modelling

Once a suitable tracer suite has been determined it is applied to the target samples. Commonly, multivariate mixing models are used (Collins *et al.,* 1997, Collins *et al.,* 2010, Smith and Blake, 2014), to assign a value for the contribution of each source to targets.

This study follows a similar procedure to a TSM, with an additional initial step of using cluster analyses to assign the sources to groups based on their compositions. The procedure used in this study is outlined in Figure 21.

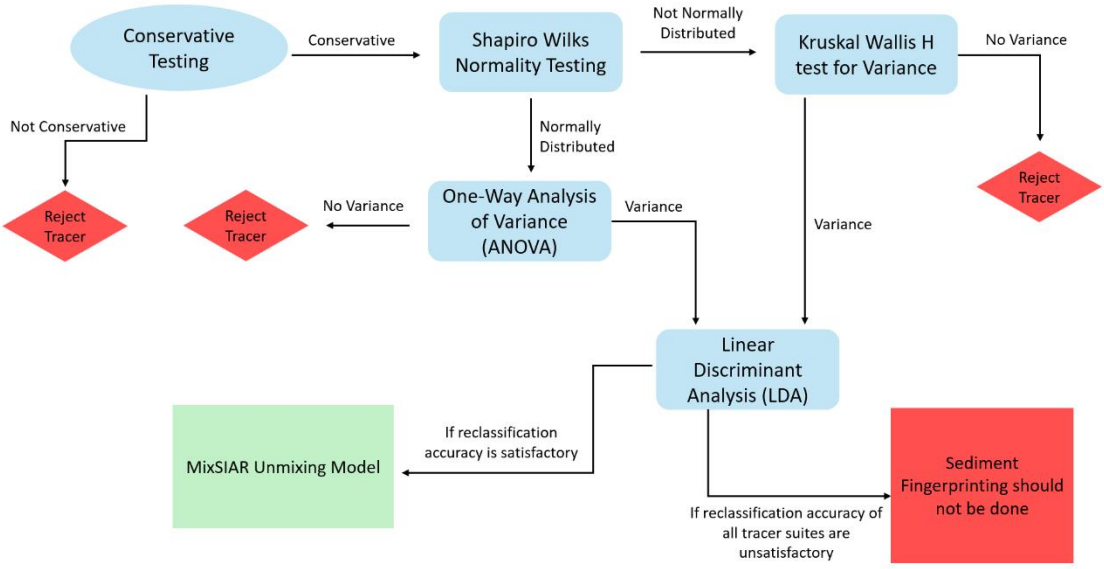

Figure 21: A flow diagram demonstrating the statistical procedure followed to complete sediment fingerprinting, starting from conservative testing and ending on the use of a MixSIAR Unmixing model to find the contributions of sediment.

6.3.1 K-Means Cluster Analysis

Initially the ghaut source samples required grouping based on their composition using k-means cluster analysis on the variables in Table 6. This identified groups or 'clusters' in which the data is more similar to other samples of the same cluster but statistically less similar than those of other clusters. K-means cluster analysis has been successfully applied to soil-related studies previously, i.e. using the cluster centres to find sampling locations based on moisture (Van Arkel and Kaleita, 2014) and for quantifying aquifer vulnerability (Javadi *et al.,* 2017). K-means cluster analysis has also been applied to sediment fingerprinting studies previously, for example, as a way of forming source group classifications when investigating sediment pollution (Pulley and Collins, 2018). K-means cluster analysis was conducted in R Studio Version 4.3.1.

The primary stage of k-means cluster analysis was to identify the optimal number of clusters which would best fit the data. K-means clustering performs a number of iterations using various cluster numbers, producing an elbow plot where the appropriate number of clusters can be

inferred. This was conducted on all source samples for all Table 6 parameters and groups then assigned.

6.3.2 Conservative Testing

In sediment fingerprinting, tracers are favoured based on their conservativeness. Conservativeness relates to how a tracer may change during transportation of the sediment from source to target site. To accurately conduct source apportionment, a tracer must be conservative in nature over the course of transport to retain the sediments chemical and mineralogical signature. Vale *et al*. (2022) discuss how identifying a tracer's conservativeness is challenging, with few techniques available and few ways of accurately accounting for all non-conservative behaviour.

An initial means of considering conservative behaviour is using boxplots as a way of visualising which potential tracers may be unsuitable. Range tests were also used, where minimums, maximums and medians for each source cluster group were compared with the values of the target samples, ensuring all target samples were within range of the sources. Those parameters outside the range were rejected from further use.

6.3.3 Testing for Normality and Variance

After grouping the samples and completing conservative testing, statistical tests of variance were conducted on the potential tracers to determine whether there were significant differences between cluster groups. If samples did not vary in chemical composition, sediment fingerprinting would not be possible.

To determine which test of variance to use on each potential tracer, Shapiro-Wilks Normality testing was conducted on the source samples to indicate whether the data follows a normal distribution. Based on the results of the normality testing, the non-parametric Kruskal Wallis H test was used for those not normally distributed, whereas the parametric equivalent, a one-way analysis of variance (ANOVA), was used for those following a normal distribution. Parameters which demonstrated significant differences and passed this test were then retained and used in the next stage of the sediment fingerprinting process.

6.3.4 Linear Discriminant Analysis

The next stage of the sediment fingerprinting process was to select the tracer suite used to classify new samples into groups. Commonly, linear discriminant analysis (LDA) is used with a greedy wilks test for two purposes:

1. To select the minimum number of tracers that can be used to maximise the source discrimination.
2. To assess the reclassification accuracy of source groups based on the selected tracer suite.

6.3.5 Unmixing Model

Finally, a MixSIAR unmixing model under a Bayesian framework with 3000 posterior realisations was used as the final step in the sediment fingerprinting process to determine the relative contributions of source groups to each of the target marine samples. The tracer suite determined from the previous statistical testing was applied to each reef target sample separately.

6.4 Particle Size Analysis Method

Particle Size Analysis was also undertaken as a key factor to consider in sediment fingerprinting studies. Particle size analysis was conducted on the samples used as part of a previous study (Stevens *et al*., 2023). Sieving using 2mm and 0.5mm sieves was completed to determine the fraction by weight of pebbles (>2mm), coarse sand (0.5-2mm) and finer sediments (<0.5mm). Particle size analysis of the finer fraction of sediment was also conducted using a Beckman-Coulter LS 13 320 Laser Diffraction Particle Size Analyzer (PSA). The PSA was used to measure a further three grain size fractions: sand (62-2000µm), silt (2-62µm) and clay (<2µm).

6.5 Sediment Fingerprinting Results

6.5.1 K-Means Cluster Analysis

K-means cluster analysis separated the ghaut source samples into four cluster groups, as indicated through Figure 22. The use of >4 groups caused the total within sum of square values to begin to plateau and show minimal differences. The group each source sample was assigned to is demonstrated in Table 7.

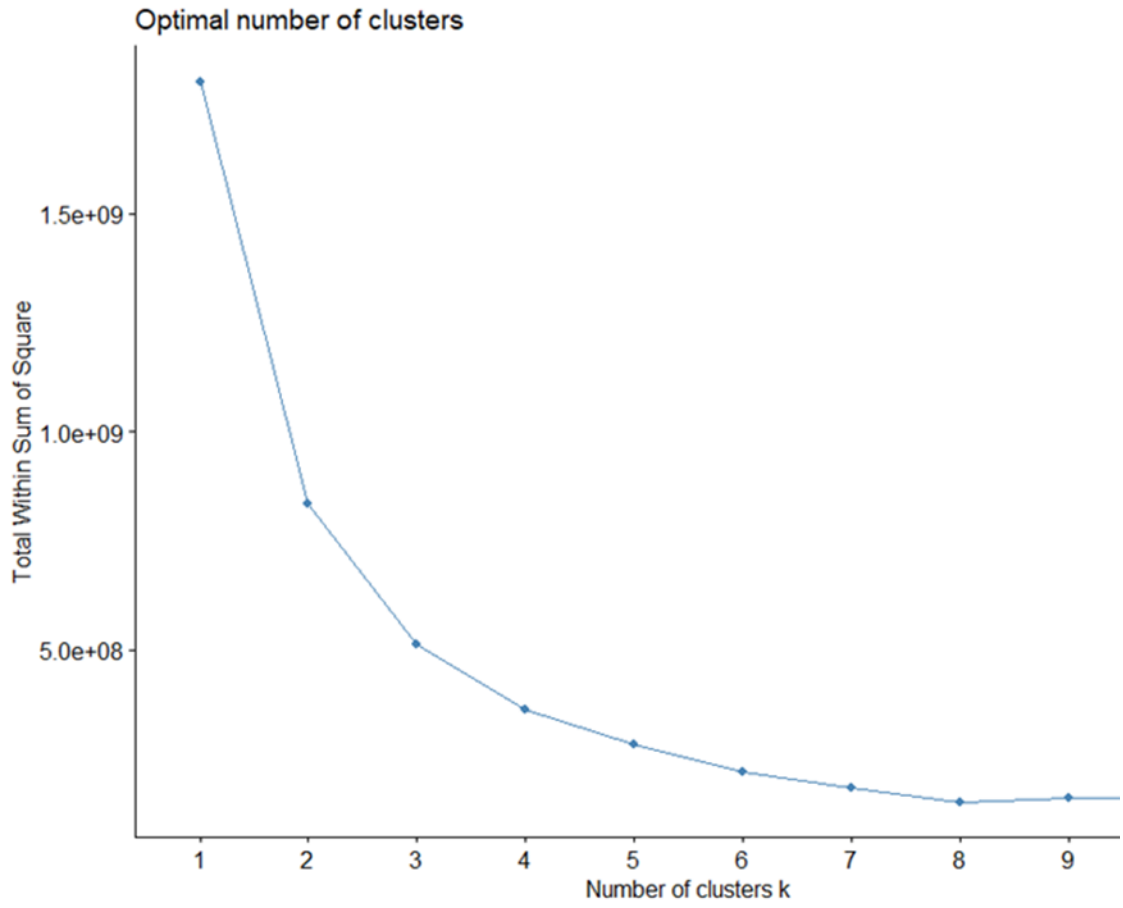

Figure 22: An elbow plot displaying the optimal number of cluster groups to be used in k-means clustering analyses based on TGA and ICP-OES data for the 40 source samples.

Table 7: The groupings of the 40 source (ghaut) samples based on the k-means cluster analysis elbow plot (Figure 22).

Cluster Group	**Samples**
Group A	LB1, LB2, LB7, LB8, LB10, LB12, COW14, COW17
Group B	LB3, COW2, COW4, COW7, COW9, COW13, COW16
Group C	LB9, BP3, BP4, BP5, BP6, BP7, BP8, BP9, BP10, BP11, BP20, BP21, COW8, EX1
Group D	LB11, BP1, BP2, COW1, COW3, COW5, COW6, COW10, COW11, COW12, COW15

These groups were plotted on a map (Figure 23) to visualise any spatial influence on the clustering groups. Figure 23 demonstrates how there are some spatial segregation of cluster groupings. Group A samples tend to concentrate in the northern regions of Montserrat, whereas

Group C consists mainly of the most south-westerly of the samples (Figure 23). Groups B and D are interspersed more alongside the western coast (Figure 23).

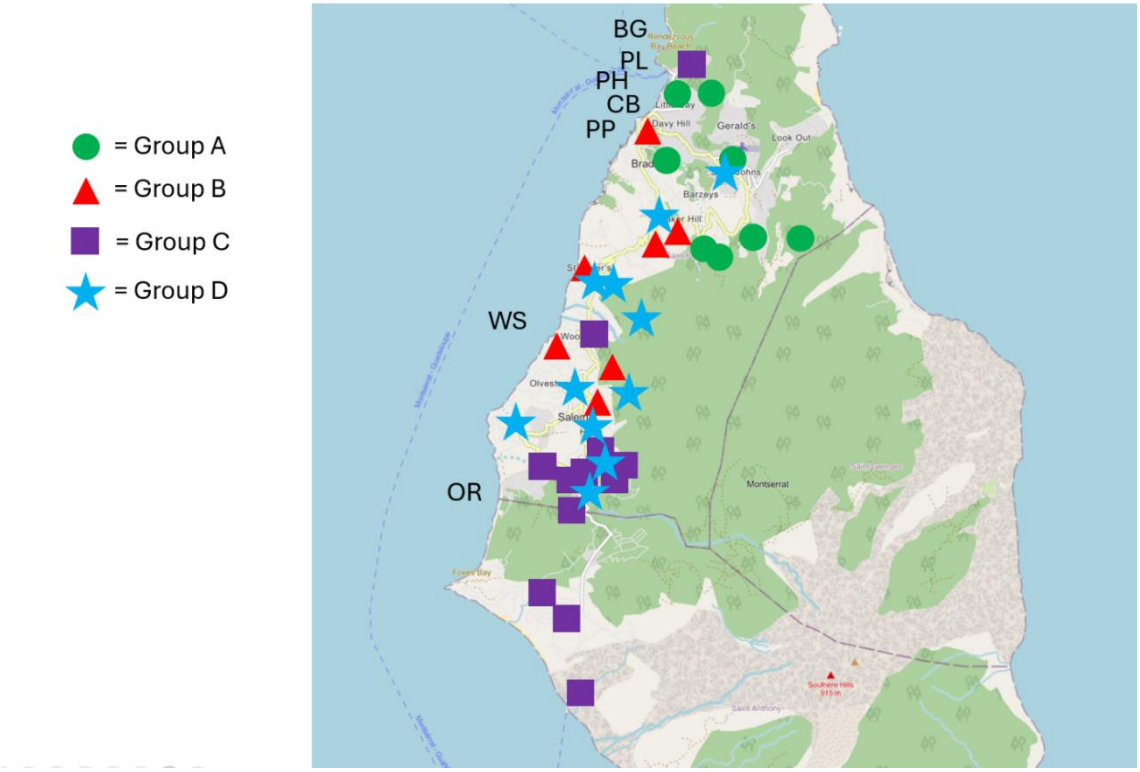

Figure 23: A map of ghaut source samples. The ghaut samples are represented by different symbols of different colours according to their assigned cluster groupings (Table 7). The locations of the marine samples are also shown. Base map from ArcGIS Pro.

6.5.2 Conservative Testing

Using Figure 24 and Tables 8 and 9 it was determined that Al, Cu and Mg were inappropriate parameters to be used and so were rejected as tracers. This was because the values of those parameters in the target samples were frequently out of range, indicative of non-conservative behaviour.

In this stage of testing, it was also decided that marine target samples PP and CB would be removed from the group of target samples. This was because they often appeared out of range, or on the limits, of the source samples for most parameters.

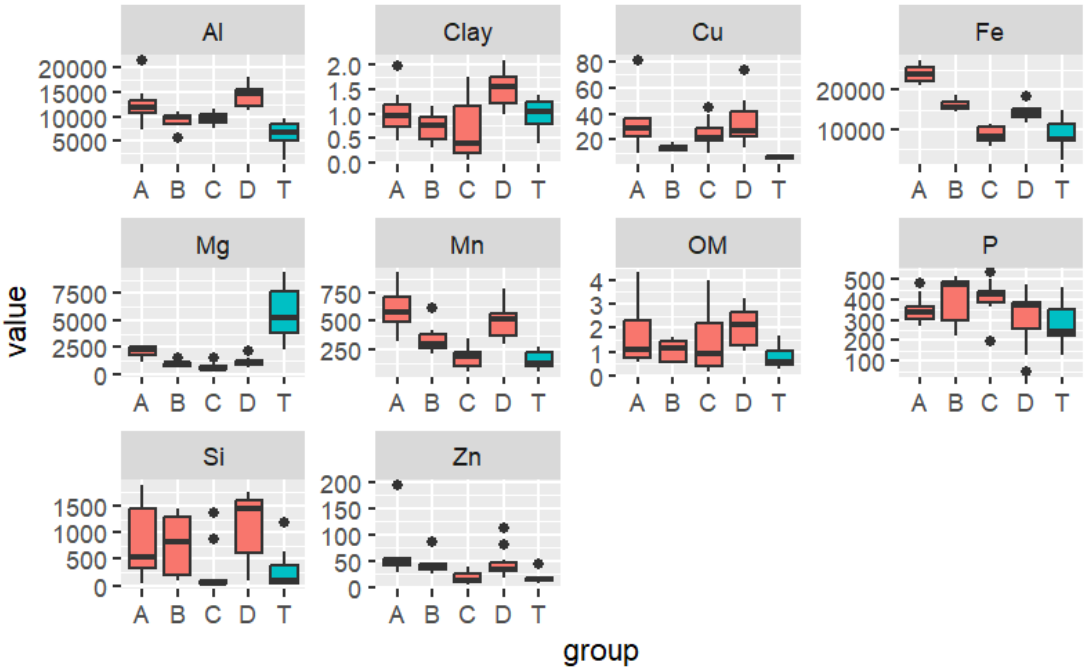

Figure 24: Boxplots of the 10 potential tracers plotted as the source ghaut sample cluster groups (A, B, C and D) and target marine samples (T). The y-axis values for Clay and OM are given as weight loss percentages and the values for Al, Cu, Fe, Mg, Mn, P, Si and Zn are given in concentrations in mg/kg.

Table 8: The minimum, maximum and median in each sediment source cluster group. Data is given for each of the 10 potential tracers. Values for OM and clay are given as percentage weight loss and those for Al, Cu, Fe, Mg, Mn, P, Si and Zn are given in units of mg/kg.

	OM	Clay	Al	Cu	Fe	Mg	Mn	P	Si	Zn
Group A										
Min	0.55	0.46	7261.48	9.93	21264.48	1163.65	321.61	267.99	51.71	28.10
Max	4.33	1.98	21425.70	81.29	27665.08	2685.63	929.96	485.04	1894.58	195.48
Median	1.11	0.97	11835.02	29.39	24142.51	2362.55	575.80	337.85	526.09	46.27
Group B										
Min	0.54	0.30	5658.58	11.06	14666.14	755.47	214.78	223.50	89.72	24.03
Max	1.64	1.17	11121.25	17.93	18826.03	1536.41	613.51	513.33	1449.72	85.07
Median	1.15	0.76	9759.54	13.09	15436.17	967.87	298.13	478.71	832.63	35.43
Group C										
Min	0.16	0.06	7717.43	9.91	5589.01	242.43	55.18	195.91	30.62	5.07
Max	3.96	1.75	11563.13	45.09	11518.91	1568.99	348.31	535.97	1356.33	38.02
Median	0.95	0.40	9582.60	21.62	8335.74	554.69	190.00	426.93	57.34	11.46
Group D										
Min	1.05	0.99	11302.61	14.29	11691.29	636.97	302.46	46.29	100.30	17.98
Max	3.22	2.11	17864.21	73.74	18516.31	2183.29	781.49	472.26	1759.30	112.67
Median	2.13	1.57	14749.50	26.82	14323.23	1026.36	521.68	371.12	1455.91	34.17

Table 9: The weight loss percentage of OM and clay along with the concentrations of Al, Cu, Fe, Mg, Mn, P, Si and Zn in mg/kg of the seven marine target samples. Values highlighted indicate those which are out of range of the sediment source samples – see Table 8.

Sample	OM	Clay	Al	Cu	Fe	Mg	Mn	P	Si
BG	0.56	1.05	7848.91	6.57	14850.89	5268.39	273.16	462.92	87.57
WS	0.26	0.38	6237.56	5.66	7656.19	2522.88	128.33	299.64	39.99
OR	0.39	0.57	9590.33	6.97	6876.50	2274.18	89.63	215.93	32.47
CB	1.42	1.33	4143.55	7.59	7555.66	9462.89	120.61	233.01	1177.73
PH	0.50	0.98	9156.05	5.13	11863.06	7143.71	280.35	241.44	56.13
PL	0.69	1.39	6675.67	7.63	11054.42	8103.24	179.27	402.76	134.45
PP	1.65	1.17	1334.59	4.95	2373.37	5166.20	57.48	129.20	631.08

6.5.3 Normality and Variance Testing

Following a 95% significance level and a null hypothesis that the data follows a normal distribution, distributions were assigned to each of the 10 potential tracers. The null hypothesis was rejected where the p-value was <0.05. The results revealed that Clay, Fe and Mn were normally distributed, whereas the remaining 7 potential tracers did not follow a normal distribution (Table 10). As a result, Kruskal Wallis H tests were conducted on the 7 not normally distributed (Table 11) whilst one-way ANOVAs were performed on the three normally distributed (Table 12).

Table 10: The results of the Shapiro-Wilks tests for normality for each of the 10 potential tracers. The W value and p-value are given for each, as well as the determination of the type of distribution each follows based on a 95% significance level. The highlighted parameters show those which follow a normal distribution.

Variable	W value	p-value	Distribution
OM	0.92612	0.01	Not normal
Clay	0.95862	0.15	Normal
Al	0.92785	0.01	Not normal
Cu	0.82024	<0.01	Not normal
Fe	0.9522	0.09	Normal
Mg	0.87378	<0.01	Not normal
Mn	0.95295	0.1	Normal
P	0.94171	0.04	Not normal
Si	0.81	<0.01	Not normal
Zn	0.71344	<0.01	Not normal

Table 11: The results of the Kruskal Wallis H tests conducted on the potential tracers that do not follow a normal distribution. The H values, degrees of freedom (df) and p-values are presented, along with whether the test indicates a statistical difference between groups based on a 95% significance level. The highlighted parameters are those which show a statistical difference across groups.

Variable	H value	df	p-value	Difference?
OM	5.4411	3	0.14	No
Al	21.324	3	<0.01	Yes
Cu	12.431	3	<0.01	Yes
Mg	22.99	3	<0.01	Yes
P	6.3456	3	0.1	No
Si	17.167	3	<0.01	Yes
Zn	20.931	3	<0.01	Yes

Table 12: The results of the one-way ANOVA conducted on the potential tracers that follow a normal distribution. The F values, degrees of freedom (df) and p-values are presented, along with whether the test indicates a statistical difference between groups based on a 95% significance level. The highlighted parameters are those which show a statistical difference across groups.

Variable	F value	df	p-value	Difference?
Clay	6.833	3	<0.01	Yes
Fe	96.53	3	<0.01	Yes
Mn	18.96	3	<0.01	Yes

Using a 95% significance level and a null hypothesis that there was no statistical variance between groups, a determination was made concerning whether or not each potential tracer demonstrated variation between groups. Statistical differences were reported where p-values were <0.05. This was observed for 8 out of 10 of the potential tracers – with OM and P being the only two where there was insufficient evidence to reject the null hypothesis (Tables 11 and 12). As a result, the 6 potential tracers passing this test and demonstrating conservative behaviour (Clay, Al, Fe, Mn, Si and Zn) were retained and progressed to the next step of the sediment fingerprinting process.

6.5.4 Linear Discriminant Analysis

A minimum of three tracers are required in the tracer suite due to the presence of four source groups. When completing LDA for a variety of potential tracer combinations, it was found that using Clay, Fe, Mn and Si as the tracer suite offered a reclassification accuracy of 100%. Further minimising the number of tracers used caused the reclassification accuracy to decrease so the final tracer suite was Clay, Fe, Mn and Si.

6.5.6 Unmixing Model

The results of the unmixing model used on five target samples (BG, WS, OR, PH and PL) are displayed in Figure 25 and Table 13 and expressed using means and standard deviations.

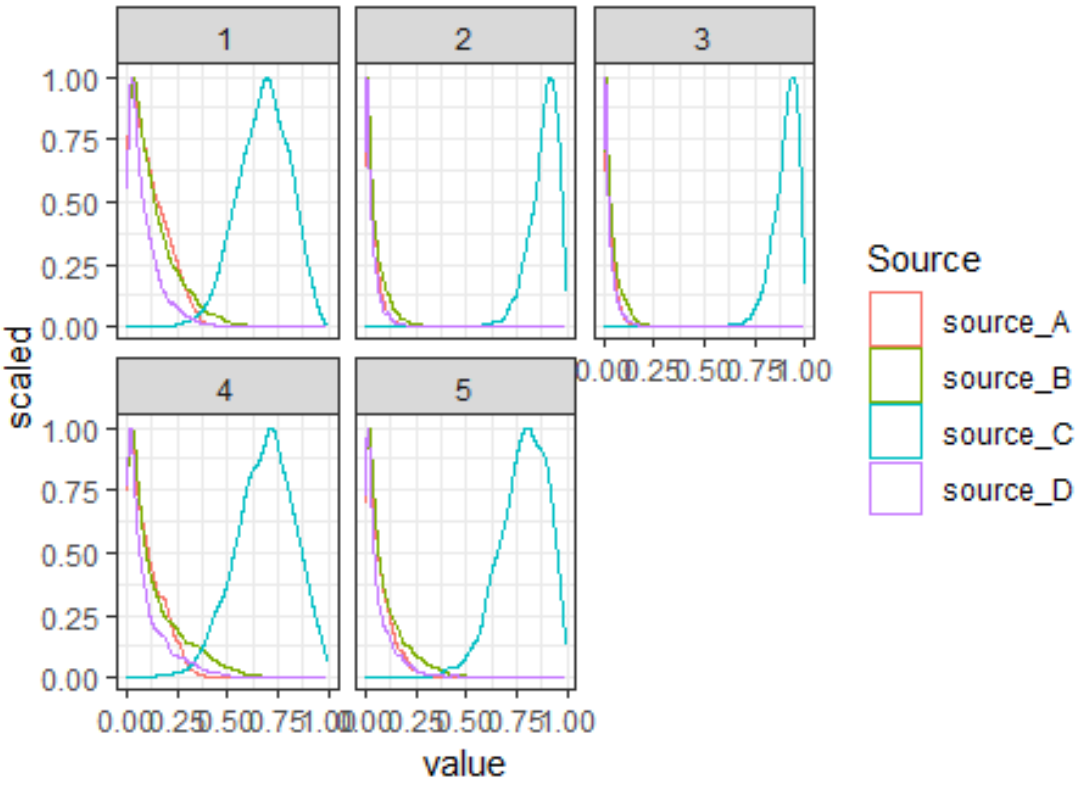

Figure 25: The results of the MixSIAR unmixing model for each of the 5 target marine samples, where 1 = BG, 2 = WS, 3 = OR, 4 = PH and 5 = PL marine samples. The curves represent the relative contribution each source group had to the respective target sample.

Table 13: The percent relative contributions and standard deviations of each source group to each target marine sample. Relative contributions and standard deviations are given to two decimal places.

Target Sample	Source Group	Relative Contribution (%)	Standard Deviation (%)
BG (1)	A	11.24	8.90
	B	12.51	11.40
	C	67.87	12.59
	D	8.38	8.13
WS (2)	A	3.36	3.31
	B	4.86	5.52
	C	88.52	12.59
	D	3.25	3.74
OR (3)	A	2.81	2.81
	B	4.13	4.72
	C	90.19	6.22
	D	2.87	3.49
PH (4)	A	9.34	8.16
	B	13.05	13.93
	C	68.27	14.52
	D	9.33	10.84
PL (5)	A	6.37	6.19
	B	8.96	9.84
	C	78.13	12.02
	D	6.53	8.22

The results of the unmixing model demonstrate that, for five target samples, the majority of sediment is transported and deposited from ghauts in source group C (Figure 25 and Table 13). All target samples have above 67% of their sediment derived from ghauts within source group C, although with large standard deviations (four out of five >12%) (Table 13). Meanwhile groups A and D are consistently the lowest contributing groups (Table 13).

6.6 Particle Size Analysis Results

The results of the sieving analyses are presented in Figure 26, demonstrating that the distribution of particle sizes vary considerably between ghaut and marine samples for all fractions. The median values for both pebbles and coarse sand were lower for marine samples than ghaut samples, but higher for fine sediment. However, the distributions of values for marine samples were broad for each grain size fraction, reflecting the variability amongst coral reefs. The percentage by weight of the three grain size fractions are also presented in Table 14 for each of the seven marine target samples.

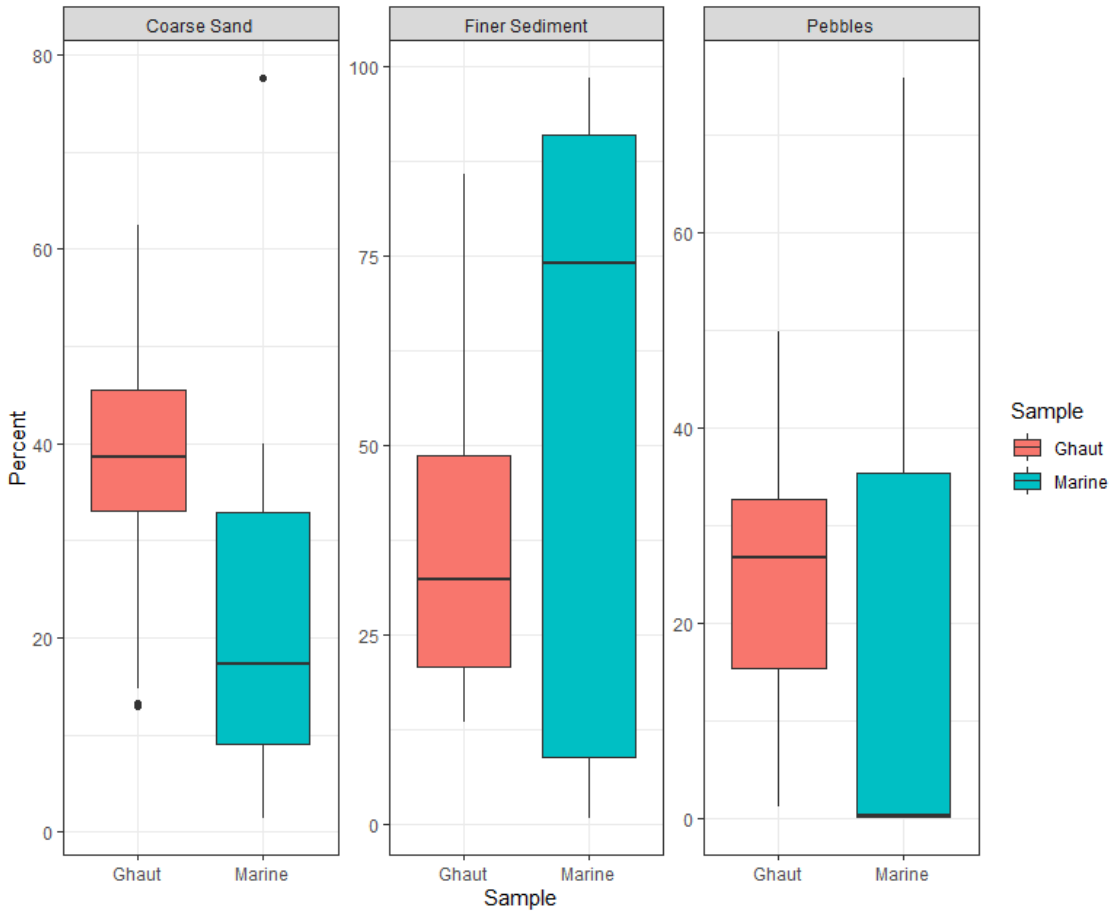

Figure 26: The percentage by weight of both ghaut and marine samples for three different grain sizes: pebbles (>2mm), coarse sand (0.5-2mm) and fine sediments (<0.5mm).

Table 14: The percentage by weight of three grain size fractions: pebbles (>2mm), coarse sand (0.5-2mm) and fine sediment (<5mm) for each of the marine samples.

Sample	Pebbles (%)	Coarse Sand (%)	Fine Sediment (%)
CB	21.49	77.64	0.91
PP	75.87	17.27	6.91
PL	49.33	40.01	10.73
PH	0.19	1.48	98.46
BG	0.09	25.95	73.99
WS	0.00	13.70	86.29
OR	0.01	4.59	95.45

The results of the Particle Size Analysis are demonstrated in Figure 27. The fractions of fine sediment have a more pronounced variation between ghaut and marine samples than the larger grains, with ghaut samples showing a greater range in values. The dominant fraction within the fine sediment fraction is that of sand, and all marine samples had high percentages (>80%), aligning with the sampling locations, rather than the preferential transfer of sand over silt or clay from the ghauts.

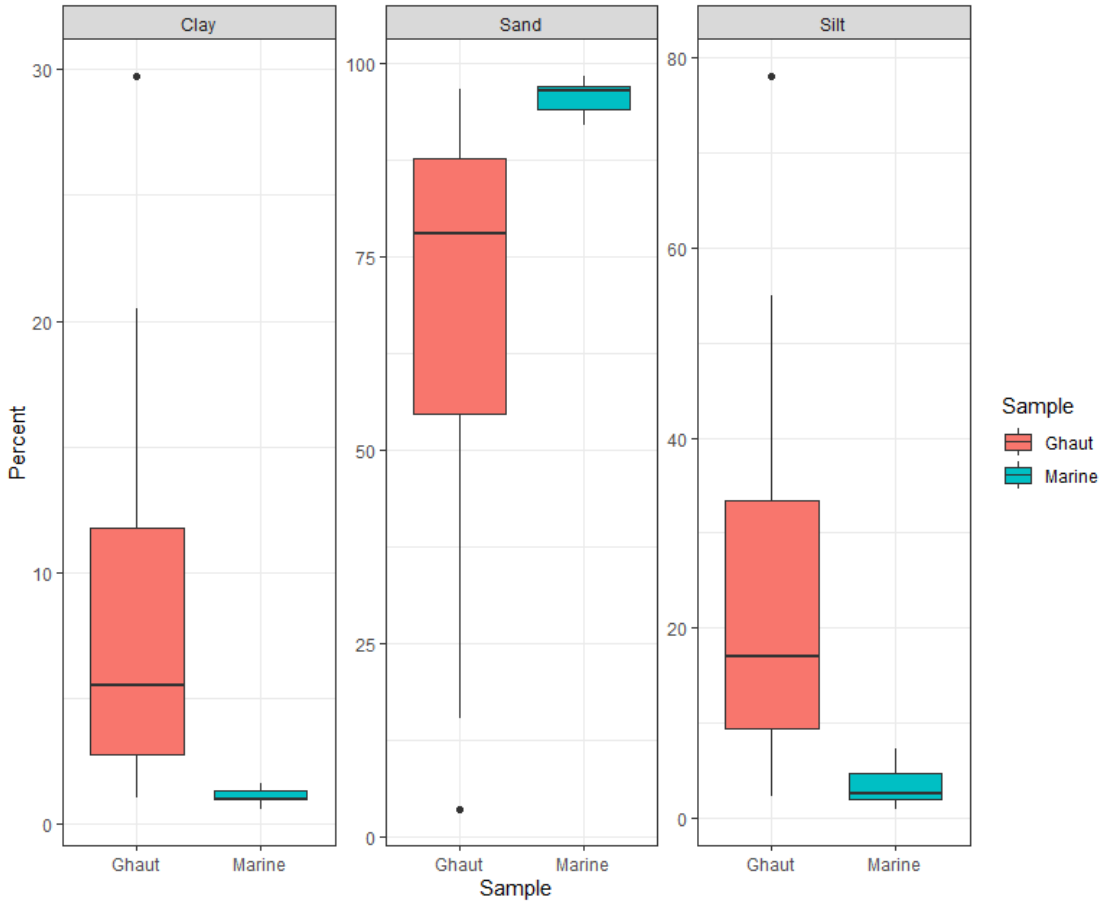

Figure 27: The percentage by volume of both ghaut and marine samples for three different grain sizes: sand (62-2000µm), silt (2-62µm) and clay (<2µm) measured using the PSA.

6.7 Discussion

6.7.1 The Use of TGA-MS Data

TGA percentage weight losses over defined temperature ranges were used as tracers rather than other signals obtained through TGA analyses, such as the position of DTG peaks, to avoid biases in terms of how various samples lose mass. For example, some samples lose mass rapidly, in a sharp distinct peak whereas others experience a loss in mass gradually across a temperature range. Therefore, use of DTG peaks as the primary sediment fingerprinting tool would be unrepresentative, where using the percentage weight loss within each range meant the bias was removed.

In terms of the CO_2 signals recorded, all but the EX1 sample (Figure 6d) displayed peaks across the duration of the experiments, aligning with the time and temperature at which DTG peaks were recorded (Appendix C). The H_2O signals, on the other hand, were more variable between samples, but after the removal of peaks within the 50-100°C temperature range and those

caused by the buoyancy effect, the H_2O signals flatlined to reveal no additional peaks in H_2O across the majority of samples (Appendix C). 15 samples did show additional peaks, all of which aligned with DTG peaks in time and temperature (Appendix C). It was concluded that all signals displayed from the mass spectrometry readings could be associated with those of the DTG signals, therefore functioning as a way of confirming the interpretations made in Chapter 5, rather than providing new insight into the samples' composition. This was also evident through testing correlations between TGA-MS variables, confirming DTG interpretations discussed in Chapter 5 (see Annex 1).

Although it was determined that mass spectrometry data alone was not suitable for sediment fingerprinting in this study, it has proved useful in many alternate applications. For instance, one prominent successful application area of TGA-MS is that of soils spiked with microplastics (Becker *et al.,* 2020; David *et al.,* 2018; Mansa and Zou, 2021). David *et al*. (2018) found the MS signal intensities responded to microplastic concentrations linearly when spiking soil samples, with positive results leading to their recommendation of its use in future studies. Alternatively, Edmondson *et al.* (2015) praised MS when distinguishing between black carbon and clay minerals in soil samples. In reflection, analysing a variety of different gases exsolved, such as scanning across AMU1-200 to find prevalent gases, may be more helpful in differentiating the samples to a higher extent and provide additional information on their composition. Therefore, the use of mass spectrometry coupled to TGA for sediment fingerprinting is encouraged despite not being applicable to this study.

The results of the study give light to the importance of considering the broader context when implementing methodologies for sediment fingerprinting. In this study, TGA was successfully implemented due to the presence of both clay minerals and organic matter in detectable quantities across all samples. Organic matter, in this context, was not a suitable tracer for sediment fingerprinting due to its inability to discriminate between source groups, however, the clay fraction was. When applying TGA to sediment fingerprinting in other catchments, very different results may be observed depending on the geology, mineralogy and physical processes of the study site. It is reasonable to conclude that in some areas TGA may provide many detectable peaks able to discriminate between sources, whilst in others, potentially no TGA results would be applicable to sediment fingerprinting. Regardless of whether TGA-derived components can act as tracers in sediment fingerprinting, this method is unequivocally useful in providing an overview of the entire sample composition to aid the understanding of the study area, as opposed to more routinely used techniques such as ICP-OES which provide information on only those elements chosen, usually requiring some previous knowledge of the study site.

6.7.2 ICP-OES Tracer Selection

For ICP-OES analysis, the elements chosen were selected based on their potential to be effective tracers and their likely prevalence in the samples. Calcium was chosen as an indicator of coral reef presence, with the expectation being that calcium concentrations would be high in the 7 marine samples and less so in the ghaut samples. Aluminium and silicon comprise the chemical signature of andisols, the main sediment type expected on Montserrat (Chapter 2). Therefore, these elements were expected to be found in high proportions in the ghaut samples. In addition, a high presence of them in the marine samples could indicate the deposition of andesitic sediment from the ghauts to the coral reefs, thus potentially making them a beneficial tracer in this study.

The remaining 8 elements were chosen based on the results of previous sediment tracing studies. Sediment fingerprinting studies often have a substantial focus on heavy metals (Table 3) due to their potential to cause great environmental harm. Nickel, zinc, copper, iron, manganese and lead are 6 of those frequently used in sediment fingerprinting. Cabral Nascimento *et al.* (2022) conducted a similar study in Brazil, whereby sediment fingerprinting was applied to ephemeral steams in a River Basin (Table 3). Although this study was concerned with the use of colour tracers, they compared them to geochemical tracers, including all the heavy metal tracers this study used, aside from copper, and determined each using ICP-OES. All the tracers mentioned above passed their conservation test in the study. Pb, Ni and Al were amongst the final tracers selected for regional source identification, whilst Fe, Al, Zn, Ni and Pb were amongst those for land use source identification. When used alone, Cabral Nascimento *et al.* (2022) found they were accurate for 98% of regional samples and 82% of land use samples, whilst in combination with colour tracers, accuracy was 95% for both. Other sediment-related studies using ICP-OES also used combinations of the chosen elements, such as Lunderberg *et al.* (2008) and Silva *et al.* (2011), but these studies focused on trace metal determination rather than sediment fingerprinting (Table 3).

Although not used as frequently in ICP-OES and sediment fingerprinting studies, Mg and P were also selected. Peña-Icart *et al.* (2017) explain how Mg (along with Ca) can indicate anthropogenic effects from events such as wastewater land flows. Giancoli Barreto *et al.* (2004) also used Mg, along with Al, Mn, Fe, Ni, Cu and Pb in ICP-OES analysis as a means of identifying potentially available metals in lake sediments, with positive results. Although phosphorous is less used as a tracer, it was included in this study due to its strong adsorption ability to soil particles (Steegen

et al., 2000). The andisols on Montserrat are comprised of volcanic glass, imogolite, allophane and halloysite in varying quantities, giving them a high phosphate fixing capacity (Padmanabhan and Reich, 2023), leading to high P concentration expectations.

6.7.3 The Removal of Calcite and Ca

Both calcite, from TGA testing, and Ca, from ICP-OES testing, were rejected as potential tracers. This was because the target samples were from coral reefs and high concentrations of Ca and calcite would be expected (Figure 28). Therefore, they would not be useful as tracers from ghaut to reef samples as the calcite and Ca would originate from the corals themselves, regardless of whether transportation and deposition from terrestrially derived sediment also occurred.

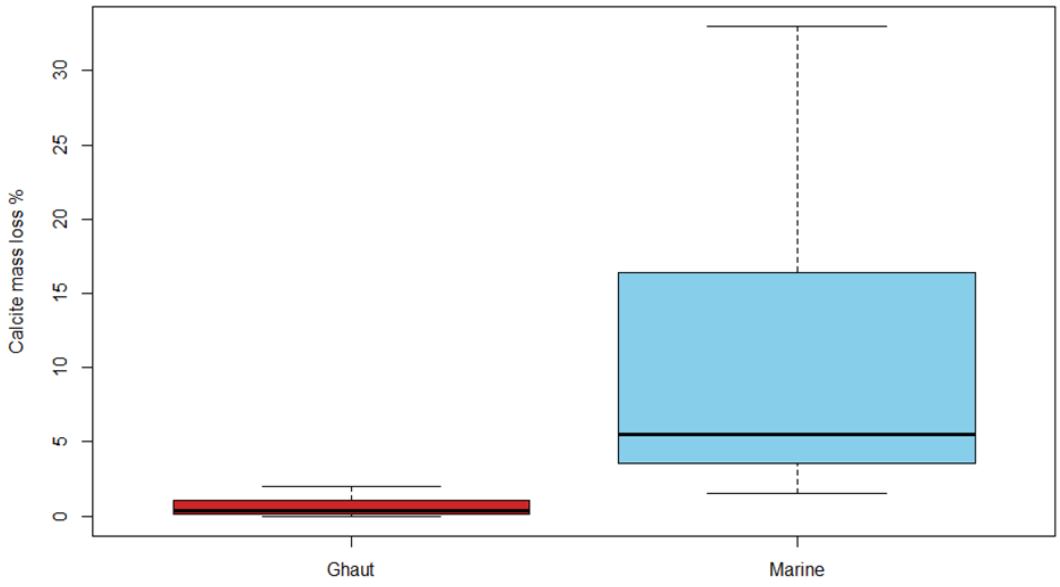

Figure 28: A boxplot of the % mass loss of calcite in both the ghaut samples and the marine samples.

6.7.4 The Removal of the CB and PP Samples

The sediment fingerprinting procedure and unmixing model successfully formed a tracer suite with a 100% reclassification rate and assigned relative contributions of each ghaut cluster group to five of the marine samples. The two additional marine samples (CB and PP) were rejected from sediment fingerprinting due to their composition. Visually, the CB and PP samples appear high in coral and shell fragments, and low on terrestrially derived sediment (Figure 18). This was also evident through the proportion of calcite and Ca in the samples in comparison to the pure shell sample (Chapter 5). The PP and CB marine samples contained the highest proportion of

calcite, at 73.35% and 50.83% respectively (Table 5), of all the marine samples and both samples' Ca concentration were too high for the detection limit of the instrument during ICP-OES analysis (Appendix D). Particle Size Analysis also reflected their low percentages of fine sediment, composed of coarser grains reflecting that of calcium carbonate (Table 14). Therefore, due to the composition of these samples and the inability to trace $CaCO_3$ to reef sites, these samples were not traced.

6.7.5 Unconservative Behaviour of Tracers

In other sediment fingerprinting studies, unconservative behaviour is often illustrated by a reduction in the parameter from source to target sample, such as occurred for copper. This is due to a range of physicochemical reactions which could occur along transportation, such as erosion or redox reactions. However, magnesium experienced the reverse, where concentrations were higher in target samples, indicative of additional Mg sources. An explanation could be the formation of high Mg-calcite. Various coral reef inhabitants precipitate calcium carbonate in different forms. For example, Sinutok *et al.* (2011) explain how the Halimeda species precipitate it as aragonite, but in contrast, foraminifera precipitate calcium carbonate as high-Mg calcite. High-magnesium calcites are those in which calcium has been replaced by magnesium atoms and is common in many marine species such as red corals and algae along with foraminifera (Long *et al.,* 2014). As a result, reefs hosting high abundances of these marine species may also exhibit high magnesium concentrations in the sediment. This could potentially explain the higher magnesium concentrations found in the target sediments, with further investigation into the types of marine species inhabiting the sites necessary for confirmation.

6.7.6 Contribution of Source Groups

The identification of which ghauts on Montserrat were depositing sediment onto coral reefs via the use of sediment fingerprinting was the overall aim of this study. This has been successfully achieved. The results of the sediment fingerprinting indicate that a large proportion (at least two-thirds) of sediment in the five marine target samples (BG, WS, OR, PH and PL) derived from ghauts in cluster group C. Group C were located on the west coast of Montserrat, consisting mainly of the most southerly ghauts sampled. These ghauts were those with closest proximity to Soufrière Hills volcano and volcanic ash fields (Chapters 1 and 3). Using the evidence gained from the laboratory analyses along with field observations (Stevens *et al.*, 2023), visual indications of the samples and knowledge of the study site, it was determined that many of the

ghaut sediment samples and sediment on the reefs were composed largely of volcanically derived material, specifically volcanic ash from current and/or past volcanic eruptions on the island. The clustering of ghaut source sample EX1 into group C (Table 7) implies the other samples in the group may contain high amounts of volcanic deposits (Chapter 5) as they are statistically similar in chemical and mineralogical composition. Geographically these locations are situated close to volcanic centres (Figure 2, Chapter 3), supporting this conclusion. The presence of clay minerals and organic matter in the reef sediment samples also provide evidence that these volcanic deposits were transported via the terrestrial landscape, i.e. the ghauts, initially before being deposited on the reefs as opposed to deposition directly from ashfalls.

In terms of location, the results stating that group C contributed most of the sediment to the coral reefs also aligned with the position of the sampling sites in relation to the Belham River, which many of the ghauts surround. With the river being a permanent watercourse, as opposed to the ephemeral nature of ghauts, this suggests the river and its tributaries provided a transportation mechanism for the sediment. Ghauts are ephemeral streams, providing a watercourse during periods of heavy rainfall. However, the wet season in Montserrat is from April to November, meaning during sampling in January-February, the ghauts were dry. As a result, the ghauts were unlikely to be providing transportation of sediment to the reefs at this time. The ghauts around the Belham River however, had additional means of transporting sediment to the sea, explaining the results of the MixSIAR model.

Three of the target samples (BG, PH and PL) were located on the northern coast of the island, where only one ghaut sampled (LB9) was placed into group C during cluster analysis. An explanation could be missing source data from a lack of ghauts sampled in the north.

6.7.7 Particle Size Analysis

Although not used for sediment fingerprinting due to unconservative behaviour, particle size analysis was conducted. Material greater in diameter than 2mm (pebbles) varies considerably between reefs, with it the majority grain size of both PP and PL marine samples (Table 14). In comparison, the percentage of pebble in the other five marine samples were below the median for the ghauts (Figure 26 and Table 14). This fraction represents large pieces of coral and shell fragments, deriving from the reefs themselves. This was reflected in the TGA weight loss data in the calcite range (Figure 18) in which the highest values of calcite were seen across the same three sample sites as the highest percentage of pebbles were seen (Table 14). This supports the

belief that the larger fraction of grains were broadly coral reef-derived. As a result, there are implications that less terrestrially-derived sediment was deposited onto the PP and PL sites.

Many coral reef studies surrounding the impacts of sediment often focus on the fine-grained sediment (Chapter 2). The results of the particle size analysis indicate that for four marine samples (BG, WS, OR and PH) the fine sediment fraction was the dominant fraction of the sample, with all >70% of the total mass (Table 14). These percentages were much higher than the median ghaut sample (Figure 26). A likely explanation is that coarser grained material is more likely to settle along the transportation route whilst fine grained sediment is more likely to remain in suspension, increasing the percentages of fine-grained sediment in the total deposited load. Additionally, physical or biogeochemical processes occurring between source and target, such as abrasion and erosion of the sediment, along with potential dilution or dissolution, may reduce grain sizes.

Particle size analysis explains the results of the range/conservative testing. The PP and CB samples contained only 0.91 and 6.91% fine sediment (Table 14). The fine sediment is that which is more likely to transport heavy metals to reefs, as well as containing the clay fraction (Uddin, 2017). As a result, a lack of fine sediment in these samples explains the observed low concentrations of heavy metals, which failed the range testing.

6.7.8 Limitations

Despite the 100% capability of the unmixing model to reclassify ghaut samples back into their correct cluster groups, the model does have limitations, evident in the large standard deviations noted in Table 13. Sediment varies in chemical, mineralogical, structural and physical properties. Therefore, tracing sediment back to a specific source is challenging, especially when limited tracers are used and not all sources can be accounted for (discussed in Chapter 7). However, the sediment fingerprinting procedure has been implemented numerous times, showing promising results and offering insightful information regardless.

6.8 Conclusions

The aim of sediment fingerprinting was to identify which ghauts transport and deposit the sediment found on the 7 coral reef samples from Montserrat. The successful application of the sediment fingerprinting procedure achieved this aim, fulfilling the objectives and indicating that the sediment on five of the seven coral reefs were likely deposited from the ghauts. The clustering and use of the unmixing model determined that the ghauts clustered into group C, containing volcanically-derived sediment mostly from recent volcanism, contributed the most.

Furthermore, the identification and successful application of the final tracer suite proved the use of geochemical and mineralogical properties of sediment are suitable tracers for sediment on Montserrat.

One of the main objectives of the project was to assess the suitability of using TGA-MS for sediment fingerprinting. Despite not applying MS signals, TGA was used successfully. Organic matter was eliminated from further use as testing found it did not vary across the sediment source groups, making it an ineffectual tracer. Clay, however, passed all tests in the tracer selection process and was one of the four tracers used in the final tracer suite. This was likely due to the nature of clay being less susceptible to transformation during transportation, in both mineralogical and chemical composition, promoting its suitability to be used as a tracer (Zöllmer and Irion, 1993). This tracer suite was then successfully applied to a Bayesian MixSIAR unmixing model and the contributions of source groups to each target site were discovered. As a result, one parameter measured using TGA-MS was successful in its application to sediment fingerprinting, fulfilling the objective.

Chapter 7: Overall Discussion and Conclusions

This final chapter aims to consolidate the work from previous chapters by drawing implications of the work to wider research areas. Recommendations for future research are made after drawing attention to the limitations of this study. The importance of this study is highlighted through exploration of the novel research presented.

7.1 Sediment Composition

TGA-MS and ICP-OES were primarily used in this study for sediment fingerprinting purposes but can also give insight into the type and nature of the sediment. Montserrat has experienced little detailed soil mapping since the onset of recent volcanic activity (see Chapter 2). The chemical analyses of collected samples aids the understanding of how sediment composition may have been altered.

Conclusions were drawn that the sediment in this study was volcanically derived as explained in Chapters 5 and 6. This was indicated through the relatively low weight loss percentages from TGA-MS analyses (Appendices B and C) in comparison to other soil/sediment studies (Kučerík *et al.,* 2012, Pallasser *et al*., 2013), reflecting that of volcanic material (Alraddadi, 2020; Denton *et al.,* 2012; Shields *et al.*, 2016).

Previous literature suggest the soils of Montserrat are andesitic (Chapter 2) and hence imply high levels of silica. Silicon is also the second most abundant element in the Earth's crust (Haynes, 2014), reflected in the high presence of silicon in many soils due to its abundance in parent material (Tubuna *et al.*, 2016). However, in this study, silicon concentrations were relatively low (Appendix D). Analyses on the chemical composition of volcanic ash from the Soufrière Hills Volcano were conducted by Baxter *et al*. in 1999. They found there were high levels of crystalline silica in the ash from the Soufrière Hills Volcano. However, an explanation for the low silicon levels found in sediment was also proposed as in situ volcanic deposits were often depleted in silica, with higher levels of Mg, Fe, Ca and Al observed (Baxter *et al.,* 1999), reflecting that of the concentrations measured in this study. This was attributed to physical alterations of the volcanic fragments such as both physical and chemical fractionation occurring during transportation of the material (Baxter *et al.,* 1999). This offers an explanation for the observed elemental concentrations whilst further implying much of the sediment was volcanically derived.

7.2 Implications of Study

7.2.1 Soil Erosion & Land Use Planning

Sediment fingerprinting is a relatively new technique with novel applications in archaeology, forensics and for health purposes by means of fingerprinting airborne particles (Owens *et al.,* 2016). However, sediment fingerprinting has been more widely used for soil mapping and erosion studies. It has the capacity to offer valuable insight into the transportation mechanisms of a catchment or larger areas. Erosion studies use this information to manage and target erosion mitigation attempts to increase their effectivity and for land-use planning.

Applications of sediment fingerprinting to erosion studies have been vast over recent decades (de Jong *et al*., 1998; Liu *et al.,* 2020; Walling and He, 1997), with Cao *et al*. (2020) explaining its significant popularity in studies on karst erosion in China. Cao *et al.* (2020) describe the issues of the expansive karst region in southwest China in terms of the poor soil stability and resultant heightened erosion, leading to a loss of fertile topsoil. This is detrimental to the food and agriculture industry, as well as the estimated 100 million people this cultivated land provides for. The use of sediment fingerprinting here has been beneficial in investigating soil loss and protecting land in order to maintain China's food security. Furthermore, de Neergaard *et al.* (2008) address the benefits gained from using sediment fingerprinting to understand how soil composition and stability may be affected by shifting cultivation and hence land use change.

This study has provided beneficial information for understanding the erosion and transportation processes occurring on Montserrat's western coast. This would benefit land surveyors if expansion of land use into the southerly regions of the Exclusion Zone of Montserrat were to begin. Due to the ongoing eruption of Soufrière Hills volcano, land use in the exclusion zone is currently prohibited and much of the land in the safe zone is under-utilised. This is true of the region surrounding the Belham River (Figures 5 and 6), where many of the ghauts in cluster group C are situated (Figure 23). Observations of land surrounding the Belham River suggest only some crop production is occurring, leaving much of the land under-utilised and of potential interest for future agricultural purposes. The results of this study could offer invaluable insight into future land-use here as much of the sediment is transported to the coral reefs (Chapter 6). Implications on the erodibility of the soil and the potential fate of fertilisers or pesticides required for agriculture may deter future land-use practices.

7.2.2 Coral Reef Conservation

Following this, the application of sediment fingerprinting to that deposited on coral reefs is important for the conservation of coral reefs. A novel study by Bainbridge *et al.* (2024) conducted similar investigations, tracing the origins of suspended particulate matter (SPM) in the Great Barrier Reef (GBR). Bainbridge *et al.'s* (2024) study also extended tracing uniquely into coral reef ecosystems with a known mechanism of transport; during flood events. The study highlighted the criticality of identifying sediment sources in order to successfully implement remediation measures for coral reef conservation. Whilst these measures would operate on a larger scale in more established reefs such as the GBR, their need is present in smaller settings such as those surrounding Montserrat. This study therefore acts as a guideline to conservationists to establish where the need for protection and remediation is most prominent.

The most vulnerable reefs are also highlighted through the particle size analysis data. The high percentages of fine sediment in four of the reef samples (Chapter 6) may indicate a higher vulnerability due to the established harmful consequences of suspended fine particulate matter to coral reef ecosystems (Chapter 2). The transport and high abundance of finer grained material and volcanic deposits may also be of concern due to the potential subsequent transport of heavy metals (Uddin, 2017). Vaithiyanathan *et al.,* (1993) describe the role of sediment as transportation mechanisms for pollutants, with sudden changes in environmental conditions allowing heavy metals to be released into water columns. This enrichment can be critical for coral reefs (Ali *et al.,* 2010, El-Sorogy *et al.*, 2012) so is of high priority to conservationists.

For Montserrat specifically, an island still rebuilding after the devastations of volcanic eruptions, areas of soil erosion and conservation may be of low priority currently, financial stability a higher concern. However, ecotourism is a sector in which many believe Montserrat has the capability to expand in the future due to its rich biodiversity, historical significance and natural beauty (Weaver, 1995). Preservation of land and coral reefs would aid the expansion of ecotourism. Therefore, this study offers potential beneficial insight into a multitude of areas, expanding beyond environmental sectors into Montserrat's economy and the future of the island.

More broadly, coral reefs surrounding volcanic islands require heightened conservation attempts due to the additional threats volcanism presents. As highlighted in Chapter 2, volcanic deposits have negative effects on coral ecosystems similar to those of sediment. However, the threats to coral reefs are exacerbated by volcanism as the sediment loads from volcanic events such as pyroclastic flows and ashfalls are much larger than sediment loads from terrestrial sources such as overland flows. Ashfalls have the potential to deposit sediment in ranges of tonnes, as

explained in Chapter 2, with these loads deposited in a short amount of time. Therefore, the coral reefs are exposed to large quantities of harmful sediment quickly, with no time to acclimatise to the new environment, thereby lessening their chances of survival and recovery.

7.3 Limitations of Study

When discussing the results of the study it is important to acknowledge associated limitations. One main limitation is in the concept of sediment fingerprinting and the procedure itself. The method used to complete sediment fingerprinting does not take into consideration multiple factors which may influence results. For instance, only sources sampled and used in the model are considered, however, other sources may be present. In this study those could include additional ghauts, cliffs which face erosion into the sea, or the Belham River. Furthermore, in sediment fingerprinting studies concerning marine environments, it must be acknowledged that sediment can be transported within the sea via ocean currents from additional sources, along with the presence of aeolian deposits, in this study, a factor which may cause the deposition of fine volcanic ash onto coral reefs.

Limitations for sediment fingerprinting also arise from large uncertainties surrounding the unmixing model. The effectiveness of the model depends on a range of parameters including the number of samples used, the reclassification ability of the selected tracer suite and the level of variation present between source groups. This is evident in the large standard deviations present in this study (Chapter 6) and is observed in a number of other sediment fingerprinting studies (Collins *et al.,* 1997; Gholami *et al.,* 2017).

Other limitations and sources of error arise from those surrounding laboratory experiments and procedures. For example, instrument error, cross contamination or the issues surrounding sample representativeness discussed in Chapter 4. Careful consideration and practice was undertaken to ensure all laboratory-based sources of error were minimised.

7.4 Future Recommendations

For future studies, recommendations are made mainly in the development of the methodology. Based on the results of this study and hypotheses surrounding the identity of the sediment analysed, initial collection and testing of volcanic ash samples from Soufrière Hills volcano and the volcanic ash fields on Montserrat are advised. Obtaining the TGA thermogram and elemental concentrations for pure volcanic deposits from the volcano they are thought to derive from

would be a way to confirm the hypotheses made in this study surrounding the sediment composition. The inclusion of microscopy for enhanced visual analysis of the samples would be of benefit, along with more extensive and detailed reef sampling methods. Field sampling ghauts further to the north and at various times of the year would also serve to enhance the rigidity of the study. Due to the ephemeral nature of the ghauts, their influence on sediment transport and deposition onto coral reefs likely varies throughout the year depending on the wet season. In this study, samples were taken prior to the wet season, when ghauts were dry. However, sampling during or after the wet season may develop different sediment fingerprinting results as their ability to act as a transfer route is enhanced.

Additionally, one of the main aims and novel concepts in this study was the suitability of using TGA-MS for sediment fingerprinting purposes. Chapter 6 explains how, in this context, mass spectrometry was not effective, however expansion of the exsolved gas analyses could rectify this, where scanning for additional gases would increase the likelihood that exsolved gas analysis could be used as well as the TGA data.

Furthermore, use of artificial tracers such as short-lived radionuclides, may prove effective in increasing confidence of assigning sources. Short-lived radionuclides would be a suitable option and have been successfully implemented in sediment fingerprinting studies previously. For example, Belmont *et al.* (2014) used excess ^{210}Pb and ^{137}Cs as two of three tracers used to distinguish between sediment sources in watersheds in mathematical models. The use of environmental radionuclides has become an established global practice, with uses across the European (Walling, 2003), North American (Nagle and Ritchie, 1999) and Asian continents (Mizugaki *et al.,* 2008). Application to Montserrat and other islands in the Lesser Antilles is therefore a likely suitable technique to incorporate for robust measurements and outcomes.

7.5 Conclusions

This study incorporates many environmental concerns and concepts: erosion, coral reef vulnerability and protection, sedimentation and the issues surrounding identifying sediment sources. Knowledge gaps and areas with a lack of research were identified. These included soil surveys and studies on the island of Montserrat, the application of sediment fingerprinting to marine environments and the use of TGA-MS for sediment fingerprinting. Aims of filling these research gaps led the study to incorporate novel applications and methodologies, applying them successfully to established sediment fingerprinting practices.

In contribution to providing modern understandings of the sediment types and compositions on Montserrat, this study opened the door for erosion mitigation, management and protection practices on Montserrat by providing statistical evidence of source areas of sediment transport on the island, as explained in Chapter 6.

The use of TGA-MS for sediment fingerprinting was specifically highlighted. Whilst information gained from the mass spectrometry component of the technique was not directly applied, it was concluded that this is a viable technique with scope to be applied to future sediment fingerprinting studies following adjustments to the method (Chapters 5, 6 and 7).

Finally, this study highlighted multiple times the importance of considering the broader context of the study area when considering methodologies and approaches to sediment fingerprinting. The fraction of samples used, pre-treatment of samples and the methods for obtaining geochemical tracers are subject to the wider area of study, with consideration needed to the uniqueness of the studied landscape and most accurate means of representing the processes taking place. For soil catchment studies taking place on volcanic islands, the processes and sediment grain sizes present will vary considerably from that of non-volcanic areas and consideration of these is essential.

References

Ajaj, R., Shahin, S., Adel, M., Salem, M., Kurup, S. and Cheruth, A.-J. (2018). *Elemental Fingerprint of Agriculture Soils of Eastern Region of the Arabian Desert by ICP-OES with GIS Mapping*. Current Environmental Engineering , 5(1), p.20. doi:https://doi.org/10.2174/2212717805666180507155251.

Alexander, J., Barclay, J., Sušnik, J., Loughlin, S.C., Herd, R.A., Darnell, A. and Crosweller, S. (2010). *Sediment-charged flash floods on Montserrat: The influence of synchronous tephra fall and varying extent of vegetation damage*. Journal of Volcanology and Geothermal Research, 194(4), pp.127–138. doi:https://doi.org/10.1016/j.jvolgeores.2010.05.002.

Ali, A.A.M., Hamed, M.A. and Abd El-Azim, H. (2010). *Heavy metals distribution in the coral reef ecosystems of the Northern Red Sea*. Helgoland Marine Research, 65(1), pp.67–80. doi:https://doi.org/10.1007/s10152-010-0202-7.

Alraddadi, S. (2020). *Surface and thermal properties of fine black and white volcanic ash.* Materials Today: Proceedings, 26, pp.1964–1966. doi:https://doi.org/10.1016/j.matpr.2020.02.429.

Álvarez-Romero, J.G., Pressey, R.L., Ban, N.C., Vance-Borland, K., Willer, C., Klein, C.J. and Gaines, S.D. (2011). *Integrated Land-Sea Conservation Planning: The Missing Links*. Annual Review of Ecology, Evolution, and Systematics, 42(1), pp.381–409. doi:https://doi.org/10.1146/annurev-ecolsys-102209-144702.

Applegarth, L.J., Tuffen, H., James, M.R. and Pinkerton, H. (2013). *Degassing-driven crystallisation in basalts*. Earth-Science Reviews, 116, pp.1–16. doi:https://doi.org/10.1016/j.earscirev.2012.10.007.

Bainbridge, Z.T., Olley, J.M., Lewis, S.E., Stevens, T. and Smithers, S.G. (2024). *Tracing sources of inorganic suspended particulate matter in the Great Barrier Reef lagoon, Australia*. Scientific Reports, 14(1). doi:https://doi.org/10.1038/s41598-024-66561-5.

Bannister, R.J., Battershill, C.N. and de Nys, R. (2012). *Suspended sediment grain size and mineralogy across the continental shelf of the Great Barrier Reef: Impacts on the physiology of a coral reef sponge*. Continental Shelf Research, 32, pp.86–95. doi:https://doi.org/10.1016/j.csr.2011.10.018.

Barclay, J., Alexander, J. and Sušnik, J. (2007). *Rainfall-induced lahars in the Belham Valley, Montserrat, West Indies*. Journal of the Geological Society, 164(4), pp.815–827. doi:https://doi.org/10.1144/0016-76492006-078.

Barclay, J., Johnstone, J.E. and Matthews, A.J. (2006). *Meteorological monitoring of an active volcano: Implications for eruption prediction*. Journal of Volcanology and Geothermal Research, 150(4), pp.339–358. doi:https://doi.org/10.1016/j.jvolgeores.2005.07.020.

Batista, P.V.G., Laceby, J.P. and Evrard, O. (2022). *How to evaluate sediment fingerprinting source apportionments*. Journal of Soils and Sediments, 22(4), pp.1315–1328. doi:https://doi.org/10.1007/s11368-022-03157-4.

Baxter, P.J., Bonadonna, C., Dupree, R., Hards, V.L., Kohn, S.C., Murphy, M.D., Nichols, A., Nicholson, R.A., Norton, G., Searl, A., Sparks, R.S.J. and Vickers, B.P. (1999). *Cristobalite in Volcanic Ash of the Soufriere Hills Volcano, Montserrat, British West Indies*. Science, 283(5405), pp.1142–1145. doi:https://doi.org/10.1126/science.283.5405.1142.

Becker, R., Altmann, K., Sommerfeld, T. and Braun, U. (2020). *Quantification of microplastics in a freshwater suspended organic matter using different thermoanalytical methods – outcome of an interlaboratory comparison.* Journal of Analytical and Applied Pyrolysis, 148, p.104829. doi:https://doi.org/10.1016/j.jaap.2020.104829.

Bell, P.R.F. (1992). *Eutrophication and coral reefs—some examples in the Great Barrier Reef lagoon*. Water Research, [online] 26(5), pp.553–568. doi:https://doi.org/10.1016/0043-1354(92)90228-v.

Belmont, P., Willenbring, J.K., Schottler, S.P., Marquard, J., Kumarasamy, K. and Hemmis, J.M. (2014). *Toward generalizable sediment fingerprinting with tracers that are conservative and nonconservative over sediment routing timescales*. Journal of Soils and Sediments, 14(8), pp.1479–1492. doi:https://doi.org/10.1007/s11368-014-0913-5.

Bish, D.L. and Duffy, C.J. (1990). Thermogravimetric Analysis of Minerals. In: Thermal Analysis in Clay Science. The Clays Mineral Society.

Biguenet, M., Sabatier, P., Éric Chaumillon, Chagué, C., Arnaud, F., Jorissen, F., Thibault Coulombier, Geba, E., Cordrie, L., Vacher, P., Anne-Lise Develle, Émilie Chalmin, Fayçal Soufi and Feuillet, N. (2021). *A 1600 year-long sedimentary record of tsunamis and hurricanes in the Lesser Antilles (Scrub Island, Anguilla). Sedimentary Geology*, 412, pp.105806–105806. doi:https://doi.org/10.1016/j.sedgeo.2020.105806.

Blake, W.H., Ficken, K.J., Taylor, P., Russell, M.A. and Walling, D.E. (2012). *Tracing crop-specific sediment sources in agricultural catchments*. Geomorphology, 139-140, pp.322–329. doi:https://doi.org/10.1016/j.geomorph.2011.10.036.

Cabral Nascimento, R., Jamil Maia, A., Jacques Agra Bezerra da Silva, Y., Farias Amorim, F., Williams Araújo do Nascimento, C., Tiecher, T., Evrard, O., Collins, A.L., Miranda Biondi, C. and Jacques Agra Bezerra da Silva, Y. (2022). *Applying geochemical and colour properties to quantify sediment sources in a Brazilian semiarid ephemeral river system*. Journal of Hydrology, 613, p.128360. doi:https://doi.org/10.1016/j.jhydrol.2022.128360.

Cao, Z., Zhang, Z., Zhang, K., Wei, X., Xiao, S. and Yang, Z. (2020). *Identifying and estimating soil erosion and sedimentation in small karst watersheds using a composite fingerprint technique*. Agriculture, Ecosystems & Environment, 294, p.106881. doi:https://doi.org/10.1016/j.agee.2020.106881.

Cantarero, S.I., Tanzil, J. T. I., and Goodkin, N.F. (2016). *Simultaneous analysis of Ba and Sr to Ca ratios in scleractinian corals by inductively coupled plasma optical emissions spectrometry*. Limnology and Oceanography: Methods, 15(1), pp.116–123. doi:https://doi.org/10.1002/lom3.10152.

Cassidy, M., Watt, S., Palmer, M.R., Trofimovs, J., Symons, W., Maclachlan, S. and Stinton, A. (2014). *Construction of volcanic records from marine sediment cores: A review and case study (Montserrat, West Indies)*. Earth-Science Reviews, 138, pp.137–155. doi:https://doi.org/10.1016/j.earscirev.2014.08.008.

Chalaux-Clergue, T., Bizeul, R., Batista, P.V.G., Martinez-Carreras, N., Laceby, J.P. and Evrard, O. (2024). *Sensitivity of source sediment fingerprinting to tracer selection methods*. European Geosciences Union , 10(1).

Chauhan, R., Kumar, R., Diwan, P.K. and Sharma, V. (2020). *Thermogravimetric analysis and chemometric based methods for soil examination: Application to soil forensics.* Forensic Chemistry, [online] 17, p.100191. doi:https://doi.org/10.1016/j.forc.2019.100191.

Collins, A.L., Walling, D.E. and Leeks, G.J.L. (1997). *Source type ascription for fluvial suspended sediment based on a quantitative composite fingerprinting technique*. CATENA, 29(1), pp.1–27. doi:https://doi.org/10.1016/s0341-8162(96)00064-1.

Collins, A.L., Walling, D.E., Webb, L. and King, P. (2010). *Apportioning catchment scale sediment sources using a modified composite fingerprinting technique incorporating property*

weightings and prior information. Geoderma, 155(3-4), pp.249–261. doi:https://doi.org/10.1016/j.geoderma.2009.12.008.

Critter, S.A.M. and Airoldi, C. (2006). *Thermal analysis of brazilian tropical soils originating from different sources*. Journal of the Brazilian Chemical Society, 17(7), pp.1250–1258. doi:https://doi.org/10.1590/s0103-50532006000700009.

David, J., Steinmetz, Z., Kučerík, J. and Schaumann, G.E. (2018). *Quantitative Analysis of Poly(ethylene terephthalate) Microplastics in Soil via Thermogravimetry–Mass Spectrometry*. Analytical Chemistry, 90(15), pp.8793–8799. doi:https://doi.org/10.1021/acs.analchem.8b00355.

De'ath, G. and Fabricius, K. (2010). *Water quality as a regional driver of coral biodiversity and macroalgae on the Great Barrier Reef.* Ecological Applications, 20(3), pp.840–850. doi:https://doi.org/10.1890/08-2023.1.

de Jong, E., Nestor, P.A., and Pennock, D.J. (1998). The use of magnetic susceptibility to measure long-term soil redistribution. CATENA, 32(1), pp.23–35. doi:https://doi.org/10.1016/s0341-8162(97)00051-9.

DeLapp, R.C. and LeBoeuf, E.J. (2004). *Thermal Analysis of Whole Soils and Sediment.* Journal of Environmental Quality, 33(1), pp.330–337. doi:https://doi.org/10.2134/jeq2004.3300.

DelValls, T.A., Forja, J.M., González-Mazo, E., Abelardo Gómez-Parra and Blasco, J. (1998). Determining contamination sources in marine sediments using multivariate analysis. Trends in Analytical Chemistry, 17(4), pp.181–192. doi:https://doi.org/10.1016/s0165-9936(98)00017-x.

de Neergaard, A., Magid, J. and Mertz, O. (2008). *Soil erosion from shifting cultivation and other smallholder land use in Sarawak, Malaysia*. Agriculture, Ecosystems & Environment, 125(1-4), pp.182–190. doi:https://doi.org/10.1016/j.agee.2007.12.013.

Denton, J.S., Tuffen, H. and Gilbert, J.S. (2012). *Variations in hydration within perlitised rhyolitic lavas—evidence from Torfajökull, Iceland*. Journal of Volcanology and Geothermal Research, 223-224, pp.64–73. doi:https://doi.org/10.1016/j.jvolgeores.2012.02.005.

Du, Y., Zhang, Y. and Shi, J. (2019). *Relationship between sea surface salinity and ocean circulation and climate change*. Science China Earth Sciences, [online] 62(5), pp.771–782. doi:https://doi.org/10.1007/s11430-018-9276-6.

Duckworth, A., Giofre, N. and Jones, R. (2017). *Coral morphology and sedimentation*. Marine Pollution Bulletin, 125(1-2), pp.289–300. doi:https://doi.org/10.1016/j.marpolbul.2017.08.036.

Dümichen, E., Eisentraut, P., Bannick, C.G., Barthel, A.-K., Senz, R. and Braun, U. (2017). *Fast identification of microplastics in complex environmental samples by a thermal degradation method*. Chemosphere, 174, pp.572–584. doi:https://doi.org/10.1016/j.chemosphere.2017.02.010.

Duprey, N.N., Yasuhara, M. and Baker, D.M. (2016). *Reefs of tomorrow: eutrophication reduces coral biodiversity in an urbanized seascape*. *Global Change Biology*, 22(11), pp.3550–3565. doi:https://doi.org/10.1111/gcb.13432.

East, C.P., Doherty, William, O.S., Fellows, C.M. and Yu, H. (2010). *Formation of thermodynamically unstable calcium oxalate dihydrate in sugar mill evaporators*. International sugar journal, 113(1346), pp.522–533.

Edmonds, M., Herd, R.A. and Strutt, M.H. (2006). *Tephra deposits associated with a large lava dome collapse, Soufrière Hills Volcano, Montserrat, 12–15 July 2003*. Journal of Volcanology and Geothermal Research, 153(3-4), pp.313–330. doi:https://doi.org/10.1016/j.jvolgeores.2005.12.008.

Edmondson, J.L., Stott, I., Potter, J., Lopez-Capel, E., Manning, D.A.C., Gaston, K.J. and Leake, J.R. (2015). *Black Carbon Contribution to Organic Carbon Stocks in Urban Soil.* Environmental Science & Technology, 49(14), pp.8339–8346. doi:https://doi.org/10.1021/acs.est.5b00313.

El-Sorogy, A.S., Mohamed, M.A. and Nour, H.E. (2012). *Heavy metals contamination of the Quaternary coral reefs, Red Sea coast, Egypt*. Environmental Earth Sciences, 67(3), pp.777–785. doi:https://doi.org/10.1007/s12665-012-1535-0.

Farivar, F., Lay Yap, P., Karunagaran, R.U. and Losic, D. (2021*). Thermogravimetric Analysis (TGA) of Graphene Materials: Effect of Particle Size of Graphene, Graphene Oxide and Graphite on Thermal Parameters*. C, [online] 7(2), p.41. doi:https://doi.org/10.3390/c7020041.

Fatahi, A., Gholami, H., Esmaeilpour, Y. and Fathabadi, A. (2022). *Fingerprinting the spatial sources of fine-grained sediment deposited in the bed of the Mehran River, southern Iran*. Scientific Reports, 12(1). doi:https://doi.org/10.1038/s41598-022-07882-1.

Feller, C., Clermont-Dauphin, C., Venkatapen, C., Albrecht, A., Arrouays, D., Bernoux, M., Blanchart, E., Cabidoche, Y.M., Cerri, C.E.P., Chevallier, T. and Larré-Larrouy, M.C., (2006). Soil Organic Carbon Sequestration in the Caribbean. *Carbon Sequestration in Soils of Latin America*, p.187.

Fernández, J.M., Clément Peltre, Craine, J.M. and Plante, A.F. (2012). *Improved Characterization of Soil Organic Matter by Thermal Analysis Using CO2/*H_2O *Evolved Gas Analysis*. Environmental science & technology, 46(16), pp.8921–8927. doi:https://doi.org/10.1021/es301375d.

Flower, J., Ramdeen, R., Estep, A., Thomas, L.R., Francis, S., Goldberg, G., Johnson, A.E., McClintock, W., Mendes, S.R., Mengerink, K., O'Garro, M., Rogers, L., Zischka, U. and Lester, S.E. (2020). *Marine spatial planning on the Caribbean island of Montserrat: Lessons for data-limited small islands*. Conservation Science and Practice, 2(4). doi:https://doi.org/10.1111/csp2.158.

Földvári, M. (2011). *Handbook of thermogravimetric system of minerals and its use in geological practice.* Budapest: Geological Institute Of Hungary.

Fourney, F. and Figueiredo, J. (2017). *Additive negative effects of anthropogenic sedimentation and warming on the survival of coral recruits*. Scientific Reports, 7(1). doi:https://doi.org/10.1038/s41598-017-12607-w.

Galan, I., Glasser, F.P. and Andrade, C. (2012). *Calcium carbonate decomposition*. Journal of Thermal Analysis and Calorimetry, 111(2), pp.1197–1202. doi:https://doi.org/10.1007/s10973-012-2290-x.

Gandais, V. (1987). *Clay mineral sources of the Grenada Basin, Southeastern Caribbean*. Clay Minerals, 22(4), pp.395–400. doi:https://doi.org/10.1180/claymin.1987.022.4.03.

García-Comendador, J., Fortesa, J., Calsamiglia, A., Garcias, F. and Estrany, J. (2017). *Source ascription in bed sediments of a Mediterranean temporary stream after the first post-fire flush.* Journal of Soils and Sediments, 17(11), pp.2582–2595. doi:https://doi.org/10.1007/s11368-017-1806-1.

García-Ruiz, J.M., Beguería, S., Nadal-Romero, E., González-Hidalgo, J.C., Lana-Renault, N. and Sanjuán, Y. (2015). *A meta-analysis of soil erosion rates across the world*. Geomorphology, 239, pp.160–173. doi:https://doi.org/10.1016/j.geomorph.2015.03.008.

Garcia-Soto, C., Garcia-Soto, C., Cheng, L., Caesar, L., Caesar, L., Schmidtko, S., Jewett, E.B., Cheripka, A., Rigor, I., Caballero, A., Chiba, S., Báez, J.C., Báez, J.C., Zielinski, T. and Abraham, J.P.

(2021*). An Overview of Ocean Climate Change Indicators: Sea Surface Temperature, Ocean Heat Content, Ocean pH, Dissolved Oxygen Concentration, Arctic Sea Ice Extent, Thickness and Volume, Sea Level and Strength of the AMOC (Atlantic Meridional Overturning Circulation)*. Frontiers in Marine Science, [online] 8. doi:https://doi.org/10.3389/fmars.2021.642372.

Gholami, H., Telfer, M.W., Blake, W.H. and Fathabadi, A. (2017). *Aeolian sediment fingerprinting using a Bayesian mixing model*. Earth Surface Processes and Landforms, 42(14), pp.2365–2376. doi:https://doi.org/10.1002/esp.4189.

Giancoli Barreto, S.R., Nozaki, J., De Oliveira, E., Do Nascimento Filho, V.F., Aragão, P.H.A., Scarminio, I.S. and Barreto, W.J. (2004). *Comparison of metal analysis in sediments using EDXRF and ICP-OES with the HCl and Tessie extraction methods.* Talanta, 64(2), pp.345–354. doi:https://doi.org/10.1016/j.talanta.2004.02.022.

Guzmán, H.M. and Jiménez, C.E. (1992). *Contamination of coral reefs by heavy metals along the Caribbean coast of Central America (Costa Rica and Panama).* Marine Pollution Bulletin, 24(11), pp.554–561. doi:https://doi.org/10.1016/0025-326x(92)90708-e.

Habibi, S., Gholami, H., Aboalhasan Fathabadi and Jansen, J.A. (2019*). Fingerprinting sources of reservoir sediment via two modelling approaches.* Science of the Total Environment, 663, pp.78–96. doi:https://doi.org/10.1016/j.scitotenv.2019.01.327.

Habineza, E., Rodgers Makwinja and Inagaki, Y. (2023). *Contamination and health risks of trace metals in water and sediments of May Sieley stream, Ethiopia*. Physics and Chemistry of the Earth, Parts A/B/C, 129, pp.103315–103315. doi:https://doi.org/10.1016/j.pce.2022.103315.

Hardy, F., Rodrigues, G. Nanton, W.R.E (1949). *The Agricultural Soils of Montserrat*. Studies in West Indian Soils, Trinidad.

Harrington, L., Fabricius, K., Eaglesham, G. and Negri, A. (2005). *Synergistic effects of diuron and sedimentation on photosynthesis and survival of crustose coralline algae.* Marine Pollution Bulletin, 51(1-4), pp.415–427. doi:https://doi.org/10.1016/j.marpolbul.2004.10.042.

Hautmann, S., Camacho, A.G., Gottsmann, J., Odbert, H.M. and Syers, R.T. (2013). *The shallow structure beneath Montserrat (West Indies) from new Bouguer gravity data*. Geophysical Research Letters, 40(19), pp.5113–5118. doi:https://doi.org/10.1002/grl.51003.

Haynes, R.J. (2014). *A contemporary overview of silicon availability in agricultural soils*. Journal of Plant Nutrition and Soil Science, 177(6), pp.831–844. doi:https://doi.org/10.1002/jpln.201400202.

Hemmings, B., Whitaker, F., Gottsmann, J. and Hughes, A. (2015). *Hydrogeology of Montserrat review and new insights*. Journal of Hydrology: Regional Studies, [online] 3, pp.1–30. doi:https://doi.org/10.1016/j.ejrh.2014.08.008.

Hou, X., Amais, R.S., Jones, B.T, Donati, G.L. (2006). *Inductively coupled plasma optical emission spectrometry*. Encyclopedia of Analytical Chemistry: Applications, Theory and Instrumentation 1-25

Idris, S.S., Rahman, N.A., Ismail, K., Alias, A.B., Rashid, Z.A. and Aris, M.J. (2010). *Investigation on thermochemical behaviour of low rank Malaysian coal, oil palm biomass and their blends during pyrolysis via thermogravimetric analysis (TGA).* Bioresource Technology, 101(12), pp.4584–4592. doi:https://doi.org/10.1016/j.biortech.2010.01.059.

Jaramillo, L., Agioutanti, E., Afrouz, S.G., Keles, C., and Sarver, E. (2022). *Thermogravimetric analysis of respirable coal mine dust for simple source apportionment*. Journal of Occupational and Environmental Hygiene, 19(9), pp.568–579. doi:https://doi.org/10.1080/15459624.2022.2100409.

Javadi, S., Hashemy, S.M., Mohammadi, K., Howard, K.W.F. and Neshat, A. (2017). *Classification of aquifer vulnerability using K-means cluster analysis*. Journal of Hydrology, 549, pp.27–37. doi:https://doi.org/10.1016/j.jhydrol.2017.03.060.

Jensen, J.L., Christensen, B.T., Schjønning, P., Watts, C.W. and Munkholm, L.J. (2018). *Converting loss-on-ignition to organic carbon content in arable topsoil: pitfalls and proposed procedure*. European Journal of Soil Science, [online] 69(4), pp.604–612. doi:https://doi.org/10.1111/ejss.12558.

Johansen, J.L., Messmer, V., Coker, D.J., Hoey, A.S. and Pratchett, M.S. (2013). *Increasing ocean temperatures reduce activity patterns of a large commercially important coral reef fish.* Global Change Biology, 20(4), pp.1067–1074. doi:https://doi.org/10.1111/gcb.12452.

Jones, M.T., Hembury, D.J., Palmer, M.R., Tonge, B., Darling, W.G. and Loughlin, S.C. (2010). *The weathering and element fluxes from active volcanoes to the oceans: a Montserrat case study.* Bulletin of Volcanology, 73(3), pp.207–222. doi:https://doi.org/10.1007/s00445-010-0397-0.

Jones, L.A., Mannion, P.D., Farnsworth, A., Bragg, F. and Lunt, D.J. (2022*). Climatic and tectonic drivers shaped the tropical distribution of coral reefs.* Nature Communications, 13(1). doi:https://doi.org/10.1038/s41467-022-30793-8.

Kaplin, C. and Brochu, M. (2014). *The effect of grain size on the oxidation of NiCoCrAlY.* Applied Surface Science, [online] 301, pp.258–263. doi:https://doi.org/10.1016/j.apsusc.2014.02.056.

Karunadasa, K.S.P., Manoratne, C.H., Pitawala, H.M.T.G.A. and Rajapakse, R.M.G. (2019). *Thermal decomposition of calcium carbonate (calcite polymorph) as examined by in-situ high-temperature X-ray powder diffraction*. Journal of Physics and Chemistry of Solids, [online] 134, pp.21–28. doi:https://doi.org/10.1016/j.jpcs.2019.05.023.

Khan, S.R., Sharma, B., Chawla, P.A. and Bhatia, R. (2021*). Inductively Coupled Plasma Optical Emission Spectrometry (ICP-OES): a Powerful Analytical Technique for Elemental Analysis*. Food Analytical Methods, 15(3), pp.666–688. doi:https://doi.org/10.1007/s12161-021-02148-4.

Kleypas, J.A., McManus, J.W. and Meñez, L.A.B. (1999*). Environmental Limits to Coral Reef Development: Where Do We Draw the Line?* American Zoologist, 39(1), pp.146–159. doi:https://doi.org/10.1093/icb/39.1.146.

Koiter, A.J., Owens, P.N., Petticrew, E.L. and Lobb, D.A. (2013). *The behavioural characteristics of sediment properties and their implications for sediment fingerprinting as an approach for identifying sediment sources in river basins*. Earth-Science Reviews, 125, pp.24–42. doi:https://doi.org/10.1016/j.earscirev.2013.05.009.

Kookana, R.S., Baskaran, S. and Naidu, R. (1998). *Pesticide fate and behaviour in Australian soils in relation to contamination and management of soil and water: a review*. Soil Research, 36(5), p.715. doi:https://doi.org/10.1071/s97109.

Kristl, M., Muršec, M., Šuštar, V. and Kristl, J. (2015). *Application of thermogravimetric analysis for the evaluation of organic and inorganic carbon contents in agricultural soils*. Journal of Thermal Analysis and Calorimetry, 123(3), pp.2139–2147. doi:https://doi.org/10.1007/s10973-015-4844-1.

Kučerík, J., Čtvrtníčková, A. and Siewert, C. (2012). *Practical application of thermogravimetry in soil science*. Journal of Thermal Analysis and Calorimetry, 113(3), pp.1103–1111. doi:https://doi.org/10.1007/s10973-012-2849-6.

Kuzminov, F.I., Brown, C.M., Fadeev, V.V. and Gorbunov, M.Y. (2013). *Effects of metal toxicity on photosynthetic processes in coral symbionts, Symbiodinium spp*. Journal of Experimental Marine Biology and Ecology, 446, pp.216–227. doi:https://doi.org/10.1016/j.jembe.2013.05.017.

Lamba, J., Karthikeyan, K.G. and Thompson, A.M. (2015). *Apportionment of suspended sediment sources in an agricultural watershed using sediment fingerprinting*. Geoderma, 239-240, pp.25–33. doi:https://doi.org/10.1016/j.geoderma.2014.09.024.

Lang, D. M. (1967). *Montserrat: Soil and Land Use Surveys, No. 22. Soil and Land Use Section*, The Regional Research Center, University of the West Indies, Imperial College of Tropical Agriculture, Trinidad, West Indies.

Lebron, I., Cooper, D.M., Brentegani, M., Bentley, L., Dos, G., Keenan, P., Cosby, J., Emmet, B. and Robinson, D.A. (2023). *Soil carbon determination for long-term monitoring revisited using thermo-gravimetric analysis.* Vadose Zone Journal. doi:https://doi.org/10.1002/vzj2.20300.

Lesser, M.P. (2021). *Eutrophication on Coral Reefs: What Is the Evidence for Phase Shifts, Nutrient Limitation and Coral Bleaching*. BioScience, [online] 71(12). doi:https://doi.org/10.1093/biosci/biab101.

Li, L., Yang, Y., Lv, Y., Yin, P. and Lei, T. (2020). *Porous calcite CaCO3 microspheres: Preparation, characterization and release behavior as doxorubicin carrier*. Colloids and Surfaces B: Biointerfaces, 186, p.110720. doi:https://doi.org/10.1016/j.colsurfb.2019.110720.

Li, X., Lv, Y., Ma, B., Wang, W. and Jian, S. (2017). *Decomposition kinetic characteristics of calcium carbonate containing organic acids by TGA.* Arabian Journal of Chemistry, 10, pp.S2534–S2538. doi:https://doi.org/10.1016/j.arabjc.2013.09.026.

Ling, S.Y., Asis, J. and Musta, B. (2023). *Distribution of metals in coastal sediment from northwest Sabah, Malaysia*. Heliyon, 9(2), p.e13271. doi:https://doi.org/10.1016/j.heliyon.2023.e13271.

Liu, L., Liu, H., Fu, S., Zhang, K., Wen, M., Yu, Y. and Huang, M. (2020). *Feasibility of magnetite powder as an erosion tracer for main soils across China*. Journal of Soils and Sediments, 20(4), pp.2207–2216. doi:https://doi.org/10.1007/s11368-020-02574-7.

Lokier, S.W. (2021). *Marine carbonate sedimentation in volcanic settings*. Geological Society, London, Special Publications, [online] 520. doi:https://doi.org/10.1144/SP520-2020-251.

Lopez-Capel, E., Krull, E.S., Bol, R. and Manning, D.A.C. (2008*). Influence of recent vegetation on labile and recalcitrant carbon soil pools in central Queensland, Australia: evidence from thermal analysis-quadrupole mass spectrometry-isotope ratio mass spectrometry*. Rapid Communications in Mass Spectrometry, 22(11), pp.1751–1758. doi:https://doi.org/10.1002/rcm.3538.

Lunderberg, J.M., Bartlett, R.J., Behm, A.M., Contreras, C., DeYoung, P.A., Hoogeveen, N.L., Huisman, A.J., Peaslee, G.F. and Postma, J.K. (2008). PIXE as a complement to trace metal analysis of sediments by ICP-OES. Nuclear Instruments and Methods in Physics Research Section B: Beam Interactions with Materials and Atoms, 266(21), pp.4782–4787. doi:https://doi.org/10.1016/j.nimb.2008.07.025.

Mansa, R. and Zou, S. (2021). *Thermogravimetric analysis of microplastics: A mini review*. Environmental Advances, 5, p.100117. doi:https://doi.org/10.1016/j.envadv.2021.100117.

Manzello, D. and Lirman, D. (2003). *The photosynthetic resilience of Porites furcata to salinity disturbance.* Coral Reefs, 22(4), pp.537–540. doi:https://doi.org/10.1007/s00338-003-0327-0.

Martí-Rosselló, T., Li, J. and Lue, L. (2018). *Quantitatively modelling kinetics through a visual analysis of the derivative thermogravimetric curves: Application to biomass pyrolysis*. Energy Conversion and Management, 172, pp.296–305. doi:https://doi.org/10.1016/j.enconman.2018.07.018.

Marubini, F. and Davies, P.S. (1996). *Nitrate increases zooxanthellae population density and reduces skeletogenesis in corals*. Marine Biology, 127(2), pp.319–328. doi:https://doi.org/10.1007/bf00942117.

McManus, J.W., Menez L.A.B., Kesner-Reyes, K.N., Vergara, S.G., Ablan, M.C. (2000). *Coral reef fishing and coral-algal phase shifts: implications for global reef status.* ICES Journal of Marine Science, 57(3), pp.572–578. doi:https://doi.org/10.1006/jmsc.2000.0720.

Miyazawa, M., Pavan, M.A., Oliveira, E.L. de, Ionashiro, M. and Silva, A.K. (2000). *Gravimetric determination of soil organic matter*. Brazilian Archives of Biology and Technology, [online] 43, pp.475–478. doi:https://doi.org/10.1590/S1516-89132000000500005.

Mizugaki, S., Onda, Y., Fukuyama, T., Koga, S., Asai, H. and Hiramatsu, S. (2008). *Estimation of suspended sediment sources using 137Cs and 210Pbex in unmanaged Japanese cypress*

plantation watersheds in southern Japan. Hydrological processes, 22(23), pp.4519–4531. doi:https://doi.org/10.1002/hyp.7053.

Mukundan, R., Radcliffe, D.E., Ritchie, J.C., Risse, L.M. and McKinley, R.A. (2010). *Sediment Fingerprinting to Determine the Source of Suspended Sediment in a Southern Piedmont Stream*. Journal of Environmental Quality, 39(4), pp.1328–1337. doi:https://doi.org/10.2134/jeq2009.0405.

Mukundan, R., Walling, D.E., Gellis, A.C., Slattery, M.C. and Radcliffe, D.E. (2012*). Sediment Source Fingerprinting: Transforming From a Research Tool to a Management Tool*. JAWRA Journal of the American Water Resources Association, 48(6), pp.1241–1257. doi:https://doi.org/10.1111/j.1752-1688.2012.00685.x.

Nagle, G.N. and Ritchie, J.C. (1999). *The Use of Tracers To Study Sediment Sources In Three Streams In Northeastern Oregon*. Physical Geography, 20(4), pp.348–366. doi:https://doi.org/10.1080/02723646.1999.10642683.

Nearing, M.A., Pruski, F.F. and O'Neal, M.R. (2004). *Expected climate change impacts on soil erosion rates: A review*. Journal of Soil and Water Conservation, 59(1), pp.43–50.

Negri, A.P., Flores, F., Röthig, T. and Uthicke, S. (2011). *Herbicides increase the vulnerability of corals to rising sea surface temperature*. Limnology and Oceanography, 56(2), pp.471–485. doi:https://doi.org/10.4319/lo.2011.56.2.0471.

Olutona, G.O. (2023). *Health Risk Assessment of Heavy Metals in Sediment of Tropical Freshwater Stream*. Journal of Nigerian Society of Physical Sciences, pp.983–983. doi:https://doi.org/10.46481/jnsps.2023.983.

Owens, P.N., Blake, W.H., Gaspar, L., Gateuille, D., Koiter, A.J., Lobb, D.A., Petticrew, E.L., Reiffarth, D.G., Smith, H.G. and Woodward, J.C. (2016). *Fingerprinting and tracing the sources of soils and sediments: Earth and ocean science, geoarchaeological, forensic, and human health applications.* Earth-Science Reviews, 162, pp.1–23. doi:https://doi.org/10.1016/j.earscirev.2016.08.012.

Padmanabhan, E. and Reich, P.F. (2023). *World Soil map based on soil taxonomy*. Encyclopedia of Soils in the Environment , 4, pp.218–231. doi:https://doi.org/10.1016/B978-0-12-822974-3.00118-X.

Pallasser, R., Minasny, B. and McBratney, A.B. (2013). *Soil carbon determination by thermogravimetrics*. PeerJ, 1, p.e6. doi:https://doi.org/10.7717/peerj.6.

Parra, M., Pons, J.C. and Ferragne, A. (1986*). Two potential sources for Holocene clay sedimentation in the Caribbean Basin: The Lesser Antilles Arc and the South American continent*. Marine geology, 72(3-4), pp.287–304. doi:https://doi.org/10.1016/0025-3227(86)90124-6.

Peña-Icart, M., Pomares-Alfonso, M.S., Wendel, F., Alonso-Hernandez, C., Yoelvis Bolaños-Alvarez and Edenir Rodrigues Pereira-Filho (2017). *Fast and direct detection of metal accumulation in marine sediments using laser-induced breakdown spectroscopy (LIBS): a case study from the Bay of Cienfuegos, Cuba†. Analytical Methods*. 9(24), pp.3713–3719. doi:https://doi.org/10.1039/c7ay00578d.

Pinheiro, F.C., Aguirre, M.Á., Nóbrega, J.A. and Canals, A. (2021). *Dispersive liquid–liquid microextraction of Cd, Hg and Pb from medicines prior to ICP OES determination according to the United States Pharmacopeia*. Analytical Methods, [online] 13(46), pp.5670–5678. doi:https://doi.org/10.1039/D1AY01566D.

Pitkanen, I.; Huttunen, J.; Halttunen, H.; Vesterinen, R (1999). *Evolved gas analysis of some solid fuels by TG-FTIR*. Journal of Thermal Analysis and Calorimetry, 56 (3), 1253−1259.

Plante, A.F., Fernández, J.M. and Leifeld, J. (2009). *Application of thermal analysis techniques in soil science.* Geoderma, 153(1-2), pp.1–10. doi:https://doi.org/10.1016/j.geoderma.2009.08.016.

Porter, J.W., Lewis, S.K. and Porter, K.G. (1999). *The effect of multiple stressors on the Florida Keys coral reef ecosystem: A landscape hypothesis and a physiological test*. Limnology and Oceanography, 44(3part2), pp.941–949. doi:https://doi.org/10.4319/lo.1999.44.3_part_2.0941.

Pulley, S. and Collins, A.L. (2018). *Tracing catchment fine sediment sources using the new SIFT (SedIment Fingerprinting Tool) open source software*. Science of The Total Environment, 635, pp.838–858. doi:https://doi.org/10.1016/j.scitotenv.2018.04.126.

Quinton, J.N., Govers, G., Van Oost, K. and Bardgett, R.D. (2010). *The impact of agricultural soil erosion on biogeochemical cycling.* Nature Geoscience, 3(5), pp.311–314. doi:https://doi.org/10.1038/ngeo838.

Ranatunga, T.D., Taylor, R.W., Bhat, K.N., Reddy, S.S., Senwo, Z.N. and Jackson, B. (2009*). Inorganic Phosphorous Forms in Soufriere Hills Volcanic Ash and Volcanic Ash-Derived Soil*. Soil Science, 174(8). doi:https://doi.org/10.1097/SS.0b013e3181b6deab.

Reichelt-Brushett, A.J. and Harrison, P.L. (2005). *The effect of selected trace metals on the fertilization success of several scleractinian coral species*. Coral Reefs, 24(4), pp.524–534. doi:https://doi.org/10.1007/s00338-005-0013-5.

Reid, I. and Laronne, J.B. (1995). *Bed Load Sediment Transport in an Ephemeral Stream and a Comparison with Seasonal and Perennial Counterparts*. Water Resources Research, 31(3), pp.773–781. doi:https://doi.org/10.1029/94wr02233.

Reuter, M. and Piller, W.E. (2011). *Volcaniclastic events in coral reef and seagrass environments: evidence for disturbance and recovery (Middle Miocene, Styrian Basin, Austria)*. Coral Reefs, 30(4), pp.889–899. doi:https://doi.org/10.1007/s00338-011-0798-3.

Rezić, I. and Steffan, I. (2007). *ICP-OES determination of metals present in textile materials.* Microchemical Journal, 85(1), pp.46–51. doi:https://doi.org/10.1016/j.microc.2006.06.010.

Riegl, B. and Branch, G.M. (1995*). Effects of sediment on the energy budgets of four scleractinian (Bourne 1900) and five alcyonacean (Lamouroux 1816) corals*. Journal of Experimental Marine Biology and Ecology, 186(2), pp.259–275. doi:https://doi.org/10.1016/0022-0981(94)00164-9.

Rogers, C. (1990). *Responses of coral reefs and reef organisms to sedimentation*. Marine Ecology Progress Series, [online] 62, pp.185–202. doi:https://doi.org/10.3354/meps062185.

Roper, W.R., Robarge, W.P., Osmond, D.L. and Heitman, J.L. (2019). *Comparing Four Methods of Measuring Soil Organic Matter in North Carolina Soils*. *Soil Science Society of America Journal*, 83(2), p.466. doi:https://doi.org/10.2136/sssaj2018.03.0105.

Saadatkhah, N., Carillo Garcia, A., Ackermann, S., Leclerc, P., Latifi, M., Samih, S., Patience, G.S. and Chaouki, J. (2019). *Experimental methods in chemical engineering: Thermogravimetric analysis—TGA. The Canadian Journal of Chemical Engineering*, 98(1), pp.34–43. doi:https://doi.org/10.1002/cjce.23673.

Scoffin, T.P. (1993). *The geological effects of hurricanes on coral reefs and the interpretation of storm deposits*. Coral Reefs, 12(3-4), pp.203–221. doi:https://doi.org/10.1007/bf00334480.

Shaheen, M.A., Tawfik, W., Mankola, A.F., Gagnon, J.E., Fryer, B.J. and Farouk El-Mekawy (2022). *Assessment of contamination levels of heavy metals in the agricultural soils using ICP-OES.* Soil and Sediment Contamination: An International Journal, pp.1–27. doi:https://doi.org/10.1080/15320383.2022.2123448.

Sherman, C.S., Simpfendorfer, C.A., Pacoureau, N., Matsushiba, J.H., Yan, H.F., Walls, R.H.L., Rigby, C.L., VanderWright, W.J., Jabado, R.W., Pollom, R.A., Carlson, J.K., Charvet, P., Bin Ali, A., Fahmi, Cheok, J., Derrick, D.H., Herman, K.B., Finucci, B., Eddy, T.D. and Palomares, M.L.D. (2023). *Half a century of rising extinction risk of coral reef sharks and rays*. Nature Communications, 14(1). doi:https://doi.org/10.1038/s41467-022-35091-x.

Sherriff, S.C., Franks, S.W., Rowan, J.S., Fenton, O. and Ó'hUallacháin, D. (2015). *Uncertainty-based assessment of tracer selection, tracer non-conservativeness and multiple solutions in sediment fingerprinting using synthetic and field data*. Journal of Soils and Sediments, 15(10), pp.2101–2116. doi:https://doi.org/10.1007/s11368-015-1123-5.

Shields, J.E., Mader, H.M., Caricchi, L., Tuffen, H., Mueller, S., Pistone, M. and Baumgartner, L.P. (2016). *Unravelling textural heterogeneity in obsidian: Shear-induced outgassing in the Rocche Rosse flow*. Journal of Volcanology and Geothermal Research, 310, pp.137–158. doi:https://doi.org/10.1016/j.jvolgeores.2015.12.003.

Siewert, C. (2004*). Rapid Screening of Soil Properties using Thermogravimetry*. Soil Science Society of America Journal, 68(5), pp.1656–1661. doi:https://doi.org/10.2136/sssaj2004.1656.

Silva, S., Bevilacqua, J. and Fávaro, D. (2011). *Major And Trace Elements Assessment in Sediment From Itupararanga Reservoir, By Activation Analysis and ICP-OES.*

Sim, K.S., Kim, H., Suel Hye Hur, Tae Woong Na, Ji Hye Lee and Ho Jin Kim (2024). *Geographical origin discriminatory analysis of onions: Chemometrics methods applied to ICP-OES and ICP-MS analysis*. Food Research International, 175, pp.113676–113676. doi:https://doi.org/10.1016/j.foodres.2023.113676.

Sinutok, S., Hill, R., Doblin, M.A., Wuhrer, R. and Ralph, P.J. (2011). *Warmer more acidic conditions cause decreased productivity and calcification in subtropical coral reef sediment-dwelling calcifiers*. Limnology and Oceanography, 56(4), pp.1200–1212. doi:https://doi.org/10.4319/lo.2011.56.4.1200.

Smith, H.G. and Blake, W.H. (2014). *Sediment fingerprinting in agricultural catchments: A critical re-examination of source discrimination and data corrections*. Geomorphology, 204, pp.177–191. doi:https://doi.org/10.1016/j.geomorph.2013.08.003.

Spalding, M., Burke, L., Wood, S.A., Ashpole, J., Hutchison, J. and zu Ermgassen, P. (2017*). Mapping the global value and distribution of coral reef tourism*. Marine Policy, [online] 82(1), pp.104–113. doi:https://doi.org/10.1016/j.marpol.2017.05.014.

Steegen, A., Govers, G., Beuselinck, L., Van Oost, K., (2000). *The use of phosphorus as a tracer in erosion/sedimentation studies*. IAHS-AISH publication, pp.59–66.

Stevens, C., Haygarth, P., Quinton, J. and Tuffen, H. (2023). *Mapping the Soils on Montserrat.* JNCC – UK Overseas Territories Report Series No. XX. JNCC, Peterborough, ISSN 2753-6270. https://hub.jncc.gov.uk/...]

Stewart, H.A., Massoudieh, A. and Gellis, A. (2014). *Sediment source apportionment in Laurel Hill Creek, PA, using Bayesian chemical mass balance and isotope fingerprinting*. Hydrological Processes, 29(11), pp.2545–2560. doi:https://doi.org/10.1002/hyp.10364.

Storlazzi, C.D., Norris, B.K. and Rosenberger, K.J. (2015). *The influence of grain size, grain color, and suspended-sediment concentration on light attenuation: Why fine-grained terrestrial sediment is bad for coral reef ecosystems.* Coral Reefs, 34(3), pp.967–975. doi:https://doi.org/10.1007/s00338-015-1268-0.

Tebbett, S.B., Goatley, C.H.R. and Bellwood, D.R. (2017*). Fine sediments suppress detritivory on coral reefs*. Marine Pollution Bulletin, 114(2), pp.934–940. doi:https://doi.org/10.1016/j.marpolbul.2016.11.016.

Tubuna, Babu, B.S., Datnoff, T. and Lawrence, E. (2016). *A Review of Silicon in Soils and Plants and Its Role in US Agriculture: History and Future Perspectives*. Soil Science, 181(9/10), pp.393–411.

Uddin, M.K. (2017). *A review on the adsorption of heavy metals by clay minerals, with special focus on the past decade*. Chemical Engineering Journal, 308, pp.438–462. doi:https://doi.org/10.1016/j.cej.2016.09.029.

Vaithiyanathan, P., Ramanathan, Al. and Subramanian, V. (1993). *Transport and distribution of heavy metals in Cauvery River.* Water, Air, & Soil Pollution, 71(1-2), pp.13–28. doi:https://doi.org/10.1007/bf00475509.

Vale, S., Swales, A., Smith, H.G., Olsen, G. and Woodward, B. (2022). *Impacts of tracer type, tracer selection, and source dominance on source apportionment with sediment fingerprinting*. Science of The Total Environment, 831, p.154832. doi:https://doi.org/10.1016/j.scitotenv.2022.154832.

Van Arkel, Z. and Kaleita, A.L. (2014). Identifying sampling locations for field-scale soil moisture estimation using K-means clustering. Water Resources Research, 50(8), pp.7050–7057. doi:https://doi.org/10.1002/2013wr015015.

Vega Thurber, R.L., Burkepile, D.E., Fuchs, C., Shantz, A.A., McMinds, R. and Zaneveld, J.R. (2013). *Chronic nutrient enrichment increases prevalence and severity of coral disease and bleaching*. Global Change Biology, [online] 20(2), pp.544–554. doi:https://doi.org/10.1111/gcb.12450.

Vernberg, W.B. and Vernberg, F.J. (2012). *Environmental Physiology of Marine Animals*. Springer Science & Business Media.

Vidal, O. and Dubacq, B., (2009). *Thermodynamic modelling of clay dehydration, stability and compositional evolution with temperature, pressure and H2O activity*. Geochimica et Cosmochimica Acta, 73(21), pp.6544–6564. doi:https://doi.org/10.1016/j.gca.2009.07.035.

Vroom, P.S. and Zgliczynski, B.J. (2011). *Effects of volcanic ash deposits on four functional groups of a coral reef. Coral Reefs*, 30(4), pp.1025–1032. doi:https://doi.org/10.1007/s00338-011-0793-8.

Walling, D.E., (2003). *Using environmental radionuclides as tracers in sediment budget investigations*. In: Proceedings of the Oslo Workshop, June 2002, Erosion and Sediment Transport Management in Rivers: Technological and Methodological Advances, IAHS Publ 283, pp. 279-301.

Walling, D.E. (2013). *The evolution of sediment source fingerprinting investigations in fluvial systems*. Journal of Soils and Sediments, 13(10), pp.1658–1675. doi:https://doi.org/10.1007/s11368-013-0767-2.

Walling, D.E. and He, Q. (1997). *Use of fallout 137Cs in investigations of overbank sediment deposition on river floodplains.* CATENA, 29(3-4), pp.263–282. doi:https://doi.org/10.1016/s0341-8162(96)00072-0.

Weaver, D.B. (1995). *Alternative tourism in Montserrat*. Tourism Management, 16(8), pp.593–604. doi:https://doi.org/10.1016/0261-5177(95)00082-8.

Wenger, A., McCormick, M., Endo, G., McLeod, I., Kroon, F. and Jones, G. (2013). *Suspended sediment prolongs larval development in a coral reef fish*. Journal of Experimental Biology. doi:https://doi.org/10.1242/jeb.094409.

Xu, W., Li, S., Whitely, N. and Pan, W.P. (2005). *Fundamentals of TGA and SDT*. pp.1–7.

Yanardağ, İ.H., Zornoza, R., Cano, A.F., Yanardağ, A.B. and Mermut, A.R. (2014). *Evaluation of carbon and nitrogen dynamics in different soil types amended with pig slurry, pig manure*

and its biochar by chemical and thermogravimetric analysis. Biology and Fertility of Soils, 51(2), pp.183–196. doi:https://doi.org/10.1007/s00374-014-0962-3.

Zainal Abidin, S.Z. and Mohamed, B. (2014). *A Review of SCUBA Diving Impacts and Implication for Coral Reefs Conservation and Tourism Management*. SHS Web of Conferences, [online] 12, p.01093. doi:https://doi.org/10.1051/shsconf/20141201093.

Zellmer, G.F., Hawkesworth, C.J., Sparks, R.S.J., Thomas, L.E., Harford, C.L., Brewer, T.S. and Loughlin, S.C. (2003). *Geochemical Evolution of the Soufriere Hills Volcano, Montserrat, Lesser Antilles Volcanic Arc.* Journal of Petrology, 44(8), pp.1349–1374. doi:https://doi.org/10.1093/petrology/44.8.1349.

Zentar, R., Ouendi, F. and Wang, H. (2023). *Effects of sample preparation methods on measured characteristics of marine and fluvial sediment*. International Journal of Sediment Research. doi:https://doi.org/10.1016/j.ijsrc.2023.09.002.

Zethof, J.H.T., Leue, M., Vogel, C., Stoner, S.W. and Kalbitz, K. (2019). *Identifying and quantifying geogenic organic carbon in soils – the case of graphite*. SOIL, 5(2), pp.383–398. doi:https://doi.org/10.5194/soil-5-383-2019.

Zöllmer, V. and Irion, G. (1993). *Clay mineral and heavy metal distributions in the northeastern North Sea.* Marine Geology, 111(3-4), pp.223–230. doi:https://doi.org/10.1016/0025-3227(93)90132-f.

Appendices

Appendix A

Table 15: The maximum, minimum and average weight loss percentages for the organic matter, clay and calcite temperature ranges, as well as total weight loss percentage for all ghaut samples. Data from TGA experiments using the TA STD Q600 instrument.

	Maximum	Average	Minimum
OM wt% loss	4.33	1.56	0.16
Clay wt% loss	2.11	0.99	0.06
Calcite wt% loss	2.02	0.59	0

Appendix B

Table 16: The TGA percentage weight losses within the temperature ranges of OM, Clay and Calcite for all ghaut and marine samples.

Sample	OM	Clay	Calcite
LB1	1.2	1.12	0.75
LB2	0.55	0.52	0.15
LB3	0.59	0.3	0
LB7	1.02	0.82	0.99
LB8	0.73	0.46	2.02
LB9	0.39	0.3	1.08
LB10	2.78	1.4	0.16
LB11	2.82	1.55	0.34
LB12	4.33	1.98	0.31
COW1	2.46	1.64	1.43
COW2	1.15	0.76	0.15
COW3	1.05	0.99	0.23
COW4	0.59	0.44	0.13
COW5	1.52	1.22	1.38
COW6	1.05	1.57	0.38
COW7	1.64	0.81	1.19
COW8	3.37	1.75	1.49
COW9	0.54	0.5	0.24
COW10	2.13	1.72	1.21
COW11	1.24	1.79	0.41
COW12	1.33	1.02	0.73
COW13	1.5	1.17	0.6
COW14	0.74	0.9	0.26
COW15	2.59	1.2	1.75
COW16	1.43	1.06	0.65
COW17	2.13	1.04	1.29
BP1	2.67	2	0.39
BP2	3.22	2.11	0.45

BP3	0.17	0.06	0.03
BP4	2.01	1.23	1.2
BP5	2.24	1.44	0.7
BP6	0.3	0.15	0.05
BP7	0.65	0.31	0.15
BP8	3.96	0.94	0.15
BP9	2.55	1.72	0.36
BP10	0.49	0.23	0.1
BP11	1.27	0.49	0.11
BP20	1.24	0.77	0.54
BP21	0.46	0.19	0.03
EX1	0.16	0.06	0.01
BG	0.56	1.05	4.89
CB	1.42	1.33	22.88
OR	0.39	0.57	1.56
PH	0.5	0.98	5.48
PL	0.69	1.39	9.92
PP	1.65	1.17	32.98
WS	0.26	0.38	2.27

Appendix C

Table 17: The peak H_2O signal (amu) within each temperature range of interest. ** represents that no significant peak was present.

Sample	200-430°C	430-590°C	590-800°C
LB1	**	**	**
LB2	**	**	**
LB3	**	**	**
LB7	**	**	**
LB8	**	**	**
LB9	**	**	**
LB10	**	**	**
LB11	**	**	**
LB12	**	9.09E-10	**
COW1	**	**	**
COW2	**	**	**
COW3	**	**	**
COW4	**	**	**
COW5	1.23E-09	1.27E-09	**
COW6	**	**	**
COW7	7.98E-10	7.15E-10	4.87E-10
COW8	1.34E-09	5.68E-10	**
COW9	**	**	**
COW10	9.03E-10	1.26E-09	**
COW11	**	**	**
COW12	**	**	**
COW13	**	**	**
COW14	**	**	**
COW15	1.72E-09	1.31E-09	**
COW16	6.23E-10	6.19E-10	**
COW17	1.49E-09	1.19E-09	**
BP1	**	**	**

BP2	**	**	**
BP3	2.61E-10	2.83E-10	**
BP4	5.05E-09	**	**
BP5	5.45E-09	**	**
BP6	2.44E-10	2.68E-10	**
BP7	**	**	**
BP8	4.81E-09	**	**
BP9	2.50E-09	2.19E-09	**
BP10	**	**	**
BP11	**	**	**
BP20	**	**	**
BP21	**	**	**
EX1	**	**	**
BG	**	**	**
CB	**	**	**
OR	**	**	**
PH	**	**	2.03E-09
PL	**	**	**
PP	**	**	**
WS	**	**	**

Table 18: The peak CO_2 signal (amu) within each temperature range of interest. ** represents that no significant peak was present.

Sample	200-430°C	430-590°C	590-800°C
LB1	5.02E-10	3.11E-10	**
LB2	3.11E-10	**	**
LB3	3.33E-10	**	**
LB7	4.92E-10	**	4.79E-10
LB8	**	**	7.56E-10
LB9	2.38E-10	**	4.62E-10
LB10	9.11E-10	**	**
LB11	7.97E-10	4.38E-10	2.21E-10
LB12	**	2.21E-10	9.24E-10
COW1	4.72E-10	**	**
COW2	1.85E-10	**	**
COW3	2.20E-10	**	**
COW4	1.86E-10	1.11E-10	**
COW5	1.11E-10	2.20E-10	1.77E-10
COW6	4.97E-10	1.77E-10	1.34E-10
COW7	2.20E-10	1.34E-10	9.99E-11
COW8	1.77E-10	9.99E-11	9.08E-11
COW9	1.34E-10	**	**
COW10	9.99E-11	1.64E-10	7.07E-11
COW11	9.08E-11	7.07E-11	**
COW12	5.23E-10	1.22E-10	**
COW13	2.83E-10	8.24E-11	8.00E-11
COW14	5.20E-11	**	**
COW15	1.44E-09	3.21E-10	**
COW16	3.52E-10	5.06E-10	3.98E-11
COW17	6.67E-11	1.68E-10	**
BP1	8.05E-10	3.74E-10	**
BP2	3.74E-10	9.46E-10	**
BP3	9.46E-10	**	**

BP4	3.02E-10	2.92E-10	**
BP5	3.84E-11	1.40E-09	1.62E-10
BP6	9.31E-10	**	**
BP7	2.92E-10	1.30E-10	**
BP8	1.40E-09	7.38E-10	1.17E-10
BP9	5.09E-10	2.92E-10	1.11E-10
BP10	1.62E-10	1.17E-10	**
BP11	4.95E-11	8.70E-10	**
BP20	1.62E-10	**	**
BP21	1.30E-10	1.73E-10	**
EX1	**	**	**
BG	2.10E-09	9.07E-10	**
CB	1.54E-08	**	**
OR	**	**	6.12E-10
PH	**	**	1.89E-09
PL	**	**	3.78E-09
PP	**	**	1.03E-08
WS	**	**	5.22E-10

Table 19: The concentrations in mg/kg of the 11 elements analysed using ICP-OES for all ghaut and marine samples. ** represent the values were outside the detection limit of the instrument.

Sample	Al	Ca	Cu	Fe	Mg	Mn	Ni	P	Pb	Si	Zn
LB1	11299.32	3946.79	35.53	25597.85	2586.69	629.04	**	346.25	**	481.17	47.72
LB2	11066.72	3879.34	22.69	21264.48	2399.12	321.61	**	311.73	**	425.39	43.37
LB3	5658.58	3541.58	17.93	16683.25	967.87	214.78	**	513.33	**	290.49	46.17
LB7	12628.56	10294.70	36.50	22725.47	2684.93	664.85	**	343.85	**	571.00	44.83
LB8	7261.48	21966.07	30.96	25658.68	2685.63	452.10	**	438.12	**	1299.40	55.03
LB9	8385.23	13675.21	45.09	10724.46	1568.99	233.52	**	398.25	**	1356.33	38.02
LB10	14548.36	3222.42	27.82	25559.55	1926.46	929.96	**	267.99	**	1843.53	53.81
LB11	15572.79	8960.82	50.17	18516.31	1355.41	521.68	**	371.12	**	1554.30	112.67
LB12	21425.70	5779.12	81.29	22520.08	1163.65	845.38	**	485.04	**	1894.58	195.48
COW1	14834.52	4100.67	73.74	13179.67	760.64	595.55	**	316.29	**	1638.10	81.11
COW2	11121.25	3100.16	11.06	18826.03	1068.53	274.23	**	478.71	**	1449.72	35.21
COW3	12285.09	2455.02	14.29	13394.64	961.92	433.33	**	211.82	**	1759.30	34.17
COW4	9759.54	3361.49	13.09	14666.14	755.47	425.18	**	262.62	**	1446.74	85.07
COW5	12154.59	6697.04	16.42	15018.02	1091.31	302.46	**	373.95	**	1513.82	50.86
COW6	17864.21	2343.63	26.35	15558.19	2183.29	701.50	**	130.54	**	1662.71	32.03
COW7	8086.23	4448.78	12.84	15436.17	1027.41	254.60	**	338.64	**	832.63	35.43
COW8	10187.77	5199.76	18.78	8806.43	862.66	191.77	**	377.45	**	884.94	26.71
COW9	9014.64	4157.10	11.54	15077.17	1536.41	343.59	**	479.82	**	1118.92	30.83
COW10	15068.63	5171.58	29.53	15391.60	765.04	781.49	**	301.37	**	1078.93	27.31
COW11	14749.50	1939.88	19.88	12324.65	1478.96	334.27	**	46.29	**	1455.91	17.98
COW12	12090.91	3952.53	26.82	14323.23	636.97	535.25	**	395.56	**	1269.70	35.91

COW13	10552.01	4332.40	15.81	15095.66	801.81	298.13	**	495.12	**	97.55	24.03
COW14	12370.72	3304.49	20.96	27665.08	2325.97	522.57	**	331.84	**	51.71	38.89
COW15	11302.61	4545.09	33.87	13086.17	979.96	345.49	**	377.35	**	100.30	33.67
COW16	9975.91	2045.36	15.36	17272.18	840.43	613.51	**	223.50	**	89.72	43.62
COW17	9259.04	3284.66	9.93	21344.85	1562.38	507.65	**	278.51	**	93.46	28.10
BP1	12340.26	6514.58	24.13	11691.29	1026.36	395.27	**	470.75	**	141.87	41.76
BP2	17654.69	5910.18	50.37	14510.98	1277.45	526.35	**	472.26	**	118.36	23.84
BP3	7717.43	4790.58	9.91	7470.94	557.92	102.71	**	535.97	**	31.16	8.77
BP4	10466.75	3172.08	15.24	10596.96	666.17	299.88	**	195.91	**	78.63	14.08
BP5	9808.00	6795.33	28.05	9640.74	787.91	209.62	**	445.37	**	47.41	34.33
BP6	9113.74	4924.57	14.77	6022.23	520.05	95.77	**	418.72	**	53.00	8.48
BP7	9357.20	4785.39	20.15	6984.34	487.49	98.76	**	367.78	**	33.77	8.83
BP8	8744.49	5300.36	21.57	7721.27	505.61	188.23	**	440.33	**	61.67	8.81
BP9	9916.63	4544.53	21.67	11518.91	1031.92	348.31	**	442.56	**	51.04	17.43
BP10	8440.79	4188.97	19.73	5589.01	434.41	92.66	**	381.29	**	30.62	4.74
BP11	10981.50	4571.60	28.96	7865.04	500.10	138.07	**	435.14	**	69.19	8.81
BP20	11563.13	4946.89	29.33	11322.65	772.75	234.47	**	444.19	**	104.91	20.24
BP21	9245.59	4757.22	39.25	11496.79	551.46	198.54	**	500.80	**	39.02	25.34
EX1	11394.42	7212.15	25.93	5644.42	242.43	55.18	**	399.30	**	111.85	5.12
BG	7848.91	49831.01	6.57	14850.89	5268.39	273.16	**	462.92	**	87.57	15.39
CB	4143.55	**	7.59	7555.66	9462.89	120.61	**	233.01	**	1177.73	17.95
OR	9590.33	15097.92	6.97	6876.50	2274.18	89.63	**	215.93	**	32.47	6.25
PH	9156.05	59494.43	5.13	11863.06	7143.71	280.35	**	241.44	**	56.13	42.71
PL	6675.67	**	7.63	11054.42	8103.24	179.27	**	402.76	**	134.45	10.86
PP	1334.59	**	1.79	2373.37	5166.20	57.48	**	129.20	**	631.08	14.28
WS	6237.56	24771.19	5.66	7656.19	2522.88	128.33	**	299.64	**	39.99	11.52

Appendix E

Table 20: The particle size analysis data for all ghaut samples. Pebbles, coarse sand and fine sediments are given as percentage by weight of the total dry weight. Sand, silt and clay are given in percentages by volume.

Sample	% Pebbles (>2mm)	% Coarse Sand (0.5-2mm)	% Fine Sediments (<0.5mm)	% Sand (62-2000µm)	% Silt (2-62µm)	% Clay (<2µm)
LB1	22.38	43.52	34.08	85.42	11.46	3.16
LB2	30.78	53.28	15.94	93.06	5.22	1.72
LB3	22.96	57.12	19.94	90.56	6.88	2.68
LB7	20.98	45.00	34.04	72.20	21.66	6.20
LB8	7.50	16.38	76.12	89.38	7.66	3.02
LB9	15.80	23.86	60.34	86.06	11.02	2.94
LB10	44.00	38.20	17.82	68.52	22.80	8.68
LB11	14.18	36.60	49.22	54.94	33.22	11.86
LB12	36.20	40.50	23.30	47.48	40.04	12.48
COW1	22.92	36.64	40.48	55.56	28.64	15.82
COW2	20.60	62.45	16.94	92.31	5.79	1.90
COW3	32.08	54.54	13.46	79.28	15.08	5.64
COW4	26.06	54.65	19.29	92.55	5.32	2.14
COW5	30.04	36.68	33.32	73.96	19.32	6.62
COW6	31.51	45.49	23.01	41.98	45.78	12.24
COW7	30.62	49.96	19.40	85.31	11.14	3.55
COW8	16.36	44.35	39.29	49.29	38.94	11.77
COW9	40.40	49.32	14.30	87.52	9.66	2.68
COW10	32.52	36.71	30.77	55.08	34.13	13.71
COW11	49.84	29.16	21.02	15.26	54.96	29.74
COW12	34.95	39.91	25.14	79.36	14.34	6.30
COW13	40.76	39.12	20.16	79.80	15.22	4.70
COW14	35.35	45.83	18.82	89.90	7.86	2.24
COW15	30.78	37.90	31.32	63.31	27.75	9.68

COW16	29.01	45.53	25.46	83.51	11.07	5.42
COW17	37.28	36.90	25.86	74.84	19.78	5.40
BP1	31.74	37.14	31.10	62.06	29.21	8.73
BP2	39.39	14.78	45.83	3.63	78.03	18.33
BP3	3.46	44.90	51.46	96.72	2.28	1.02
BP4	17.93	33.67	48.43	42.81	43.07	14.12
BP5	14.10	26.43	59.47	42.06	46.93	8.41
BP6	10.06	52.14	36.48	90.80	7.19	2.02
BP7	1.06	13.25	85.69	84.28	12.97	2.76
BP8	7.16	30.12	62.72	36.83	50.28	12.86
BP9	32.86	38.41	28.73	82.93	13.20	3.88
BP10	5.39	31.37	63.24	76.80	18.72	5.12
BP11	3.41	12.90	83.68	40.08	50.38	9.53
BP20	5.84	25.39	68.77	53.90	25.62	20.48
BP21	22.00	43.26	34.74	88.12	8.99	2.69
EX1	27.33	38.90	33.77	92.80	5.69	1.51

Table 21: The particle size analysis data for all marine samples. Pebbles, coarse sand and fine sediments are given as percentage by weight of the total dry weight. Sand, silt and clay are given in percentages by volume.

Sample	**% Pebbles (>2mm)**	**% Coarse Sand (0.5-2mm)**	**% Fine Sediments (<0.5mm)**	**% Sand (62-2000µm)**	**% Silt (2-62µm)**	**% Clay (<2µm)**
BG	0.09	25.95	73.99	96	3.05	0.95
CB	21.49	77.64	0.91	96.51	2.54	0.95
OR	0.01	4.59	95.45	97.05	1.95	1
PH	0.19	1.48	98.46	96.92	1.95	1.13
PL	49.33	40.01	10.73	92.03	6.47	1.5
PP	75.87	17.27	6.91	92.04	7.36	1.6
WS	0.00	13.70	86.29	98.4	1	0.6

Annexes

Annex 1 – Mass Spectrometry Correlations

The use of mass spectrometry to analyse exsolved H_2O and CO_2 gases during thermogravimetric analyses was a significant component of this study. Whilst this analysis was originally conducted with the aims of using the data for sediment fingerprinting purposes, this was later disbanded due to the nature of the data collected (Chapter 6). However, the mass spectrometry data is still valuable. One way in which it can be used is to give insight into potential correlations between the amount of each gas exsolved and the mass loss. This was conducted across three different temperature ranges: 200-430°C (to represent organic matter), 430-590°C (for clay minerals) and 590-800°C (for calcite) (Chapter 5). The purpose behind the correlations was to determine whether the mass spectrometry data collected could give evidence for the hypotheses made that with an increase in organic matter or clay or calcite in the sample (represented by their mass loss), an increase in CO_2 or H_2O exsolved would occur.

Prior to conducting correlation tests, initial Shapiro Wilks tests for normality were conducted on the percentage weight loss, the H_2O peaks and the CO_2 peaks within each of the three temperature ranges representing OM, clay and carbonates. These results are displayed in Table 22. These tests were done to determine whether each variables dataset was normally distributed. This informs whether a Spearman's rank or Pearson's correlation should be conducted.

Table 22: The W-values and p-values given from the Shapiro-Wilks tests for normality conducted on the percentage weight loss, CO_2 peaks and H_2O peaks within the temperature ranges representing OM, clay and calcite. Those highlighted show a normal distribution.

Variable	W-Value	p-Value
% Weight Loss – OM	0.9151	0.002
% Weight Loss – Clay	0.9693	0.237
% Weight Loss – Calcite	0.3942	8.45e-13
CO_2 Peaks – OM	0.2620	1.3e-12
CO_2 Peaks – Clay	0.8253	0.0005
CO_2 Peaks - Calcite	0.5607	2.85e-06
H_2O Peaks – OM	0.8371	0.0703
H_2O Peaks – Clay	0.7693	0.0043
H_2O Peaks - Calcite	0.7894	0.0155

With a null hypothesis claiming the data is normally distributed and a 95% significance level, there is sufficient evidence to suggest that the % weight losses of OM and calcite, all CO_2 peaks and the H_2O peaks of clay and calcite are not normally distributed. This conclusion has arisen as the p-values are all less than 0.05, so therefore the null hypothesis can be rejected. The % weight loss of clay and the H_2O peak of OM have p-values > 0.05 and therefore there is insufficient evidence to reject the null hypotheses (these display a normal distribution).

Correlation testing was conducted between the percentage weight loss and the peak CO_2 or H_2O for each of OM, clay and calcite. As in all pairs of variables tested there was at least one variable not normally distributed, Spearman's rank correlations were used for all sets of variables. The results are shown in Table 23 and Figures 29 and 30.

Table 23: ρ-values (Spearman's rank correlation coefficients), p-values and n values from the Spearman's rank correlation testing conducted. Results are given for all 6 tests completed on % weight loss vs CO_2/H_2O peaks within three temperature ranges (OM, clay and calcite). Those highlighted indicate positive correlations.

Variables	ρ - value	p- value	n
% weight loss vs CO_2 peaks:			
OM	0.77	1.60e-08	38
Clay	0.33	0.10	26
Calcite	0.7	1.14e-03	18
% weight loss vs H_2O peaks:			
OM	0.61	0.11	8
Clay	0.68	0.01	12
Calcite	-0.35	0.35	9

The Spearman's rank correlations use a 95% significance level and a null hypothesis stating that no correlation is present. As p-values are <0.05, there is sufficient evidence to reject the null hypothesis and say that there is positive correlation for the relationship between % weight loss and CO_2 exsolved for OM and calcite, along with that for the H_2O peaks of clay. However, for that of the clay CO_2 peaks and the H_2O peaks of OM and calcite, p-values are greater than 0.05 and therefore there is insufficient evidence to suggest correlation is present.

These results are as expected. When OM is heated, CO_2 is given off, therefore suggesting that more OM will release more CO_2, as the data indicates is true. This also occurs for calcite, where calcium oxide and carbon dioxide gas are the products of heating calcium carbonates, again suggesting more calcite present will result in more CO_2 gas exsolved, as indicated by the results. For the correlation demonstrated between clay and H_2O, this can be explained by the loss of water adsorbed onto the clay minerals, so as more clay is heated, more water escapes this chemical binding and H_2O peaks increase.

Overall, the results of the Spearman's rank correlation tests conducted are insightful in justifying the conclusions drawn about the identities of the sample components and demonstrate how mass spectrometry data can be used to aid the chemical analysis of sediment samples.

a)

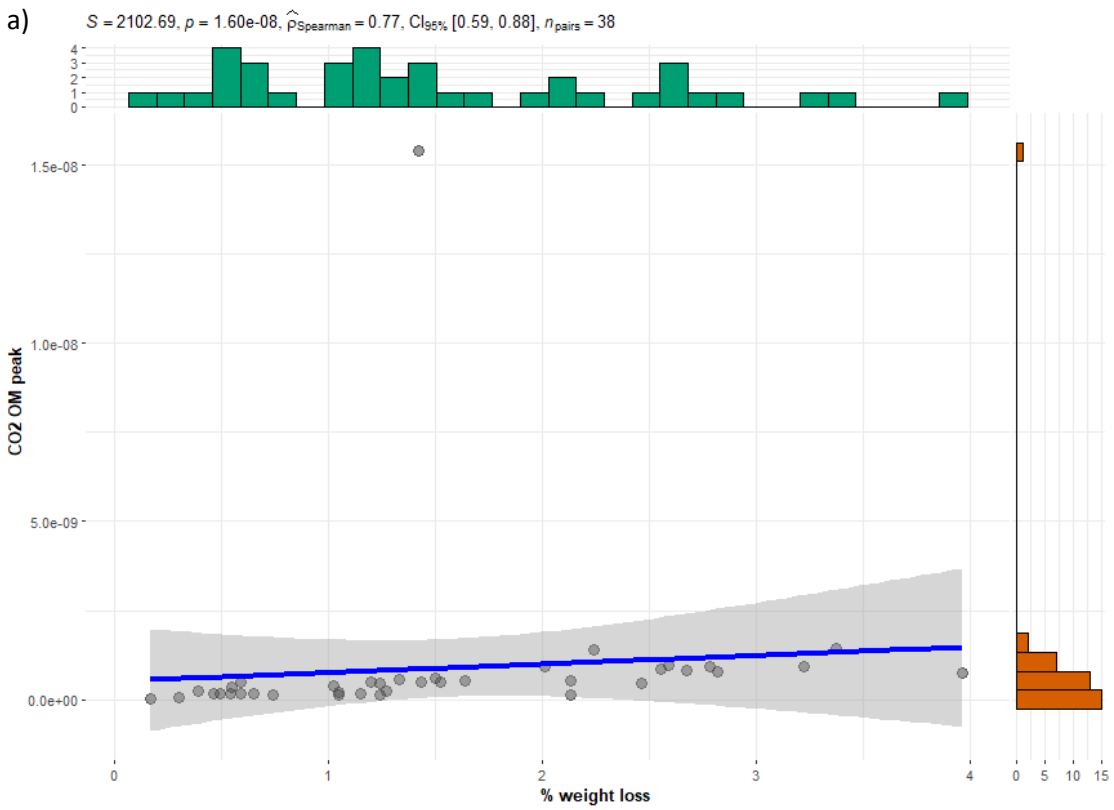
S = 2102.69, p = 1.60e-08, ρ̂Spearman = 0.77, CI95% [0.59, 0.88], npairs = 38
CO2 OM peak
% weight loss

b)

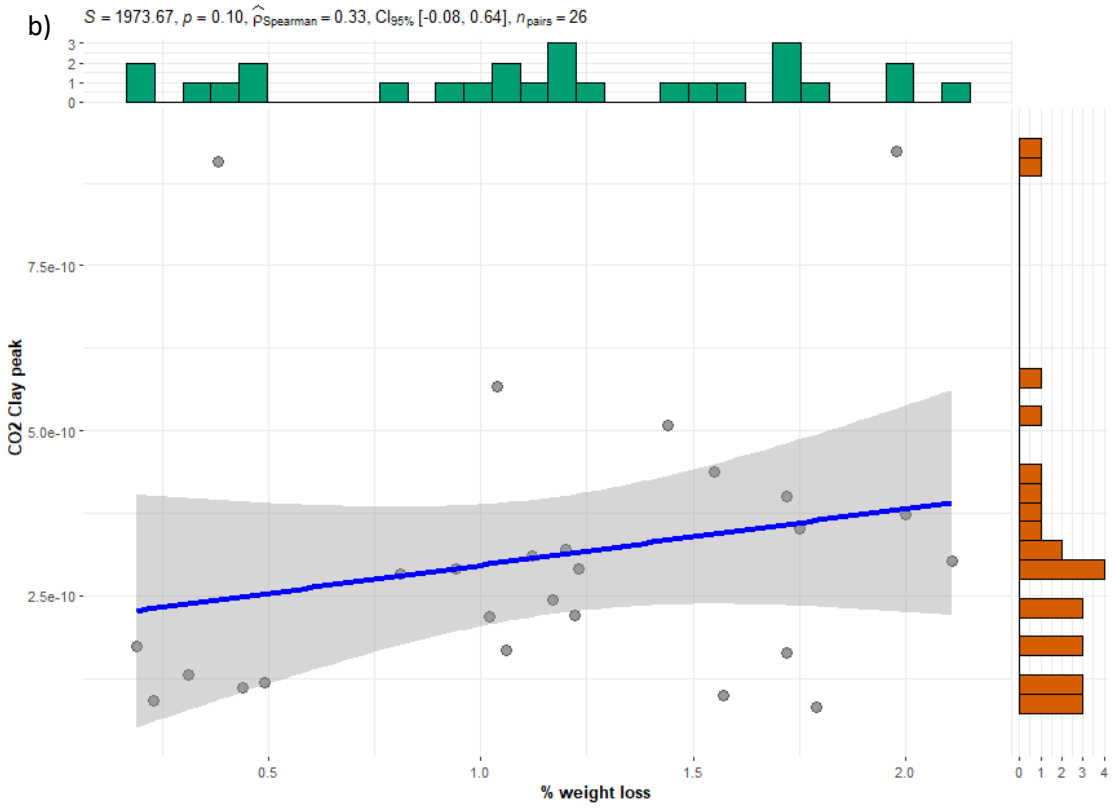
S = 1973.67, p = 0.10, ρ̂Spearman = 0.33, CI95% [-0.08, 0.64], npairs = 26
CO2 Clay peak
% weight loss

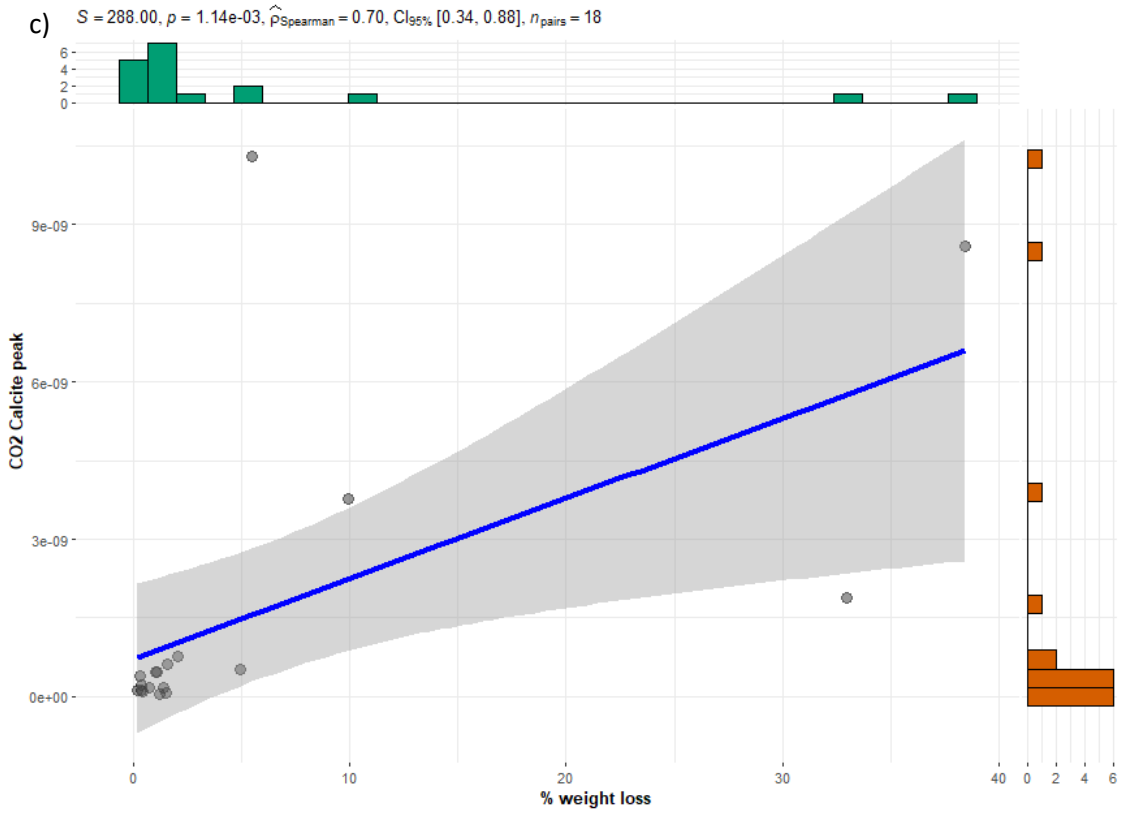

Figure 29: The results of the Spearman's rank correlations conducted on % weight loss vs CO_2 peaks (in amu) for a) OM, b) clay and c) calcite. % weight loss is displayed on the x-axis against CO_2 peaks on the y-axis. A line of best fit is displayed along with bar graphs of the two variables including each sample point alongside their corresponding axis.

a)

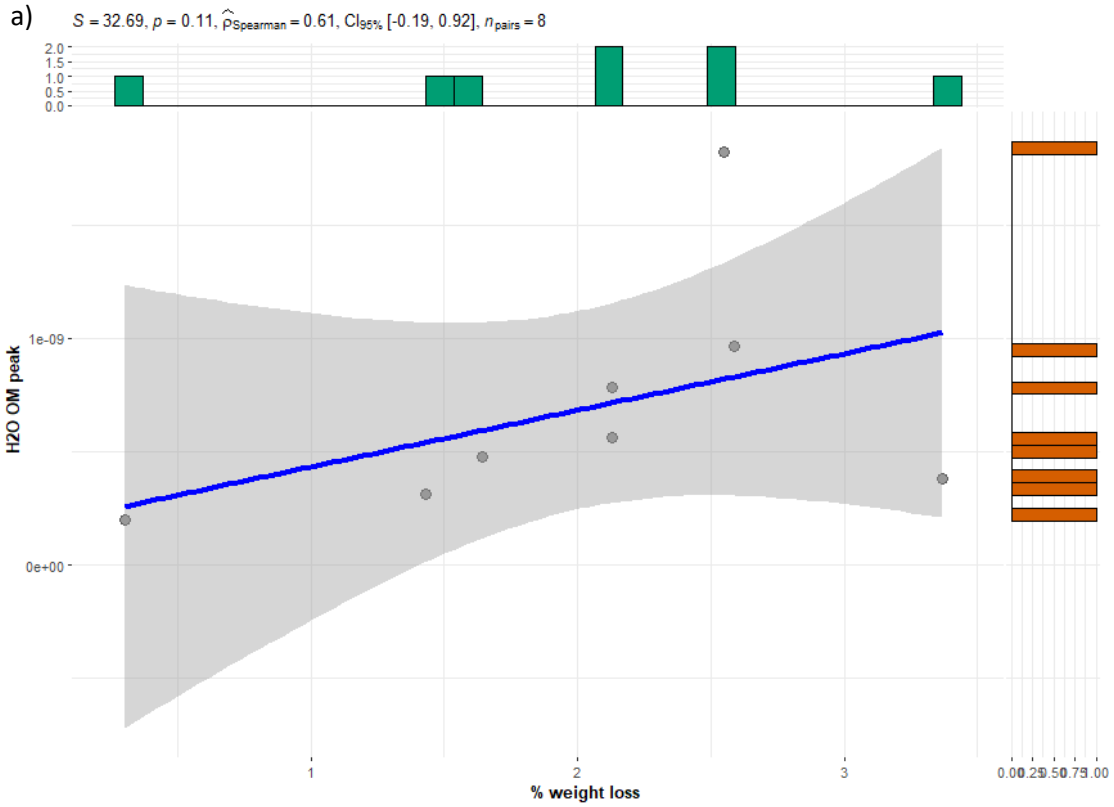
S = 32.69, p = 0.11, ρ̂Spearman = 0.61, CI95% [-0.19, 0.92], npairs = 8
H2O OM peak
% weight loss

b)

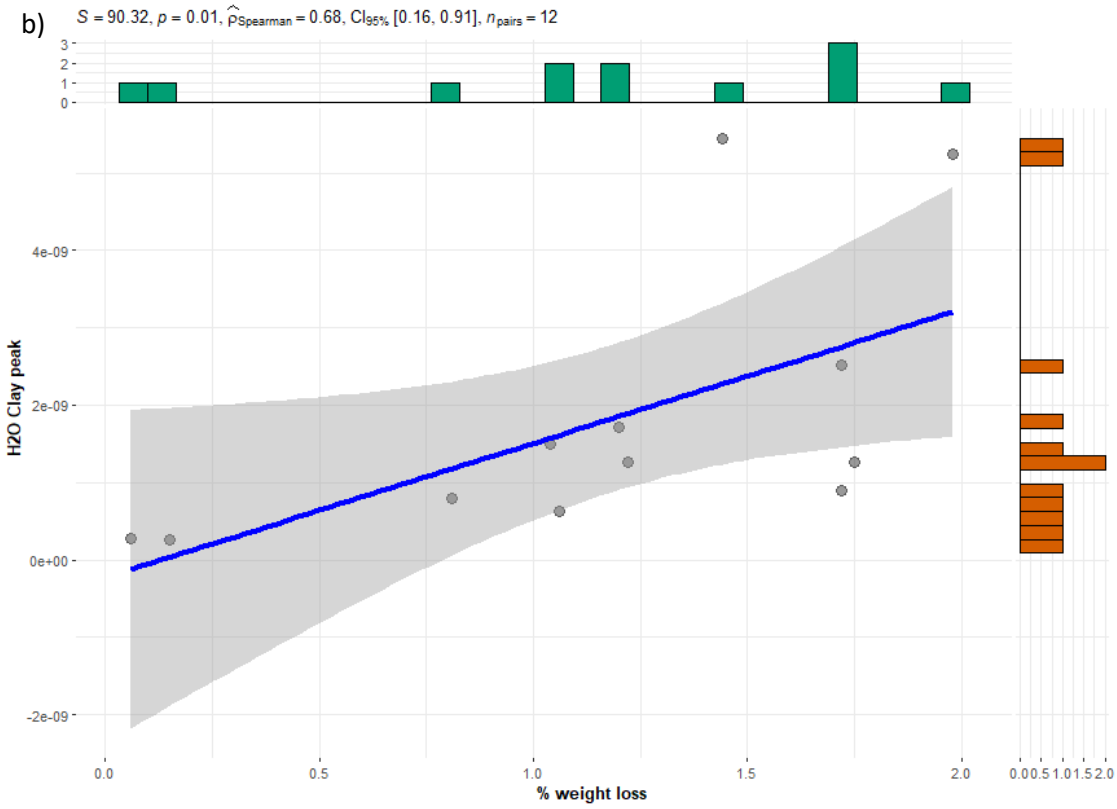
S = 90.32, p = 0.01, ρ̂Spearman = 0.68, CI95% [0.16, 0.91], npairs = 12
H2O Clay peak
% weight loss

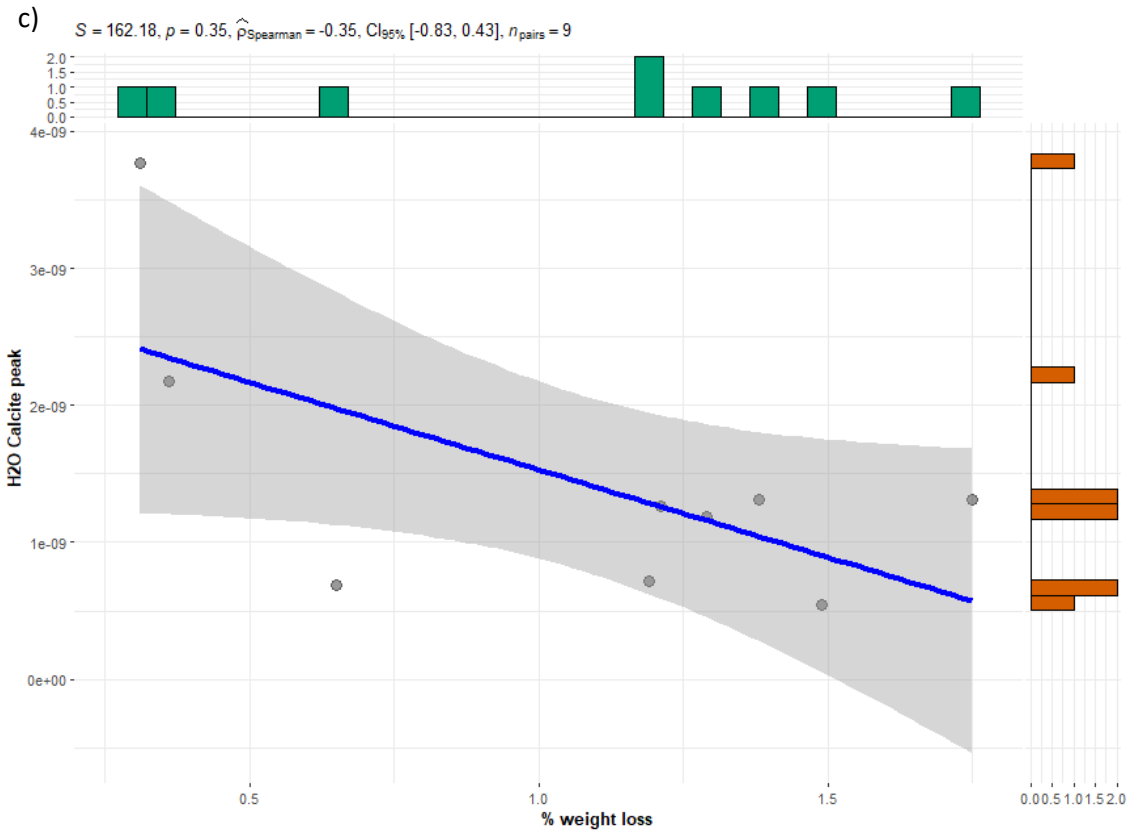

Figure 30: The results of the Spearman's rank correlations conducted on % weight loss vs H_2O peaks (in amu) for a) OM, b) clay and c) calcite. % weight loss is displayed on the x-axis against H_2O peaks on the y-axis. A line of best fit is displayed along with bar graphs of the two variables including each sample point alongside their corresponding axis.